Mutational Analysis of the ubiquitin binding domains of TOL proteins in *Arabidopsis thaliana*

Masterarbeit

eingereicht von

Christina Artner, BSc

Betreuer: Assoc. Prof. Dr. Christian Luschnig

Mitwirkende: Mag. Dr. Barbara Korbei

Durchgeführt am Department für Angewandte Genetik und Zellbiologie der Universität für Bodenkultur Wien

Wien, am 24.5.2016

1. Contents

I. Acknowledgements

This work was performed at the Department of Applied Genetics and Cell Biology (DAGZ, BOKU Vienna)

First of all I would like to thank my official supervisor Christian Luschnig for providing a pleasant working atmosphere and for his support regarding my Ph.D. application.

Special thanks to my co-supervisor Barbara Korbei for assisting me in every step of my master thesis and throughout my writing period. Your positive feedback and motivation facilitated my personal and scientific development and opened up new enriching possibilities I am going to focus soon within my Ph.D.. The certainty that I can always come to you with every kind of problem or question gave and still give me the feeling of being save and independent the same time, I cannot thank you enough!

Of course, Lucinda de Araujo! I will never forget working with you side by side solving together every problem (in the lab and everything in between). Thanks for all the time you spend with me explaining and discussing any problem, it was well worth! For me coming back to the lab feels like coming home again.

I am grateful to Katarzyna Retzer and her cooperativeness (from the beginning on) regarding everything in the lab and more! I will miss our delightful and refreshing conversations in the evening.

Additionally I want to thank Doris Lucyshyn and Jürgen Kleine-Vehn for the kindly and helpful conversations we had (and hopefully we will have in future) and the grateful possibilities they opened to me. If it would be possible, I would accept both of them without hesitation!

Special thanks to Eva Maria Gelb, Barbara Svoboda and Nora Lieskonig, who always promptly advised me in one or other ways.

Last but not least I want to thank my best friends and my family, including my parents Ingrid, Rudolf and my boyfriend Markus, for never becoming tired of listening to me whenever I couldn`t stop talking about all the lab and master stuff. It´s done now!

II. Abstract

Regulation of plasma membrane protein abundance controls responses to changing environmental conditions. Membrane proteins destined for degradation are marked by ubiquitin, endocytosed and subsequently transferred by the ESCRT (Endosomal Sorting Complex required for Transport) machinery to the final degradation compartment. The ESCRT machinery, consisting of four complexes, is highly conserved with the exception of the ESCRT-0, which as such is not found in plants. Yet, first contact with ubiquitinated cargo is initiated by the ubiquitin binding domain (UBD) of the ESCRT-0 complex. Thus the discovery of a family of nine proteins, called TOLs (Tom1 like), as potential ESCRT-0 orthologs in Arabidopsis thaliana gave a new perspective to plant endosomal trafficking. As mammalian and yeast ESCRT-0 subunits share similar UBDs with the TOLs, related functionality was assumed. In order to characterize the unique TOL proteins, I mutated the highly conserved amino acids reported to be important for ubiquitin binding. With these mutated constructs, I performed in vitro binding studies and could successfully show a substantial decrease in ubiquitin binding. I used these constructs to design in vivo TOL constructs to analyze the effect of the lack of ubiquitin binding in planta. Initial analysis of these plant lines showed that the mutation of the UBDs not only affects the binding to ubiquitin but also the localization of the TOL proteins. These results not only verify the importance of these UBDs of the TOL proteins but further suggest their interplay in the regulation of the function of the proteins and potentially the entire machinery that is responsible for the degradation of plasma membrane localized proteins. Further analysis will be needed to confirm these results. Nevertheless, this study serves as a solid corner stone to unravel the interplay between ubiquitinated plasma membrane proteins destined for degradation and the endosomal sorting machinery.

III. Zusammenfassung

Die Aktivität membran-assoziierter Plasmamembranproteine (PMP) an der zellulären Oberfläche ermöglicht die Interaktion einzelner Zellen untereinander als auch mit ihrer Umwelt. Die Reaktion auf veränderte Umwelteinflüsse erfolgt unter anderem durch eine Regulation der Degradation dieser Proteine. PMP, welche für die Degradierung bestimmt sind, können mittels Ubiquitin-Kopplung markiert, durch Endocytose in die Zelle aufgenommen und mithilfe der ESCRT Maschinerie zum endgültigem Abbau transportiert werden. Die ESCRT Maschinerie, bestehend aus vier Komplexen, ist besonders konserviert, wobei ESCRT-0 in pflanzlichen Zellen nicht vorhanden und daher eine Ausnahme bildet. Die initiale Kontaktaufnahme mit Ubiquitin-markierten PMP erfolgt durch die Ubiquitin-Bindungsdomänen (UBDs) des ESCRT-0 Komplexes. Die Entdeckung der Tom1-like Proteine (TOL) als mögliche Orthologe für ESCRT-0 in Arabidopsis thaliana eröffnet einen neuen Blickwinkel in den endosomalen Mechanismus in pflanzlichen Zellen. Die Ähnlichkeit zwischen den tierischen und pflanzlichen UBDs der ESCRT-0 und TOL Proteinen lässt auf eine gemeinsame Funktionalität schließen. Zur Charakterisierung dieser TOL Proteine in *Arabidopsis thaliana* wurden innerhalb dieser Masterarbeit die entsprechend höchst konservierten Aminosäuren der UBDs mutiert und analysiert. In *in vitro* Experimenten konnte ich eine reduzierte Ubiquitin-Bindungsaktivität nachweisen. Darauf folgende *in vivo* Experimente bestätigten nicht nur die Änderung der Ubiquitin-Interaktion, sondern auch eine veränderte zelluläre Lokalisierung des Proteins. Diese Resultate weisen nicht nur auf die Wichtigkeit der UBDs der TOL Proteine hin, sondern eröffnen auch eine neue Sichtweise auf ihre Interaktion mit anderen Proteinen und der Sortierungsmaschinerie. Dementsprechend stellt diese Masterarbeit einen wichtigen Meilenstein für zukünftige Studien zur Analyse des Zusammenspiels zwischen ubiquitinierten PMP und dem endosomalen Sortierungssystem dar.

2. Introduction

To interact with the environment, cells adjust their exterior surface by altering the composition of the plasma membrane (PM) (recently reviewed by (Sorkin and von Zastrow, 2009)). The lipid bilayer, providing the basic structure of the cellular membrane, is furnished with a distinct set of plasma membrane proteins (PMP) to determine its characteristic functional properties (recently reviewed by (Engel and Gaub, 2008)). These incorporated proteins fulfill different functions like acting as an anchor for different carbohydrates and other molecules or arranging to form certain transporters or receptors (recently reviewed by (Engel and Gaub, 2008)). To ensure efficient communication and interaction with the changing environment, the cell surface need to be adapted by exchanging or discarding distinct PMPs (recently reviewed by (Sorkin and von Zastrow, 2009)). This adjusting process is performed by the intracellular endosomal system (recently reviewed by (Scott et al., 2014)).

2.1 Endosomal system

The endosomal system is the major membrane-sorting apparatus and provides the transport machinery for intracellular protein sorting (recently reviewed by (Sorkin and von Zastrow, 2009)). It is composed of different types of compartments with distinct structure and function (recently reviewed by (Lemmon and Traub, 2000)). Generally it operates as a regulatory machinery to sort endocytosed PMPs for either degradation or recycling and newly synthesized proteins to their final destination (recently reviewed by (Huotari and Helenius, 2011)). As shown in Figure 1 different types of endosomes are responsible for sorting certain proteins to their ultimate location.

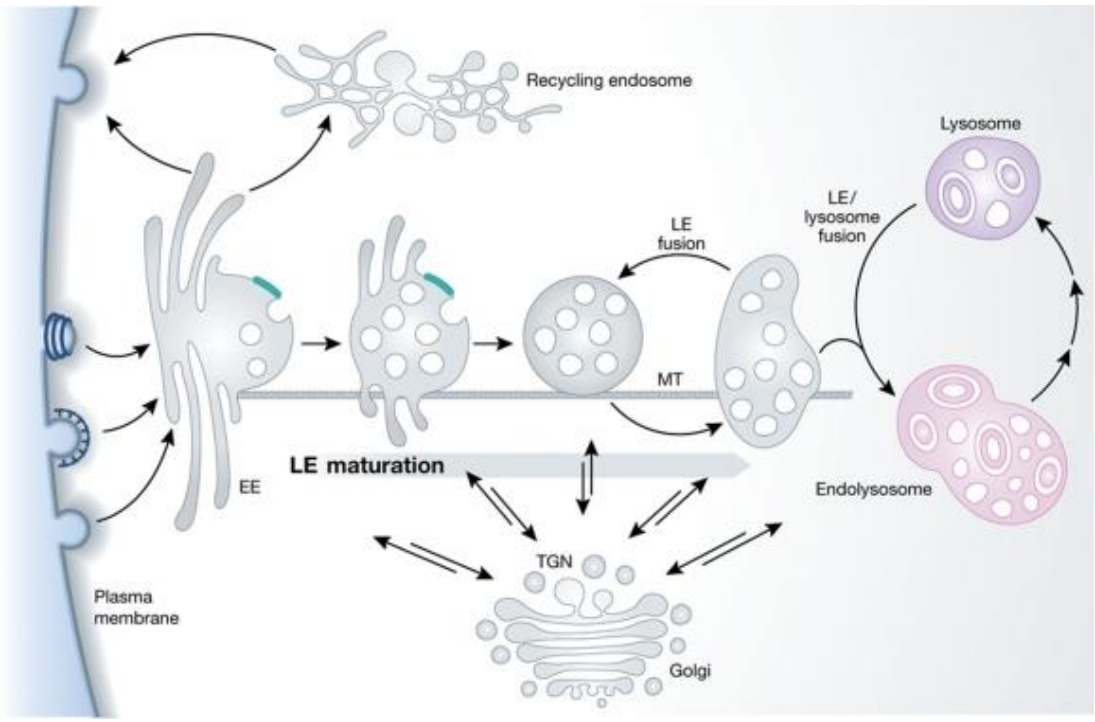

Figure 1: Endosomal system ; Endocytosed PMP is transported to the early endosome (Sommerville and Hartshorne) and sorted either via the recycling endosome back to the PM or via multivesicular bodies to the lysosomes for degradation. EE: early endosome, LE: late endosome, MT: microtubule, TGN: trans Golgi network. (adapted from (Huotari and Helenius, 2011))

2.1.1 Post-Golgi endosomal system

Early endosomes (EE) are recognized as an important sorting station in the mammalian endocytic pathway (recently reviewed by (Scott et al., 2014)). They are the first compartment to receive endocytosed material from the PM as well as proteins destined for secretion from the Golgi (Scott et al., 2014). EE regulate the efficient transport back to the PM, to the trans-Golgi network or to the lysosome for final degradation (Scott et al., 2014). Due to their high surface to volume ratio EE are highly accessible for vesicle fusion and budding off (recently reviewed by (Huotari and Helenius, 2011)). Most of them are small with tubular extrusion and preferentially move close to the PM along microtubules (Huotari and Helenius, 2011). However, EE cannot be seen as stationary compartments as their continuous fusion and separating process gives rise to the next compartments (recently reviewed by (Saftig and Klumperman, 2009)). Membrane sub-domains constantly mature, according to the composition of their cargo, either to recycling endosomes (RE) or late endosomes (LE) by recruitment of distinct proteins (Saftig and

Klumperman, 2009). During maturation from EE to late endosome/multivesicular bodies (LE/MVB) protein composition in the membrane changes as exemplified by the switch from Rab5 to Rab7 and by the elevated incorporation of H^+ ATPases, which is accompanied by a progressive decrease of pH (Saftig and Klumperman, 2009). Acidification during the maturation process plays an important role for the function of the compartment (Huotari and Helenius, 2011). The LE/MVB are characterized by a roundish morphology and the formation of ILVs induced by ESCRT (Endosomal Sorting Complex required for Transport) -machinery (Huotari and Helenius, 2011). The transformation process from LE to endolysosome finally resulting in the lysosome is continuous and therefore the different maturation stages cannot be clearly distinguished (Huotari and Helenius, 2011). Lysosomes represent the terminal degradation compartment of the endocytic pathway, they depend on influx of new component to maintain their intactness, acidity and localization (Huotari and Helenius, 2011). These include soluble hydrolytic enzymes for controlled intracellular digestion of macromolecules (recently reviewed by (Luzio et al., 2007). The proteolytic activity of the enzymes is regulated by proteolytic cleavage in the acidic environment provided by the organelle itself (Luzio et al., 2007). Due to the wide variety of digestive functions the organelle can be found in most cell types.

2.2 Endocytosis: transport from plasma membrane into the cell

Clathrin mediated endocytosis, as the most abundant route for cargo uptake, can be used by all known eukaryotic cells (recently reviewed by (McMahon and Boucrot, 2011)). The formation of clathrin-coated pits at the PM generally represent a potential starting point for clathrin-regulated endocytosis of PMPs (McMahon and Boucrot, 2011). Adaptor and accessory proteins are recruited to the PM and interact with the PMP destined for endocytosis, forming an interaction-interface for the clathrin proteins (McMahon and Boucrot, 2011). The pit starts invagination until the resulting vesicle, including the PMP as cargo, pinches off and finally fuses with the EE (McMahon and Boucrot, 2011).

2.2.1 Lysosomal degradation pathway

Proteins destined for lysosomal degradation are marked by ubiquitination, endocytosed and consequently sorted into EE (recently reviewed by (Williams and Urbe, 2007; Dikic et al., 2009)). Rab5 as an important marker for EEs recruits and interacts with Phosphoinositide-3-kinase (PI-3-kinase), which ultimately induces local lipid Phosphoinositide 3-Phosphate (PI-3P) production (recently reviewed by (Stenmark, 2009)). Inositol phospholipids (Erpapazoglou et al.) are inserted into the membranes via their unpolar tail-structure (fatty acids) (recently reviewed by (Hirsch et al., 2007)). Their inositol sugar head can be phosphorylated at various hydroxyl groups, resulting in different types of Phosphoinositides (PIPs) (Hirsch et al., 2007). The distribution of the PIPs their corresponding kinases and phosphatases vary from organelle to organelle, predominantly also within an organelle defining specialized organelle membrane domain (Hirsch et al., 2007). As PIPs label the membrane–cytosol interface, they regulate organelle identity as well as vesicular trafficking (Hirsch et al., 2007).

Ubiquitin and PI-3P together play a crucial role for protein sorting in the EEs for further lysosomal degradation by advertising a surface for interaction with the endosomal sorting complex required for transport (ESCRT) (recently reviewed by (Williams and Urbe, 2007)). The ESCRT machinery itself regulates the formation of ILVs (intraluminal vesicles) during the maturation from early through LE/MVB and finally to lysosomes (Williams and Urbe, 2007). The formation of ILVs is of utmost importance as only cargos located within the final lysosome, but not integrated in its outer membrane, are degraded properly (recently reviewed by (Saksena et al., 2007)). The covalent addition of ubiquitin as frequent post translational modification (recently reviewed by (Hicke et al., 2005)), is the best characterized signal for cargo proteins to enter the degradative lysosomal pathway (Williams and Urbe, 2007). If the endocytosed cargo is not marked by ubiquitin, as the ubiquitin was removed by a deubiquitinating enzyme, it passes the PI-3P enriched environment of the EEs to the Rab4-containing RE and is finally recycled back to the PM (recently reviewed by (Grant and Donaldson, 2009)).

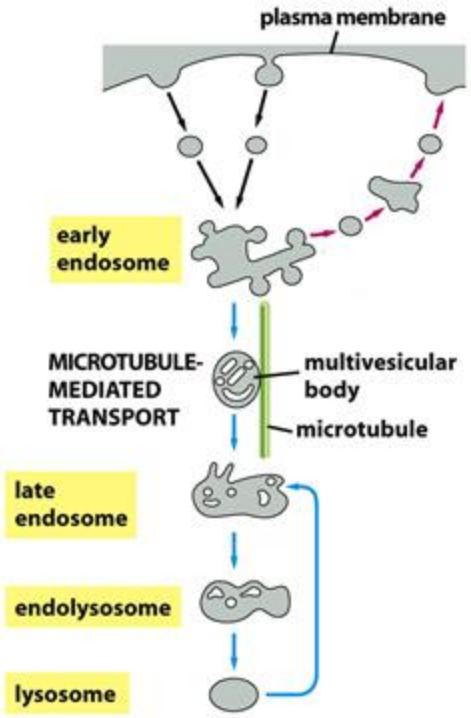

Figure 2: Endocytosis of PM proteins destined for lysosomal degradation and recycling back to the PM from EE ; PMPs are endocytosed at the PM and subsequently transported to the EE as main sorting station. Ubiquitin marked cargo follow the lysosomal degradation pathway via the MVB. Deubiquitinated proteins are recycled back to the PM. (Recently adapted from (Alberts, 2008)).

2.3 ESCRT machinery

The endosomal sorting complex required for transport (ESCRT) machinery is responsible for endosomal sorting of ubiquitinated PMPs into ILVs of LE/MVB, thus regulating protein abundance on the cellular surface (recently reviewed by (Williams and Urbe, 2007)). Generally the highly conserved ESCRT machinery consist of 4 protein complexes, namely ESCRT-0, I, II and III, which bind and interact with the ubiquitinated cargo and other protein domains enriched at the endosomal membrane to mediate the sorting process into the internal vesicles of the LE/MVB (Williams and Urbe, 2007). ESCRT complexes are soluble localized in the cytosol until recruited to the endosomal membrane (Williams and Urbe, 2007). Although cell fractionation studies support this assumption, quantitative ultrastructural studies suggest, that ESCRT-0 and ESCRT-I are predominantly membrane-associated (80%) and preferentially accumulate on tubule-vesicular structures (45%) (Welsch et al., 2006; Williams and Urbe, 2007). This discovery

reflects the extended involvement of the ESCRT machinery in the continuous lysosomal degradation process of endocytosed cargo (Williams and Urbe, 2007).

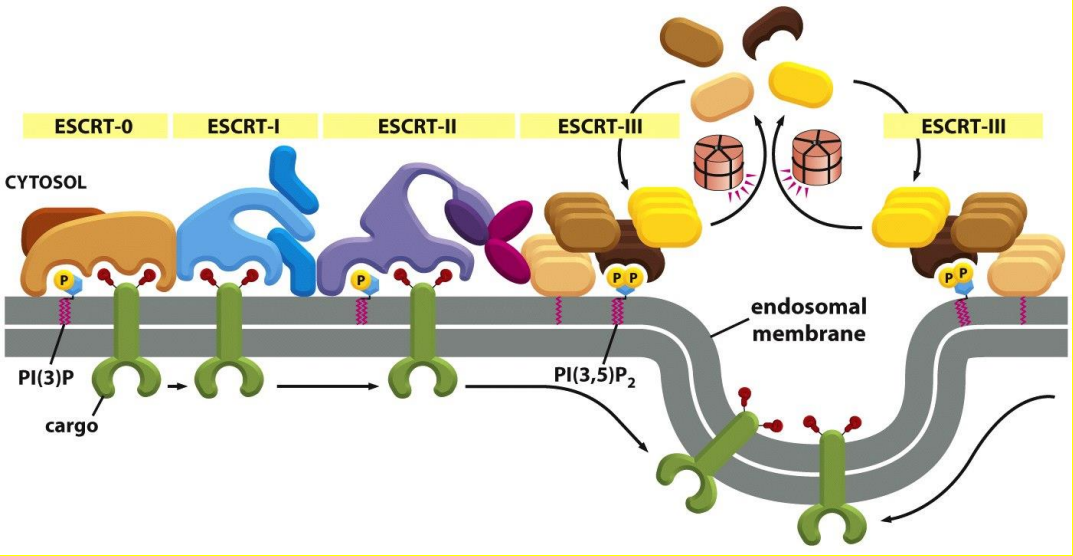

Figure 3: Assembling of the ESCRT machinery ; Cascade-like recruitment of the ESCRT-machinery including ESCRT-0,I,II and III. (adapted from (Alberts, 2008))

The assembling of the ESCRT machinery (Figure 3) starts with the recruitment of ESCRT-0 to the endosomal membrane, where it binds the ubiquitinated cargo (recently reviewed by (Hurley, 2010)). Beside the ubiquitin-marked cargo, ESCRT-0 also interacts with the PI-3P enriched in the endosomal membrane of EE (Hurley, 2010). In addition ESCRT-0 is thought to be responsible for clathrin targeting to the endosomes, as the two subunits (Hrs and STAM) of the mammalian ESCRT-0 bind to clathrin (Williams and Urbe, 2007). Hrs interact with clathrin by a Leu-Ile-Ser-Phe-Asp motif at its C-terminus, but the binding site of STAM to clathrin has not been mapped yet (Williams and Urbe, 2007). Assembly of ESCRT-I complex is further promoted by direct interaction with the ESCRT-0 complex (Hurley, 2010). The main role of ESCRT-I is the recognition of ubiquitinated cargo (Bilodeau et al., 2003; Babst, 2011) and handing it over to ESCRT-II for further direct activation of ESCRT-II downstream functions (Hurley, 2010). Beside interaction with ubiquitinated substrate and PI-3P, ESCRT II also initiates ESCRT-III complex formation (Hurley, 2010). In contrast to all other ESCRT complexes, ESCRT-III does not directly interact with ubiquitin-marked cargo (Hurley, 2010). ESCRT-III is composed of different subunits that are involved in cargo trapping, membrane deformation and ILV abscission (Hurley, 2010).

Finally the Vps4 complex (ATPase) regulates dissociation of the ESCRT-III for further reuse of the ESCRT machinery (Hurley, 2010).

2.3.1 ESCRT-0 complex

The initial sorting process of ubiquitinated cargo destined for lysosomal degradation in EE is accomplished by the ESCRT-0 complex (Williams and Urbe, 2007; Hurley, 2010). In yeast Vps27 (Vacuolar protein sorting-associated protein 27) and Hse1 make up the ESCRT-0 complex, whereas in mammals HRS (hepatocyte growth factor (HGF) regulated Tyr-kinase substrate) function as homologue protein for yeast Vps27 and STAM (signal transducing adaptor molecule) for Hse1 in yeast (Williams and Urbe, 2007; Hurley, 2010). Vps27 and the mammalian homologue Hrs include a FYVE (Fab 1 (yeast orthologue of PIKfyve), YOTB, Vac 1 (vesicle transport protein), and EEA1) domain as an example for membrane lipid-directed targeting mechanism (Williams and Urbe, 2007; Hurley, 2010). The FYVE domain consists of eight conserved cysteins coordinating two Zn^{2+} ions and several other features for interaction with PI-3P (recently reviewed by (Driscoll)). Accordingly this domain within Vps27 and Hrs can target the ESCRT-0 complex to the early endosomal membrane via PI-3P (Williams and Urbe, 2007; Hurley, 2010). Src homology 3 (SH3) domain, present in the Hse1 and STAM proteins, recruit the deubiquitinating enzyme (UBPY) to the ESCRT-0 complex regulating the degradation process by modeling the ubiquitination pattern (Hurley, 2010).

Both ESCRT-0 components share a common N-terminal VHS (Vps27-Hrs-STAM) domain (Williams and Urbe, 2007; Hurley, 2010) thought to be responsible for intracellular trafficking and cargo binding (Williams and Urbe, 2007). Another Ubiquitin interaction domain, so called GAT (GGA and Tom) domain, was discovered by sequence similarity analysis (Hurley, 2010). It lies within the coiled coil region of Vps27/Hse1 and Hrs/STAM and is involved in complex formation and stability (Bilodeau et al., 2003; Mizuno et al., 2003; Prag et al., 2007).

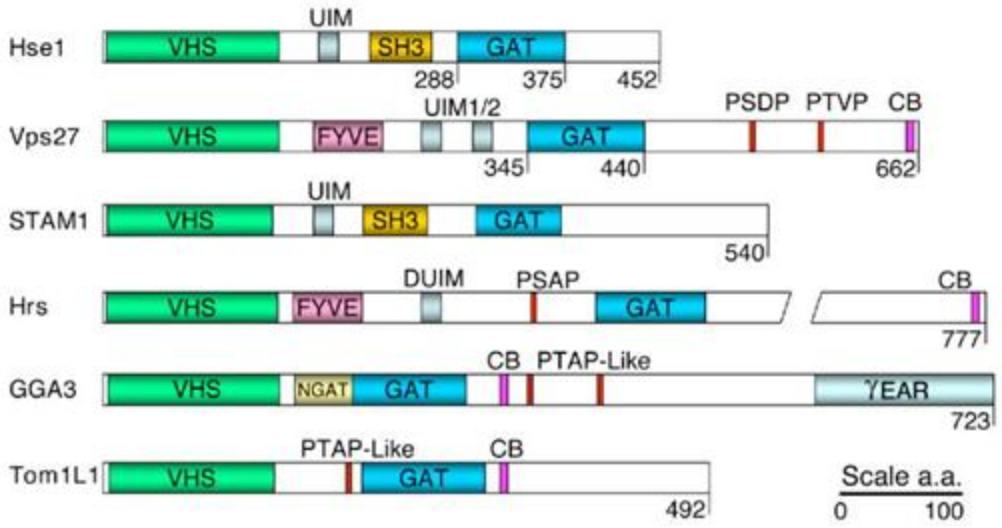

Figure 4 structure of different ESCRT-0 subunits, GGA3 and Tom1L1 ; abbreviations as follows: Vps27 (Vacuolar protein sorting-associated protein 27), HRS (hepatocyte growth factor (HGF) regulated Tyr-kinase substrate), Vps27 and STAM (signal transducing adaptor molecule) VHS (Vps27-Hrs-STAM), GAT (GGA and Tom), FYVE (Fab 1 (yeast orthologue of PIKfyve), YOTB, Vac 1 (vesicle transport protein), and EEA1), SH3 (Src homology 3 domain) (recently adapted from (Prag et al., 2007))

2.4 Ubiquitin and ubiquitin binding domains

Ubiquitin is a 76 amino acid protein with a molecular weight of 8 kDa (recently reviewed by (Dikic et al., 2009)). It is a post-translationally added modification of proteins, which acts as a regulator for different cellular processes, especially for degradation, endocytosis and vesicular trafficking (recently reviewed by (Hurley et al., 2006; Dikic et al., 2009))

Ubiquitination as a widespread inducible and reversible regulatory modification, can influence the interactions, molecular landscape, location and activity of proteins (Hicke et al., 2005; Dikic et al., 2009). Generally, the C-terminus of Ubiquitin is covalently attached to a Lysin residues of the target protein via a three step procedure including Ubiquitin-activating (E1), Ubiquitin conjugating (E2) and Ubiquitin-ligating (E3) enzymes (recently reviewed by (Erpapazoglou et al., 2014)). Proteins can be modified by different ubiquitin signals including monoubiquitination, multiple monoubquitination and polyubiquitination (Dikic et al., 2009; Erpapazoglou et al., 2014), which have a different influence on the protein activity.

Ubiquitin binding proteins contain small (20-150 amino acid long) ubiquitin binding domains (UBDs) for direct interaction with mono and/or poly-ubiquitin chains (Hicke et al., 2005;

Erpapazoglou et al., 2014). Their structural diversity reflect their abundant modes of action within different biological processes (Hicke et al., 2005). However, the largest class of UBDs share a common α-helical structure, like the UBA (ubiquitin associated), UIM (ubiquitin interacting motive), DUIM (double sided UIM), MIU (motive interacting with ubiquitin), CUE (coupling of ubiquitin conjugation to endoplasmatic reticulum degradation), GAT (GGA and TOM) and the octahelical VHS (Vps27/Hrs/STAM) (Hurley et al., 2006) . Nearly all α-helical UBDs interact with ubiquitin via its hydrophobic Isoleucin44 patch (Hurley et al., 2006; Dikic et al., 2009; Erpapazoglou et al., 2014). ESCRT-0 subunits Vps27/Hse1 and Hrs/STAM contain functional UBDs to enrich ubiquitinated cargo at a distinct endosomal membrane sites initiating lysosomal degradation (Dikic et al., 2009).

2.4.1 VHS domain

The octahelical VHS (Vps27-Hrs-STAM) domain (Figure 5B) is a common UBD, which is predominantly present at the N-terminus of proteins involved in vesicular trafficking in eukaryotes (recently reviewed by (Wang et al., 2010)). In mammals the VHS domain is present in 9 proteins: Hrs, STAM1+2, GGA 1+2+3, Tom1, Tom1L1, Tom1L2 (Wang et al., 2010). Due to its super-helical structure it was suggested to provide a common protein-protein interaction surface (Mao et al., 2000; Mizuno et al., 2003). The importance of the VHS domain as UBD was elucidated by *in vitro* assays analyzing the N-terminal part of the STAM protein including UIM and VHS domain (Mizuno et al., 2003). Although analysis of the individual domains revealed similar ubiquitin binding affinities, deletion of the VHS impaired ubiquitin binding activity more severely than deletion of UIM in the mammalian ESCRT-0 subunit STAM (Mizuno et al., 2003). The tandem location of VHS and UIM in Hse1 and STAM might have a synergistic effect in their ubiquitin binding affinity, whereas in Vps27 and Hrs the FYVE domain located in between may disturb (Mizuno et al., 2003). Nevertheless these domains can interact with ubiquitin independently, although it's still not clear whether VHS and UIM bind to different sites of ubiquitin or if they bind different ubiquitin molecules simultaneously (Mizuno et al., 2003).

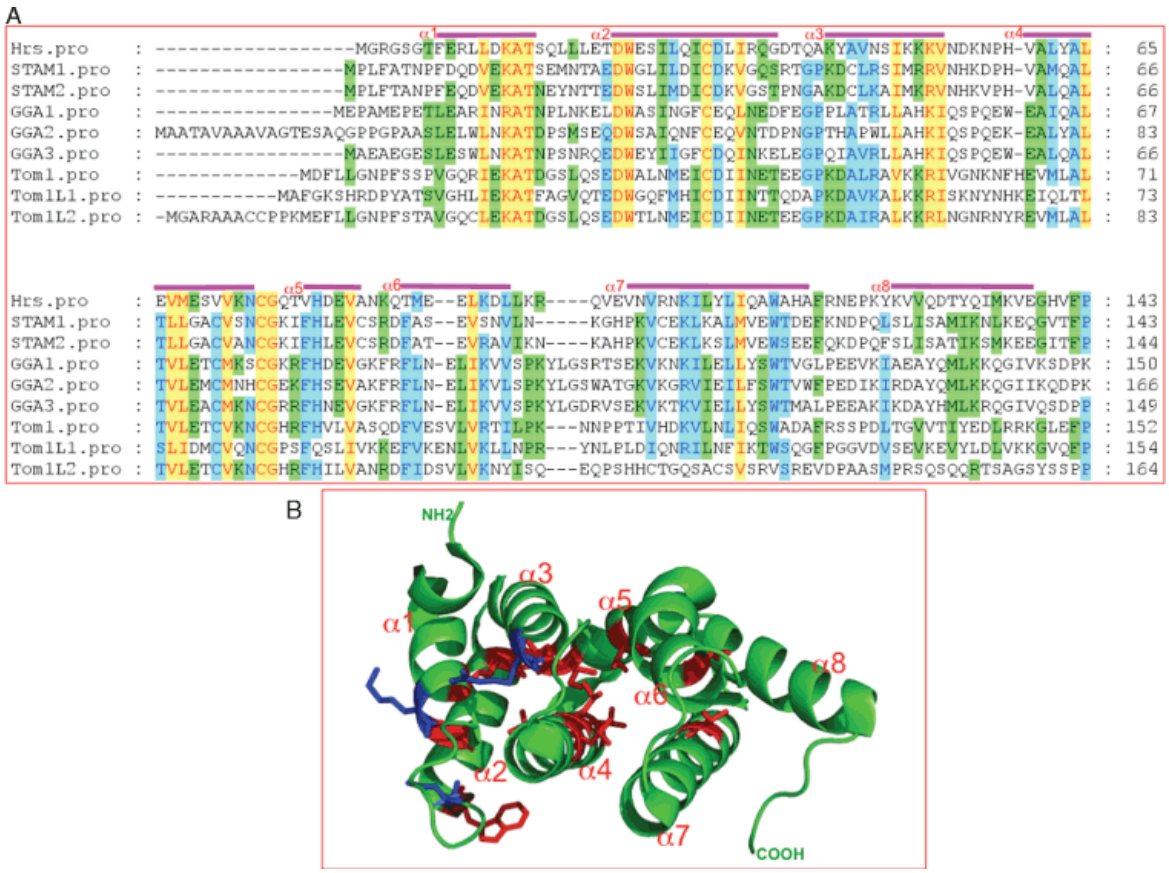

Figure 5: Sequence and structure of the VHS domain ; A) Alignment of amino acid sequence of the VHS domain of nine human VHS domain containing proteins, residues identical or conserved in all proteins are written in red with yellow background, mostly conserved residues are written in blue with blue background and less conserved residues are written in black with green background, **B)** structure of VHS domain of Tom1, some conserved hydrophobic residues are shown in red, some conserved polar or charged residues are marked in blue (recently adapted from (Wang et al., 2010))

The most conserved amino acids liable for ubiquitin binding are located in the α2- and α4-helix of VHS (Wang et al., 2010), oriented towards the surface of the protein to promote ubiquitin interaction (Lange et al., 2011). The binding affinity for VHS to ubiquitin is relatively low, reflecting the fast dissociation rate and the rapid assembly and disassembly of the protein complex for ubiquitinated cargo sorting (Lange et al., 2011).

2.4.2 GAT domain

The GAT (GGA and Tom) domain was initially discovered in GGA (Golgi-localized, gamma-ear containing, ADP-ribosylation factor binding) proteins as a family of monomeric clathrin adaptor proteins regulating vesicular transport between the trans Golgi network (TGN) and the endosomal system (Dell'Angelica et al., 2000; Collins et al., 2003b). The structural organization

of the GGA GAT domain includes two independent subdomains: the C-terminal and the N-terminal GAT domain (Collins et al., 2003b). Whereas the N-terminal hook (171-210 residues) interact with the ARF1-GTP targeting the GGA to the Golgi (recently reviewed by (Bonifacino, 2004)), the C-terminal helical bundle (211-299 residues) is responsible for ubiquitin binding (Bilodeau et al., 2004). Within the C-terminal α3-helix of the GGA GAT domain, one uncharged and two hydrophobic amino acids are well conserved residues involved in ubiquitin binding (Puertollano and Bonifacino, 2004; Shiba et al., 2004) The second ubiquitin interaction region was discovered in the α1-helix including an acidic, hydrophobic and another acidic amino acid pointing to the same surface of the helix more or less well conserved in Tom and GGA proteins (Bilodeau et al., 2004; Prag et al., 2005).

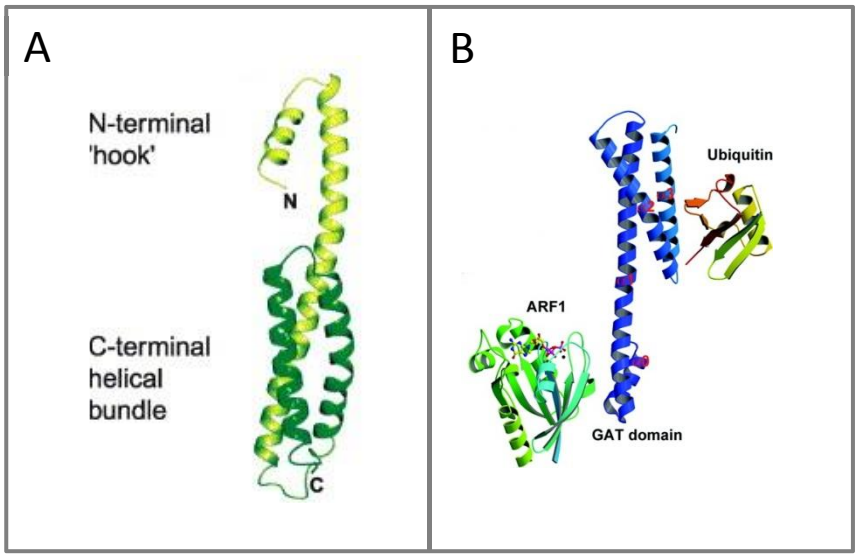

Figure 6: GAT domain of GGA1 ; A) secondary structure of GAT domain of GGA1 including 4α-helices (α 0-3), the green part represent the C terminal part interacting with the ARF1-GTP whereas the yellow part correspond to the N terminal part of the domain responsible for ubiquitin binding, (adapted from (Collins et al., 2003b)) **B)** GGA GAT domain bind to ubiquitin via its C-terminus and ARF1 with its N-terminal part, (adapted from (Shiba et al., 2004))

Two intertwined GAT domains, each consist of 3 α-helices, built up the core complex of Vps27/Hse1 and Hrs/STAM with a barbell-like structure (Prag et al., 2007). One bundle of the barbell is composed of α1 and α3-N-terminus of Hse1 and α3-C-terminus of Vps27, whereas the other one is patterned mirror-inverted (Prag et al., 2007). The central part of each α3-helix together form the two-stranded coiled coil of the barbell (Prag et al., 2007). The GAT domains

therefore are essential domains in assembling the multivalent ubiquitin binding machinery of the ESCRT-0 (Prag et al., 2007).

2.5 Plant endosomal compartments

As plants belong to the group of sessile organisms, quick and efficient communication, as well as consequent response mechanisms according to changing environmental conditions are of utmost importance. Cells regulate PMP levels by transcriptional/translational control mechanisms, but also by vesicular trafficking from and to the cellular surface (recently reviewed by (Geldner, 2004)).

In contrast to mammals, plant endosomal compartments are still not as well defined. Furthermore, plants have unique features in the organization of their endosomal system (Reyes et al., 2011b). The EEs are defined as the first compartment that receive cargo after endocytosis from the PM (Geldner, 2004). By establishing a TGN marker, Dettmer et al identified the TGN as an EE-like compartment (Dettmer et al., 2006; Uemura and Nakano, 2013). Further studies confirmed this hypothesis by showing TGN/EE to move independently of the Golgi and only transiently associated with the Golgi stack (Viotti et al., 2010). The EE coincide with the TGN and are therefore considered as the crossing point between the biosynthetic and the endocytic pathway (Reyes et al., 2011a). The EE/TGN are a system of interconnected tubular membranes with clathrin coated regions (recently reviewed by (Foresti and Denecke, 2008)). Their function as sorting hub indicate a similar role to that of the mammalian EE, which sort proteins destined for recycling to the PM or Golgi and cargo destined for degradation through the MVB to the lytic vacuole (recently reviewed by (Foresti and Denecke, 2008)). Two endosomal organelles were defined and characterized in plants: the TGN/EE and finally the late endosomes or MVB, also known as prevacuolar compartments (Reyes et al., 2011a).

In contrast to mammals, plant and fungal cells contain a lysosomal related compartment called vacuoles covering different functions (recently reviewed by (Zhang et al., 2014)). They are responsible for storage of nutrients and waste products as well as for degradation of macromolecules and maintenance of the cell homeostasis (Zhang et al., 2014). Due to their

extensive functions, different types of vacuoles are generally present in plant and yeast cells (recently reviewed by (Xiang et al., 2013)). Vacuoles are highly dynamic and vary their size due to changing cell types and growth conditions (Zhang et al., 2014). Analogous to mammalian lysosomes degradative vacuoles are acidic and contain hydrolytic enzymes (Xiang et al., 2013). Due to their multi-functionality plant vacuoles cannot be seen simply as lysosome-substitute (Xiang et al., 2013).

2.6 From the plasma membrane to the vacuole

The TGN/EE in plants share some common structural features with the mammalian EE (Scheuring et al., 2011), suggesting similar functional properties as sorting hub for cargo molecules. Proteins destined for degradation are generally marked by ubiquitination and subsequently transported to the vacuole (Reyes et al., 2011b).

In plants, the ESCRT machinery is also involved in this sorting mechanism by associating with the endosomal membrane, recognizing ubiquitinated cargo and further formation of ILVs (Winter and Hauser, 2006a; Reyes et al., 2011b). The presence of homologs for this generally in eukaryotes well conserved ESCRT machinery was verified in plants (Shen et al., 2003; Spitzer et al., 2006; Winter and Hauser, 2006b; Leung et al., 2008) with the exception of ESCRT-0, yet their exact location remains unclear (Scheuring et al., 2011). In mammalian cells proteins are sorted mainly via clathrin coated vesicles (McMahon and Boucrot, 2011). In contrast molecule trafficking from TGN/EE to MVB/LE in plants is not restricted to this transport mechanism (Scheuring et al., 2011). Inhibition of clathrin mediated vesicle transport do not prohibit arrival of cargo in the MVB/LE and subsequently in the vacuole, suggesting a maturation of MVB/LE from the TGN/EE (Scheuring et al., 2011). In accordance to the assumption of maturation-mechanism, the localization of ESCRT complexes already in the TGN/EE can be expected (Scheuring et al., 2011). The finding of ILVs within the TGN/EE confirm the suggestion that ESCRT starts assembling there (Scheuring et al., 2011). It's still not clear whether the ESCRT-I assembles at the Golgi or the TGN/EE, as long as the localization of an ESCRT-0 ortholog *in planta* is not verified.

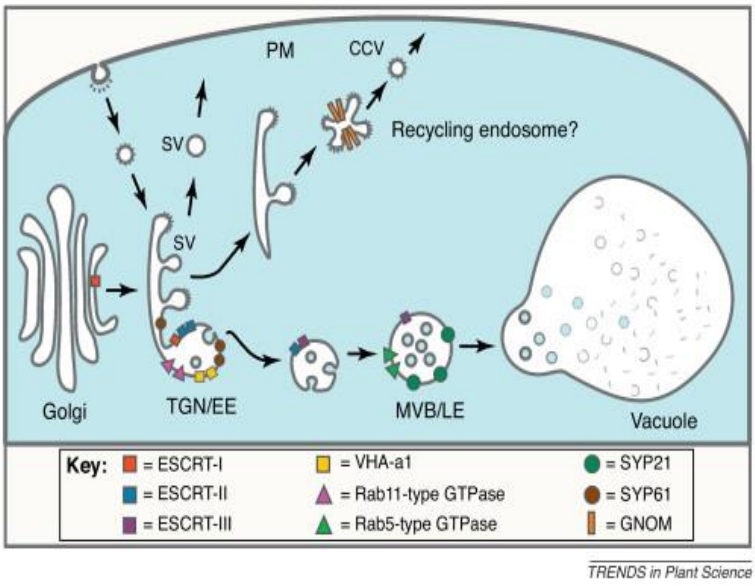

Figure 7 ESCRT assembling in *planta* : TGN/EE: trans Golgi network/early endosome, MVB/LE: multivesicular bodies/late endosome.(adapted from (Scheuring et al., 2011))

2.6.1 TOL proteins as ESCRT-0 orthologs

Although arrangement and components of the four ESCRT complexes (ESCRT 0-III) are well conserved in all major eukaryotic taxa, clear orthologs for ESCRT-0 in plants are absent (Winter and Hauser, 2006b; Williams and Urbe, 2007; Shahriari et al., 2011). Tom (Target of Myb) proteins found in mammals can interact with ubiquitinated cargo, bind ESCRT-I and therefor represent an alternative to ESCRT-0 (Winter and Hauser, 2006b; Wang et al., 2010; Herman et al., 2011; Richardson et al., 2011). The lack of ESCRT-0 orthologs in plants might indicate a distinct cargo selection in plants (Richardson and Mullen, 2011).

The discovery of a family of nine so called TOL (Tom1-like) proteins as potential substitutes for ESCRT-0 in *Arabidopsis thaliana* revealed a new perspective in the functionality of ubiquitinated protein sorting in higher plants (Korbei et al., 2013; Moulinier-Anzola et al., 2014).

Our experiments identify TOL proteins as gatekeepers at the PM and moreover provide essential insights into the evolution of the eukaryotic sorting machinery, supporting a model, in which TOL proteins represent ancesteral cargo recognition determinants (Korbei et al., 2013). Thus, life without ESCRT-0 could be substituted by TOL proteins, which are seemingly adequate to organize the numerous responses that characterize the development of higher plants (Korbei

et al., 2013). TOL proteins can be seen as counterparts to the human and yeast ESCRT-0 substituent (Korbei et al., 2013). They share common protein domains, in particular the VHS and GAT domain and putative clathrin-binding motifs, for sorting and targeting ubiquitinated cargo proteins (Korbei et al., 2013).

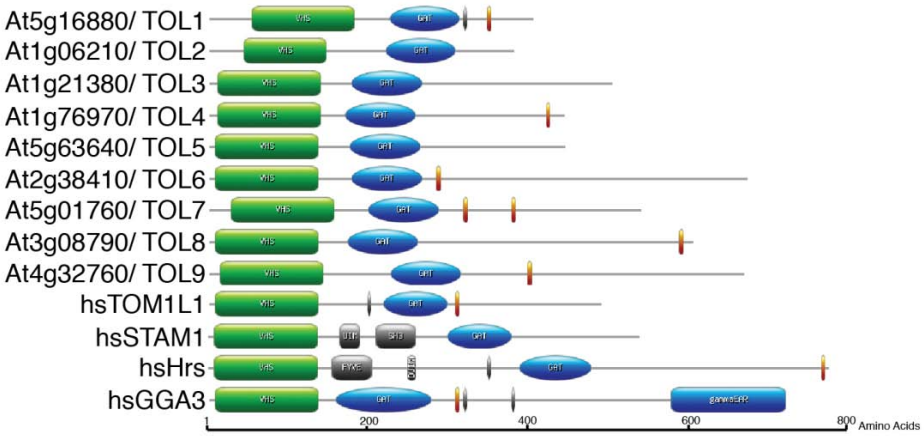

Figure 8: In silico analysis of the domain organization of VHS-GAT proteins in *Arabidopsis thaliana* and *Homo sapiens* ; (http://prosite.expasy.org/; adapted from [S1]): Domain name abbreviations are as follows: VHS (Vps27/Hrs/STAM domain; green); GAT (GGA and TOM domain, blue); FYVE (Fab1/YOTP/Vac1/EEA1 domain), UIM (ubiquitin-interacting motif), DUIM (double UIM) and SH3 (Src homology-3), (adapted from (Korbei et al., 2013))

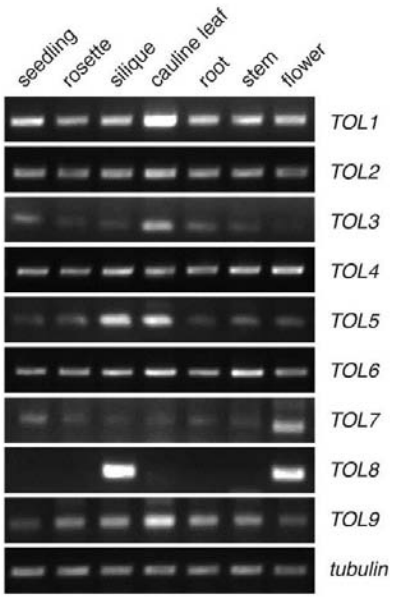

Figure 9: Expression analysis of TOLs: Expression of 9 *TOLs* in different tissues ; RT-PCR performed on cDNA, derived from adult plants for the siliques, flowers, cauline leaves, and stems, from plants 13 days after germination (DAG) for the rosette leaves and roots or 5 DAG total seedlings. A *TOL*-specific fragment is detectable in most tissues tested. *Tubulin* was used as an internal standard, (adapted from (Moulinier-Anzola et al., 2014))

A ubiquitous expression pattern was shown for all TOL genes *in planta* (Figure 9) including adult organs, roots, stem and leaves, with the exception of TOL8, which was exclusively found in siliques and flowers of adult plants (Moulinier-Anzola et al., 2014).

The wide distribution of most TOL proteins *in planta* with concurrent limited location of few TOLs indicate their extensive role in different steps of endosomal protein sorting and could potentially be indicative of redundancies within the gene family (Moulinier-Anzola et al., 2014). Korbei et al identified T-DNA insertion mutants of *Arabidopsis thaliana* for all TOL loci, which did not express full length TOL transcripts (Korbei et al., 2013). The resulting homozygous single T-DNA plant mutant lines show no obvious phenotype, however higher-order mutant combinations, especially *tol2-1/tol2-1 tol3-1/tol3-1 tol5-1/tol5-1 tol6-1/tol6-1 tol9A-1/tol9A-1* (*tolQ*), show pronounced growth defects (Korbei et al., 2013). As several of these pleiotrophic defects suggest a misregulation of the plant hormone auxin, the vacuolar degradation of PIN2, an auxin influx carrier, was assessed in more detail (Korbei et al., 2013). It was shown that the ubiquitin dependent downregulation of PIN2 was defective in *tolQ* plants This was not only applied to PIN2, but also to other known PMPs, known to be down regulated by degradation in the vacuole upon ubiquitination (Korbei et al., 2013) . Thus the TOLs can be seen as potential gatekeepers for PMPs on their route to the vacuole for degradation (Korbei et al., 2013; Sauer and Friml, 2014).

2.7 TOL6 protein

As TOL6 loss of function in *tolQ* contributes to developmental defects in *Arabidopsis thaliana*, we focused on TOL6 as a TOL representative for further analysis (Korbei et al., 2013). *In vitro* ubiquitin binding activity of TOL6 (Figure 10 A) contributes to the hypothesis, that TOL proteins act as orthologs for ESCRT-0 *in planta,* targeting ubiquitinated endocytosed PMPs to the vacuoles/lysosomes (Korbei et al., 2013).

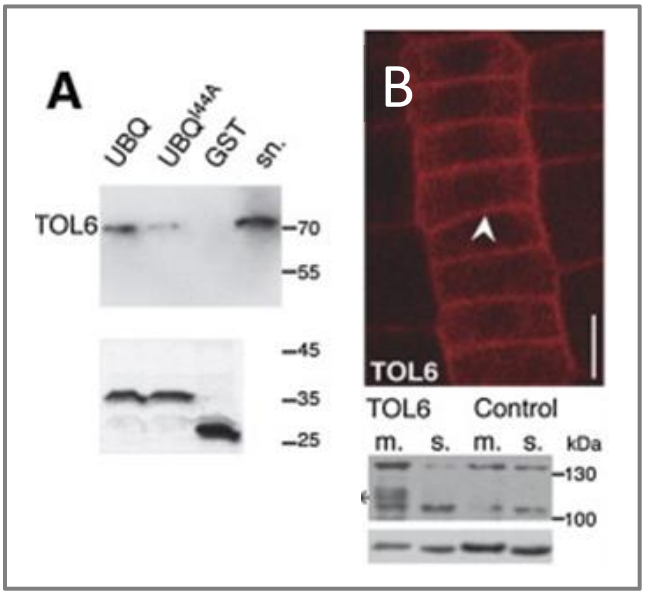

Figure 10: Ubiquitin binding activity and localization of TOL6 proteins : A) TOL6:His (75kDa) coprecipitated with GST:ubq (34,5kDa) , but not with GST:ubq ^{I44A} or GST (26kDa) , probed with anti-His. Bottom panel show comparable amounts of proteins used for the pull down assay stained with coomassie. **B**) CLSM analysis of *TOL6p*::TOL6:mcherry in *tol6-1* root meristem cells (6DAG). Bottom: membrane (m.) and soluble (s.) protein extracts from *tol6*-1 TOL6p::TOL6:mcherry and Col-0 probed with anti-mcherry. Tubulin was used to visualize protein loading. (adapted from (Korbei et al., 2013))

In Figure 10 B, the localization of TOL6 in *tol6-1* mutant *Arabidopsis thaliana* to the cellular periphery at the PM is visualized by CLSM (Confocal Laser Scanning Microscopy). Subsequent analysis of TOL6 proteins extracted from plant tissue, fractionated into a cytosolic soluble (s.) and a membrane associated (m.) fraction, indicate association of TOL6 protein with the PM (Korbei et al., 2013).

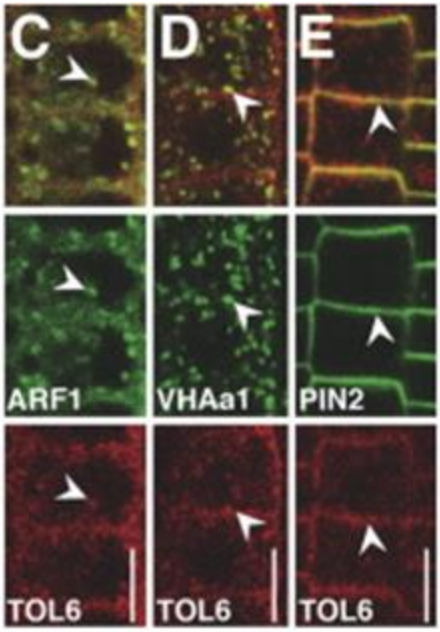

Figure 11: Localization of TOL6: TOL6p::TOL6:mcherry in *tol6-1* root meristem cells at 6 DAG with different markers : C) ARF1p::ARF1:GFP (green) **D)** VHa1p::VHA1:GFP (green) **E)** PM marker PIN2p::PIN2:GFP (green) (adapted from(Korbei et al., 2013))

TOL6 co-localizes with the TGN/EE marker ARF1 and VHAa1 as well as with the PM localized PIN2 (Figure 11). These data taken together indicate early assembling of the potential ESCRT machinery in plants at the TGN/EE (Scheuring et al., 2011) and their involvement in early cargo recognition and sorting potentially already at the PM (Korbei et al., 2013).

3. Aim of this work

The ESCRT-0 complex, as key regulator of PMP abundance in mammals, is responsible for targeting and sorting of ubiquitinated cargo to the lysosomes for final degradation. Accordingly the discovery of ESCRT-0 orthologs, the TOL proteins, in *Arabidopsis thaliana* revealed a new perspective for endosomal trafficking of proteins destined for degradation in higher plants. TOL proteins were shown to interact with ubiquitinated cargo and share common structural ubiquitin binding domains (UBDs) with the human and yeast orthologs.

The aim of this work is to examine the functionality of the UBDs and to assess their importance in cellular processes of cargo sorting. For this purpose I mutagenized the two reported conserved UBDs of TOL6, as a representative of the TOL family. The amino acids mutagenized were well conserved and reported as being relevant for ubiquitin binding in the mammalian and yeast system. With these mutagenized constructs, mutagenized in either the first or the second or both UBDs, I performed *in vitro* binding studies to test for their ability to bind ubiquitin. With these results I subsequently constructed mutagenized translational reporter constructs for *in planta* transformation. Analysis of the transformed plant lines will allow assessment of the *in vivo* importance of the UBDs for endosomal trafficking in higher plants.

The characterization of the TOL UBDs will contribute to understanding how TOL proteins interact with ubiquitin-marked PMP and how they contribute to their subsequent sorting for their final degradation in the plant vacuole.

4. Materials and Methods

4.1 Chemicals and enzymes

Used chemicals for the production of solutions, buffers and media were purchased, if nit indicated otherwise, from the following companies: Roth, Fluka, Merck, Aplichem and Sigma. Enzymes were purchased from Roche, Invitrogen, MBI Fermentas and New England Biolabs.

4.2 Bacterial strains

4.2.1 *Escherichia coli* strains

Strain	Genotype	Reference
DH10B	F⁻ *mcr*A Δ(*mrr-hsd*RMS-*mcr*BC) Φ80d*lac*ZΔM15 Δ*lac*X74 *end*A1 *rec*A1 *deo*R Δ(*ara*, *leu*)7697 *ara*D139 *gal*U *gal*K *nup*G *rps*L λ-	Grant *et al.*, 1990
BL21(DE3)	F⁻ *omp*T *gal [dcm] [lon] hsdS*$_B$ (r_B –m_B -; an *E.coli* strain) with DE3, a λ prophage carrying the T7 RNA polymerase gene	Studier *et al.*, 1990

4.2.2 *Agrobacterium tumefaciens* strains

Strain	Reference
GV3101/pMP90 (RifR/ GentR)	Koncz and Schell, 1986

4.3 Antibodies

Epitope	Type	Dilution	Producer, catalog number or Reference
His epitope	Mouse monoclonal	1:2000	Novagene
HRP α mouse	Goat polyclonal	1:10000	Dianova 115-035-164

4.4 *Arabidopsis thaliana* mutants and reporter lines

Arabidopsis thaliana wild type ecotype Columbia (Col-O) and following *Arabidopsis* mutants and reporter lines were used in this work. Col0, *tol6-1* and *tolQ(2/3/5/6/9A)* were obtained from Barbara Korbei.

Mutant/Reporter	Background	Drug Resistance (plant, E.coli)
stol6	Col0	Gent, Spec
stol6	*tol6-1*	Gent, Spec
stol6	*tolQ(2/3/5/6/9A)*	Gent, Spec
Mutated *stol6* ^{mVHS}	Col0	Gent, Spec
Mutated *stol6* ^{mVHS}	*tol6-1*	Gent, Spec
Mutated *stol6* ^{mVHS}	*tolQ(2/3/5/6/9A)*	Gent, Spec
Mutated *stol6* ^{mGAT}	Col0	Gent, Spec
Mutated *stol6* ^{mGAT}	*tol6-1*	Gent, Spec
Mutated *stol6* ^{mGAT}	*tolQ(2/3/5/6/9A)*	Gent, Spec
Mutated *stol6* ^{mTOTAL}	Col0	Gent, Spec
Mutated *stol6* ^{mTOTAL}	*tol6-1*	Gent, Spec
Mutated *stol6* ^{mTOTAL}	*tolQ(2/3/5/6/9A)*	Gent, Spec

4.5 Oligonucleotides

Synthetic oligonucleotides were purchased from MWG-Biotech AG. Lyophilized oligonucleotides were dissolved in dH_2O to a final stock concentration of 100 µM and stored at -20°C. Following abbreviations are used in the table below Mut:Mutagenesis, Amp:Amplification, Gen:Genotyping

Primer	Internal Number	Purpose	Orientation	5`-3` Sequence
TOL6 N73A f	1995	Mut	forward	GAG ACG TTG GTA AAG GCC TGT GGA G
TOL6 N73A r	1996	Mut	reverse	C TCC ACA GGC CTT TAC CAA CGT CTC
TOL6 AAA1f	1997	Mut	forward	GG GAT GTG ATG GCT GCC GCG GGC GAC ATG
TOL6 AAA1R	1998	Mut	reverse	GAT GTC GCC CGC GGC AGC CAT CAC ATC CC
TOL6 AAA2f	1999	Mut	forward	CTC TTG GGC GCC GCG GCA CAA GCT GTG G
TOL6 AAA2r	2000	Mut	reverse	C CAC AGC TTG TGC CGC GGC GCC CAA GAG
TOL6 W25Af	1841	Mut	forward	GTTAGGTCCTGATGCGACTACGAATA TGGAAATCTGC
TOL6 W25Ar	1844	Mut	reverse	GCAGATTTCCATATTCGTAGTCGCATC AGGACCTAAC
LB1.3	1953	Gen		ATTTTGCCGATTTCGGAAC
TOL3u (TOMl152u)	1241	Gen	forward	GCTCAGGCAACTGCATCAG
TOL3d (TOMl152u)	1242	Gen	reverse	CGGTATTGGAGTGGGAGCTG
NotImcherryu	1465	Mut	forward	GCGGCCGCATGGTGAGCAAGGGCGA

				GGAG
NotImcherryd	1466	Mut	reverse	GCGGCCGCTTACTTGTACAGCTCGTCC ATG
TOL6q-f1	2005		forward	ACCAGTGAGTCATCCACCGT
TOL6q-r1	2006		reverse	ACCTCAGTTGCCATTGCTTCA
TOL6f (TOMlE11u)	1377	Gen	forward	GTGGATATTTTCCCTCTGGACC
TOL6r (TOMlE11d)	1378	Gen	reverse	GCGACGGTGGCTGTTGATAAAG
TOL6-NotISalIr	1850		reverse	GGG GGT CGA CGC GGC CGC AAA TCA TTT TCC TTC CTC C
TOL6-SalIu	1594	Amp	forward	GGGGGTCGACATGGCGTCGTCTTCAG CTTC
TOL6-SalId	1595	Amp	reverse	GGGGGTCGACGTAAATCATTTTCCTTC CTCC

4.6 Plasmids/vectors

4.6.1 pTZ57R/T

The ready-to-use T/A pTZ57R/T plasmid contains 3'-ddT overhangs at both ends of the cloning site to ensure efficient cloning of DNA sequences with 3'-dA overhangs into the vector, whilst concurrently blocking plasmid recirculation. The pTZ57R/T vector was used for general cloning procedures due to its high content of different restriction sites within the multiple cloning site in contrast to the overall small size of the vector (Provided by Thermo Fisher Scientific).

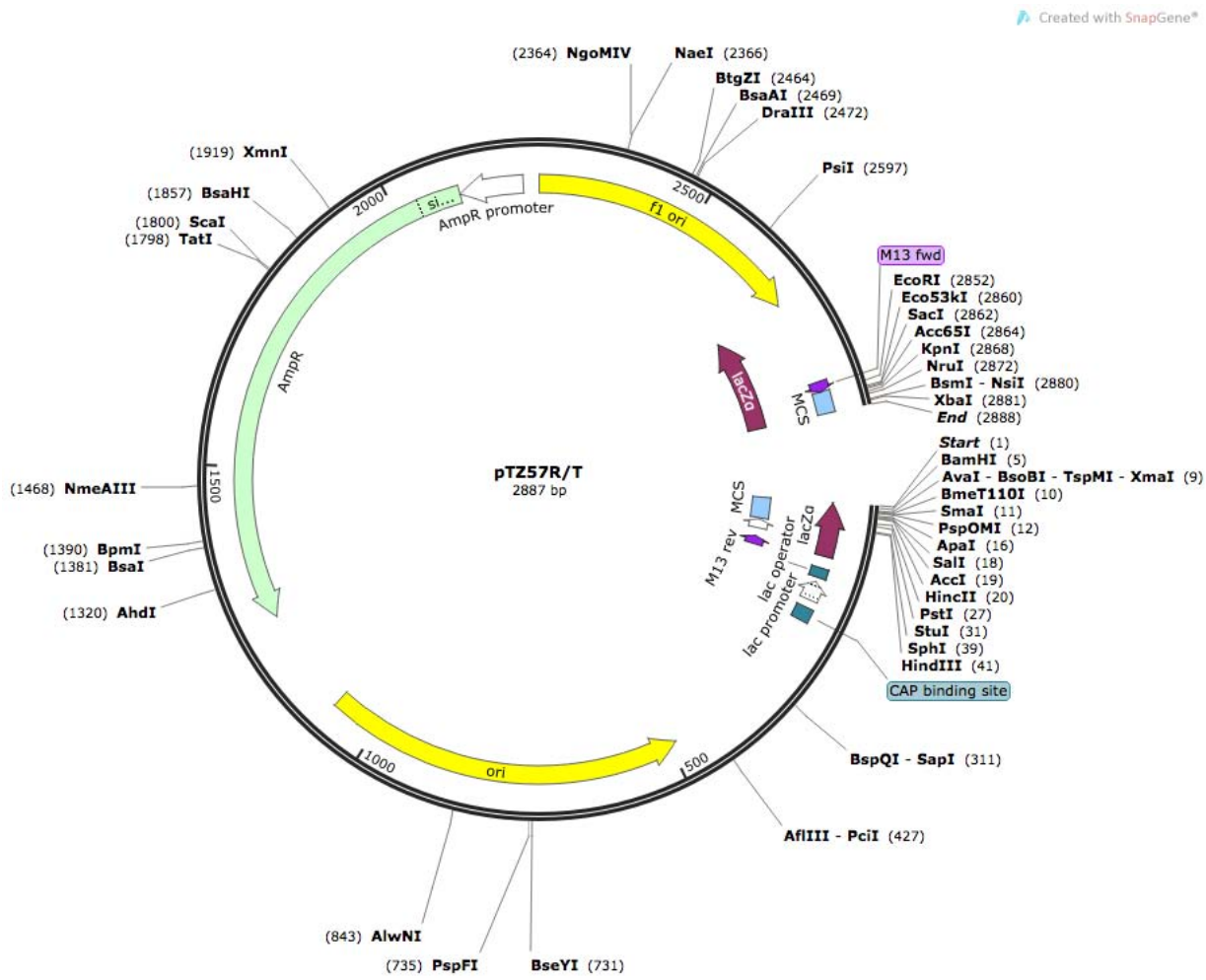

Figure 12: pTZ56R/T plasmid is 2887 bp in size carrying one antibiotic resistance gene for ampicillin, which was used for selection of transformed bacteria. In this case SalI was used for further cloning strategies. For insert sequencing M24f and M24r can be used. source: www.snapgene.com

4.6.2 pET24a

For fast and high quality protein expression in bacteria, the pET24a vector was used as expression vector in BL21 (DE3). Target genes are cloned into the pET24a plasmids under control of strong bacteriophage T7 transcription. Expression is induced by the addition of IPTG to the bacterial culture, since in the host bacteria the T7 RNA polymerase gene is under *lacUV5* control. T7 RNA polymerase is so selective and active that, when fully induced, almost all of the cell's resources are converted to target gene expression.

The multiple cloning site is flanked by the T7 promoter and a 6x His-tag, resulting in expression of fusion proteins with C-terminal 6x His-tag, which was be used for further (Antibody based) detection procedures.

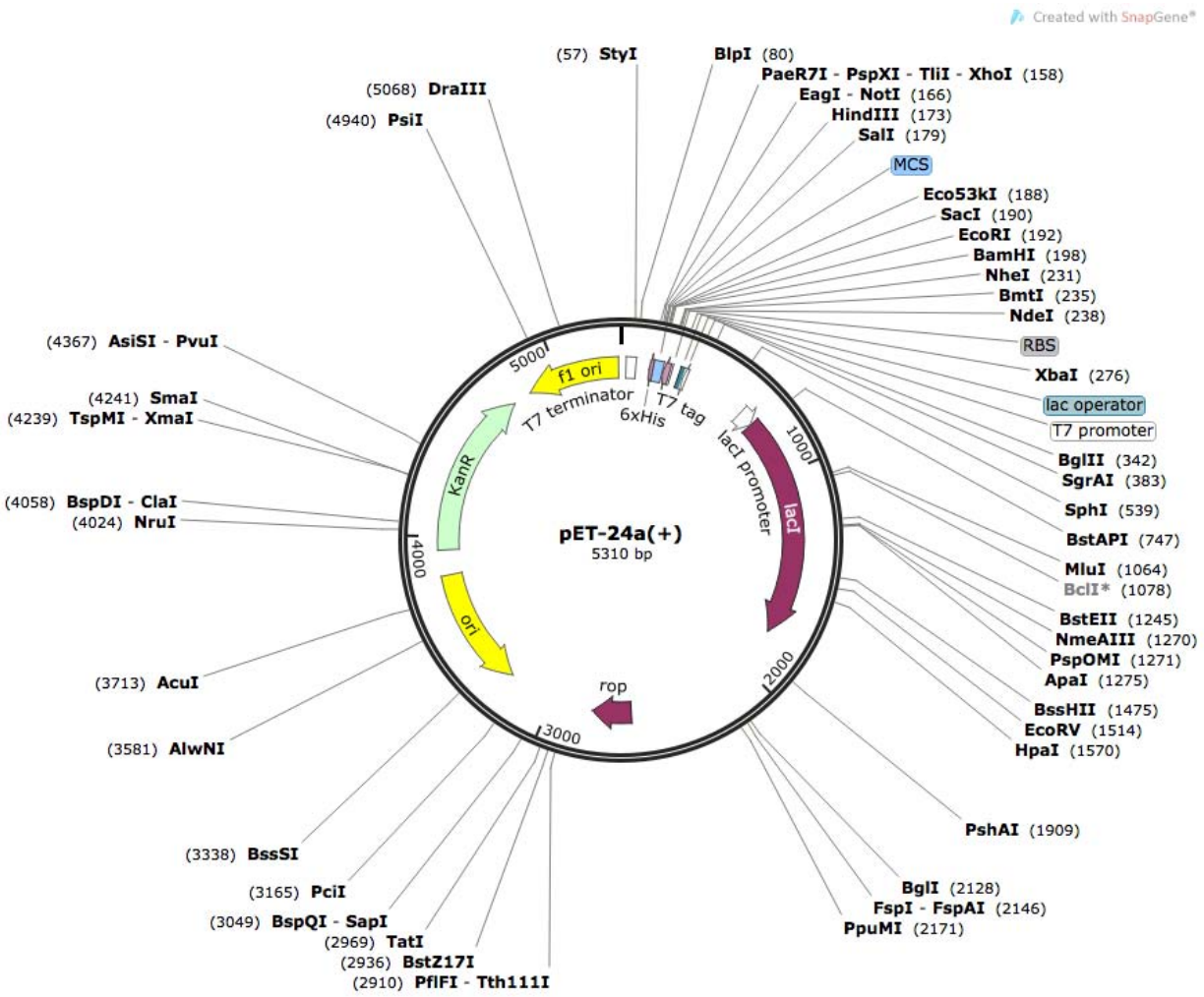

Figure 13: pET24a vector is 5310 bp in size and capable of Kanamycin resistance gene used for selection in bacteria. 6x His taq can be used for final purification or detection of the desired protein. T7-expression system saves high expression level with concurrent lower plasmid copy number. source: www.snapgene.com

4.6.3 pPZP221

To transfer the gene of interest into *Arabidopsis thaliana,* the floral dip method (Clough and Bent, 1998) (see 4.9.5) for transformation was performed using the pPZP221 plasmid containing the desired gene. For endogenous TOL6 protein expression *in planta,* a TOL6 specific promoter was inserted.

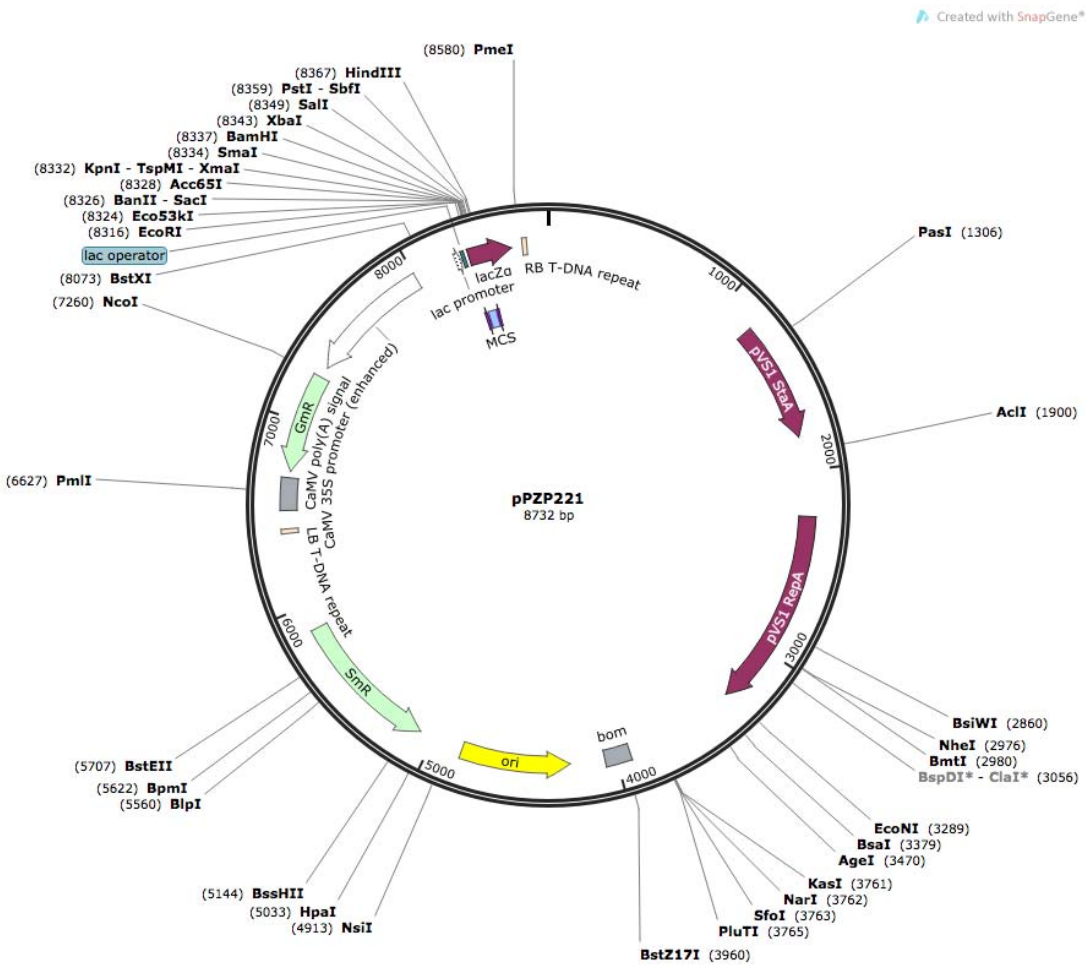

Figure 14: pPZP221 vector with 8732 bp in size including 2 antibiotic resistance genes. Spectinomycin and Gentamycin were used for *Agrobacterium tumefaciens* selection, Gentamycin alone was used for selection of transformed plants. The construct was cloned into the plasmid via SalI. source: www.snapgene.com

4.7 Molecular biological methods

4.7.1 Plasmid DNA Isolation with kits

Column-based kits provided by Fermentas were used to obtain high quality plasmid DNA for further cloning strategies. Isolation procedure was performed according to the supplier`s protocol. To test the quality and the amount of DNA agarose gel electrophoreses and spectrophotometry was used.

4.7.2 Mini-Preparation of *E.Coli* plasmid DNA by the "boiling method"

A single colony of *E.Coli* was inoculated in 5 mL LB medium containing the corresponding selection antibiotic. The culture was incubated overnight on a rotary plate (180 rpm) at 37°C. 1.5 mL of the overnight culture was centrifuged at 13000 rpm for 2 minutes. The supernatant was removed by pipetting and the remaining pellet was resuspended in 100 µL STET buffer. After the addition of freshly made lysozyme solution the sample was vortexed and incubated at 100°C for 2 minutes to inactivate the lysozyme. Afterwards, the sample was centrifuged for 30 minutes at 13000 rpm and the pellet, including cellular protein debris, was removed with a toothpick. The supernatant was mixed by inversion with 105 µL ice-cold isopropanol (stored at -20°C) and further centrifuged for 10 minutes at 13000 rpm and 4°C to precipitate the DNA. The supernatant was removed and the remaining pellet washed with 400 µL ice-cold 70% Ethanol and centrifugation for 5 minutes at 13000 rpm and 4°C The pellet was air dried and dissolved in 35 µL dH_2O and 1 µL RNase (200 µg RNase/mL) by gently mixing for 15 minutes at 37°C.

STET buffer: 8 g sucrose (8% w/v), 500 µL Triton-X (0.05% v/v), 5 mL 1 M Tris/HCl pH 8.0 (50 mM), 10 mL 0.5 M EDTA (50 mM), dH_2O to 100 mL, filter sterilized and stored at room temperature.

1 M Tris/HCl pH 8.0: 60.6 g Tris (2-amino-2-hydroxymethyl-1,3-propanediol) dissolved in 480 ML dH_2O and brought to the pH 8.0 with concentrated HCl, dH_2O to 500 mL, autoclaved and stored at room temperature.

Lysozyme solution: 5 mg lysozyme dissolved in 500 µL dH_2O

RNAase A: 100 mg RNAase in 10 mL dH_2O, heat at 95°C for 10 minutes and cool down slowly. 1 mL aliquots are stored at -20°C

4.7.3 Spectrophotometric quantification of DNA using Nano drop

Spectrophotometric quantification was performed to determine the concentration of the DNA in a solution. Based on the Beer-Lambert law an OD of 1 (optical density) correspond to 50 ng/µL for dsDNA and 33 ng/µL for ssDNA. For optimal measurement the OD should range between 0.1 and 1.0. The $A_{260/280}$ ratio estimates the purity of the DNA sample. According to the

fact, that aromatic amino acids have their absorption maximum at 280nm, the $A_{260/280}$ ratio ≥ 1.8 result in a low protein contamination and the $A_{260/280}$ ratio ≤ 1.8 in a high protein contamination level of the DNA. Concentration of the samples was calculated with the following equations.

A_{260} * dilution factor * 50 = ng/µL ds DNA

A_{260} * dilution factor * 33 = ng/µL ss DNA

4.7.4 Plant genomic DNA isolation with the CTAB method

To get PCR-quality plant genomic DNA (gDNA) in a short time, 1-2 rosette leaves of a 2-3 weeks old seedling were harvested in a 1.5 mL microtube and immediately frozen in liquid nitrogen. Frozen plant material was homogenized to a fine powder by using a plastic pestle (precooled in liquid nitrogen) driven by a drilling machine at maximal speed for some seconds and frozen again in liquid nitrogen. Afterwards 200 µL 2xCTAB buffer were added to the sample, mixed and incubated at 65°C for 5 minutes, shaking gently. After addition of 200 µL Chloroform, the sample was vortexed and spun down for 5 minutes at 13000 rpm, and room temperature (RT). The aqueous upper phase was transferred into a new tube, avoiding transfer of the interface. The DNA in the aqueous phase in the new tube was precipitated by using 2.5 volumes of ethanol absolute, incubating for at least 20 minutes at -20°C and then centrifuge at 13000 rpm for 15 minutes at 4°C. The supernatant was removed ant the pellet washed with 700 µL ice-cold 70% Ethanol (stored at -20°C) by centrifuging the sample for 5 minutes at 13000 rpm and 4°C. After removing the supernatant the pellet was air dried and dissolved in 30 µL dH_2O for 15 minutes at 37°C, shaking gently. 1-2 µL were used for further PCR for genotyping.

2xCTAB buffer: 2 g CTAB (Cetyl trimethylammonium bromide, s% w/v), 10 mL 1 M Tris/HCl pH 8.0 (100 mM), 4 mL 0.5 M EDTA pH 8.0 (20 mM), 8.18 g NaCl (1.4 M), 1 g PVP (Polyvinyl pyrrolidone Mr 40000, 1 % w/v), dH_2O to 100 mL, autoclaved and stored at RT.

1 M Tris/HCl pH 8.0: 60.6 g Tris (2-amino-2-hydroxymethylö-1,2-propanediol) dissolved in 480 mL dH_2O and brought to the pH 8.0 with concentrated HCl, dH_2O to 500 mL, autoclaved and stored at RT

0.5 M EDTA pH 8.0: 93.06 g Na_2-EDTA* $2H_2O$ (Ethylendiaminetetraacetic acid disodium salt dehydrate) dissolved in 450 mL dH_2O and brought to a pH of 8.0 with 10 M NaOH, dH_2O to 500 mL, autoclaved and stored at RT.

4.7.5 Polymerase Chain Reaction (PCR)

PCR was usually performed in 50 µL reaction volume:

Component	Volume	Final concentration
Template DNA		10-50 ng
10 x PCR buffer	5 µL	1.5 mM $MgCl_2$
2 mM dNTP mix	5 µL	0.2 mM
2 µM oligo forward	2.5 µL	100 nM
2 µM oligo reverse	2.5 µL	100 nM
Taq-Hifi-Polymerase	1 µL	1 U
dH_2O	Up to 50 µL	

PCR was performed with an Eppendorf Thermocycler.

Step	Temperature	Time
Preheating	95 °C	5 ‘
Denaturation	95 °C	30’’
Annealing	Oligo-specific (50-60 °C)	60’’
Elongation	72 °C	30’’/kb
Extension	72 °C	5’

The 3 PCR steps colored in grey including denaturation, annealing and elongation provide the core amplification part of the method exponentially increasing the DNA concentration with every cycle. They are repeated 19-29 times depending on the sensitivity of the PCR reaction.

For direct screening of *E. Coli* colonies (colony PCR), single colonies were picked from a agar plate with a sterile toothpick and resuspended in the following reaction mixture

Component	Volume
Template DNA	Colony from the toothpick
10x PCR buffer	2 µL
2 mM dNTP mix	2 µL
2 µM oligo forward	2 µL
2 µM oligo reverse	2 µL
Taq-Polymerase	0.3 µL
dH_2O	Up to 20 µL

Then a standard PCR (see above) was performed with an initial preheating step of 10min.

10xPCR buffer: 500 µL 1 M Tris/HCl pH 9.0 (100 mM), 2500 µL 1 M KCl (0.5 M), 75 µL 1 M $MgCl_2$ (15 mM), 250 µL 20% Triton X-100 (1% v/v) and 1000 µL of 10 mg/mL NSA (2 mg/mL), 675 µL dH_2O to a final volume of 5 mL, divided in 500 µL aliquots and stored at -20°C.

1 M Tris/HCl pH 9.0: 60.6 g Tris (2-amino-2-hydroxymethylö-1,2-propanediol) dissolved in 480 mL dH_2O and brought to the pH 9.0 with concentrated HCl, dH_2O to 500 mL, autoclaved and stored at RT

1 M KCl: 7.46 g KCl, dH_2O to 100 mL, autocalved and stored at RT.

1 M $MgCl_2$: 10.15 g $MgCl_2$ * 6 H_2O, dissolved in 50 mL dH_2O, autoclaved and stored at RT.

20% (v/v) Triton X-100: 1 mL 100% Triton X-100 diluted in 5 mL dH_2O, stored at 4°C.

10 mg/mL BSA: 100 mg bovine serum albumin (BSA, Fraktion V, Fluka) dissolved in 10 mL dH_2O and stored in 1 mL aliquotes at -20°C.

2 mM dNTP mix: 40 µL of each 100 mM deoxyribonucleotide triphosphate stock (dATP, dTTP, dGTP, dCTP), with 1840 µL dH_2O to a final volume of 2 mL, 500 µL aliquots stored at -20 °C.

Oligo stocks (Primers): lyophilized oligonucleotides were dissolved in an appropriate volume of dH_2O to get a 100 µM stock solution. For the 2 µM working stock solutions, 10 µL of the 100 µM stock were

diluted in dH_2O to a final volume of 500 µL, whereas for the 10 µM working solution 50 µL of the 100 µM stock were diluted in dH_2O to a final volume of 500 µL.

4.7.6 Site-directed Mutagenesis by Polymerase Chain Reaction (PCR) with proof-reading Kappa Hifi Kit

KAPA HiFi HotStart PCR Kit was used according to manufacturer's manual to perform a site-directed mutagenesis.

Typically PCR was performed in 50 µL reaction volume:

component	Volume	Final concentration
Template DNA		30-100 ng
10 x PCR buffer with Mg	10 µL	3 mM $MgCl_2$
10 mM dNTP mix	1.5 µL	0.3 mM
10 µM oligo forward	1.5 µL	0.3 mM
10 µM oligo reverse	1.5 µL	0.3 mM
Taq-Hifi-Polymerase	1 µL	1 U
dH_2O	Up to 50 µL	

PCR was performed with an Eppendorf Thermocycler.

Step	Temperature	Time
Preheating	95 °C	5 '
Denaturation	98 °C	20''
Annealing	Oligo-specific (50-60 °C)	60''
Elongation	72 °C	30''/kb
Extension	72 °C	5'

The 3 PCR steps colored in grey including denaturation, annealing and elongation provide the core amplification part of the method exponentially increasing the DNA concentration with every cycle. Generally 20 cycles were used.

To amplify DNA for T/A cloning approaches the Kappa Hifi Kit was used according to manufacturer's manual.

Step	Temperature	Time
Preheating	98 °C	3 '
Denaturation	98 °C	30''
Annealing	Oligo-specific (50-60 °C)	45''
Elongation	72 °C	30''/kb
Extension	72 °C	10'

Generally 30 cycles were used to amplify the desired DNA fragment.

Oligo stocks (Primers): lyophilized oligonucleotides were dissolved in an appropriate volume of dH_2O to get a 100 µM stock solution. For the 2 µM working stock solutions, 10 µL of the 100 µM stock were diluted in dH_2O to a final volume of 500 µL, whereas for the 10 µM working solution 50 µL of the 100 µM stock were diluted in dH_2O to a final volume of 500 µL.

10 mM dNTP mix: was provided by the PCR kit

10 x PCR buffer with Mg: was provided by the PCR kit

4.7.7 Polymerase Chain reaction (PCR) to get DNA with T/A overhang

For further ligation into pTZ57R/T vector T/A (sticky ends) ends need to be added to a blunt ended insert by using a short PCR reaction.

Component	Volume	Final concentration
Template DNA		30-50 ng
10 x PCR buffer	5 µL	1.5 mM $MgCl_2$
2 mM dNTP mix	5 µL	0.2 mM
10 µM oligo forward	-	
10 µM oligo reverse	-	

Taq- Polymerase	1 µL	1 U
dH_2O	Up to 50 µL	

PCR was performed with an Eppendorf Thermocycler.

Step	Temperature	Time
Denaturation	98 °C	3''
Elongation	72 °C	30'
Extension	72 °C	5'

see above (standard PCR)

4.7.8 DNA gel-electrophoresis

To estimate the size and the amount of plant or bacterial plasmid DNA or for elution of digested DNA fragments, horizontal agarose gel-electrophoresis was performed with 1 % agarose gels. The gels were prepared by heating up a mixture of 1 % agarose in 1 x TAE buffer in a microwave until the agarose has melted completely. After cooling down, ethidium bromide was added to a final concentration of 0.5 µg/mL. The DNA samples were mixed with 6x loading buffer and finally loaded on the gel. According to the range of the loaded DNA fragment sizes 5 µL of an appropriate DNA size marker was used. The gels were run in 1xTEA buffer at 100-120 V and the bands were visualized under UV light (254 nm) using a transiluminator.

6x orange gel-loading buffer: 0.25 % Orange G (w7v), dissolved in 87 % glycerol

50x TAE electrophoresis buffer: 242 g Tris base (2 M) dissolved in 800 mL dH2O, 57.1 mL glacial acetic acid (1 M), 18.62 g Na2EDTA*2 H2O (0.05 M) or 100 mL 0.5 M EDTA pH 8.0, dH2O to 1000 mL, autocalved and stored at RT

0.5 M EDTA pH 8.0: 93.06 g Na2EDTA*2 H2O dissolved in 450 mL dH2O and brought to a pH 8.0 with 10 M NaOH, with dH2O to 500 mL, autoclaved and stored at RT.

Ethidium bromide stock (10 mg/mL): Roth, stored at 4°C

4.7.9 DNA digestion with restriction endonucleases

Digestions were performed in recommended supplied buffers according to the manufacturer's manual. Preparative / Quantitative digestions for further cloning strategies were generally done in 50 µL reaction volume and incubated for 2 h, whereas for control digestions the reaction volume can be reduced to 20 µL and incubated for 30 minutes to 1 h according to the enzyme activity. Heat inactivation was performed either at 65 °C or 80 °C according to the enzyme specifications.

Enzymes: MBI Fermentas and New England Biolabs

4.7.10 Purification of DNA fragments from agarose gels

For DNA purification from agarose gels the Gel Extraction Kit from peqGOLD Gel Extraction Kit from Thermo Scientific was used. The procedure was done according to the manufacturer's manual.

4.7.11 Dephosporylation of enzyme-digested DNA ends

To prevent vector re-ligation after digestion with restriction endonucleases, the 5`-phosphate groups were enzymatically removed with shrimp alkaline phosphatase. Dephosphorylation reaction was performed directly after inactivation of the restriction endonuclease by addition of 1 µL fastAP and incubation for 15-20 minutes at 37 °C. No additional fastAP buffer was added, as this enzyme is active in all common restriction enzyme buffers.

fastAP: MBI Fermentas

4.7.12 Cloning of PCR fragments

PCR fragments with T/A overhangs (4.7.7) were purified from agarose gels (4.7.1) and ligated into T/A cloning vector according to the ligation protocol (4.7.13). Transformation into *E.Coli* was accomplished by electroporation (4.8.4). Blue-white selection was performed to identify positive clones due to their color (4.7.14).

4.7.13 T4 DNA Ligation

Prior to the ligation reaction, the purified vector and insert were analyzed on an agarose gels to estimate DNA quality and amount. Ligation reaction was performed in 20 µL using 5 U of T4 DNA Ligase and 2 µL T4 DNA Ligase buffer. The molar ratio of vector and insert should be approximately 1:3 according to the size of the vector and the insert. The reaction was incubated for 45 minutes at RT and finally at 14°C overnight. Prior to transformation the T4 DNA ligase was inactivated for 10 minutes at 65°C, ligation reaction was stored at -20°C.

T4 DNA Ligase and Buffer: MBI Fermentas, New England Biolabs

4.7.14 Blue-White Selection of positive clones

The pTZ57R/T plasmid is a *lacZ*-bearing vector backbone, encoding for β-galactosidase. IPTG (Isopropyl-β-D-thiogalactopyranoside) induces the *lacZ* gene expression. X-Gal (5-bromo-4-chloro-3-indolyl- β-D-galactopyranoside) is a substrate for the β-galactosidase, which is cleaved, then dimerizes and oxidizes to form a bright blue insoluble precipitate. If the gene of interest is inserted in the multiple cloning site, expression of the *lacZ* gene is disrupted, no enzyme produced and the X-Gal remains colorless. 75 µL of IPTG – X-GAL mixture was spread on the surface of a selective agar plate prior to plating of the bacterial culture. After incubation of the plates at 37°C overnight they were placed at 4°C to promote the formation of blue precipitate. Cells transformed with vectors containing the gene of interest will produce white colonies; cells transformed with only the vector grow into blue colonies.

100 mM IPTG stock: 23.8 mg/mL in dH_2O, 500 µL aliquots stored at – 20 °C

X-Gal stock: 60 mg/mL in DMF, 500 µL aliquots stored at – 20 °C

IPTG – X-Gal mixture: 25 µL of 100 mM IPTG, 25 µL of X-Gal stock, 25 µL dH_2O, mixed before spread on the agar plates

4.8 Microbiological methods

4.8.1 Media and growth conditions for bacteria

E. Coli was grown in LB liquid medium with appropriate antibiotics under vigorous shaking (rotary shaker, 180 rpm) or on LB solid medium in Petri dishes (1.5 % agar), overnight at 37 °C.

Agrobacterium tumefaciens was grown (rotary shaker, 180 rpm) in liquid or solid LB medium (1.5 % agar) with appropriate antibiotics for one or two days at 29 °C.

Antibiotics: were filter sterilized, divided in 10 mL aliquots and stored at – 20 °C

Antibiotic	**Stock concentration in dH_2O**	**Final concentration for *E.Coli***	**Final concentration For *A. tumefaciens***
Ampicillin	50 mg/mL	50 µg/mL	
Kanamycin	50 mg/mL	50 µg/mL	100 µg/mL
Gentamycin	100 mg/mL		50 µg/mL
Rifampicin	50 mg/mL		50 µg/mL
Spectinomycin	50 mg/mL	50 µg/mL	100 µg/mL

LB medium: 10 g tryptone (1 %), 5 g yeast extract (0.5 %), 10 g NaCl (172 mM), dH_2O to 1000 mL, autoclaved and stored at RT. For solid media, 4.5 g agar was added to 300 mL liquid medium, autoclaved and stored at RT. Before use the solid media need to be molten in a microwave oven, cooled down to 55 °C in the water bath and an appropriate amount of selective antibiotic was added prior to use.

2x TY medium: 16 g tryptone (1.6 %), 10 g yeast extract (1 %), 5 g NaCl (86 mM), dH_2O to 900 mL, pH brought to 7.4 with 10 M NaOH, dH_2O to 1000 mL, autoclaved and stored at RT. For solid medium 4.5 g agar was added to 300 mL liquid medium, autocalved and stored at RT. Before use the solid media need to be molten in a microwave oven, cooled down to 55 °C in the water bath and an appropriate amount of selective antibiotic was added prior to use.

4.8.2 Preparation of electrocompetent *E.coli*

A single colony of the appropriate E. Coli strain (DH10B or BL21(DE3)) was inoculated in 5 mL of LB and grown overnight at 37 °C, 180 rpm. Next day 2 mL of the overnight culture was added to fresh 500 mL LB medium and grown at 37 °C until OD_{600} = 0.5. Cultures were chilled on ice for 1 hour and then centrifuged for 15 minutes at 5000 rpm at 4°C (Hettich Zentrifugen, type 1610 D-78532 Tuttlingen, Rotor E819) in prechilled 50 mL Falcon tubes. The bacterial pellet was resuspended with 200 mL of ice-cold sterile dH_2O in each tube and centrifuged again. The washing step was repeated once. Afterwards the water is removed from the tubes. Within each washing step the number of used tubes was reduced until 2 tubes remaind. 5 mL of prechilled 10% Glycerol in dH_2O was added to both tubes, pellet was resuspended and centrifuged again. Finally the pellet is resuspended in 1 mL prechilled 10% Glycerol in dH_2O, 50µL aliquots were shock frozen in liquid nitrogen and stored at – 80 °C

10 % Glycerol: 1000 µL 100% Glycerol to 9 mL dH_2O, autoclaved and stored at 4 °C.

4.8.3 Preparation of electrocompetent *A. tumefaciens*

A single colony of a the appropriate A. tumefaciens strain was inoculated in 5 mL of LB and adequate selection antibiotic and grown overnight at 29 °C, 180 rpm. 2x 2 mL liquid culture were inoculated in 2x 500 mL LB containing selection antibiotic and grown at 29 °C until reaching an OD_{600} = 0.5-0.6. Further steps were exactly the same as for the preparation of electrocompetent *E. coli.*

4.8.4 Electroporation of *E. coli* and A. *tumefaciens*

Plasmid DNA (1-3 µL, equals 1-10 ng DNA) was added to 50 µL of electrocompetent cells (thawed on ice for some minutes). The suspension was gently mixed and transferred in to ice cold electroporation cuvettes (2mm path length, Equinio, Peqlab) and kept on ice until high voltage pulse was applied at 2.5 kV (for *E.coli*) or 2.2 kV (for *A. tumefaciens*), 200 Ω and 25 µF in a BIO-RAD Gene Pulser™. After the electropulse, 550 µL of LB or 2xTY medium was added to the cells, gently mixed and finally transferred into a 1.5 mL tube and incubated for 1 hour at 37

°C or at RT in the dark for *A. tumefaciens.* Aliquotes of the cell suspension were plated on LB plates with the appropriate selection antibiotic.

4.8.5 Preparation of bacterial -80 °C glycerol stocks

A single colony of the desired clone of *E.coli* was grown in 5 mL of selective medium. 600 µL of the overnight culture were mixed with 600 µL 100 % glycerol by vortexing in a cryo-tube and directly shock frozen in liquid nitrogen, finally stored at -80 °C.

4.8.6 Induction of Protein expression in BL21(DE3)

Plant proteins were expressed in *E.coli* strain BL21 (DE3) by induction with IPTG for further biochemical analysis. A desired colony was inoculated in 5 mL LB medium containing appropriate selection antibiotic and grown overnight at 37 °C shaking (180 rpm). Next day 1-2 mL of the overnight culture was used to inoculate a new culture of 50 mL LB medium with adequate selection antibiotic and grown until OD_{600} = 0.5-0.6. Prior to the addition of IPTG to induce protein expression 1 mL of the cell culture was saved for further analysis, centrifuged and the remaining pellet frozen at -20 °C. IPTG (100 mM) was added to the remaining cell culture (49 mL) to a final concentration 0.5 mM IPTG Protein expression by IPTG induction achieved by incubation of the cell culture for at least 5 hours at 37 °C with shaking at 180rpm. Afterwards 1 mL of the cell suspension was saved, centrifuged and the pellet was saved at -20 °C for further analysis. The remaining cell culture (48 mL) was centrifuged in 50 mL falcon tubes for 15 minutes at 5000 rpm, 4 °C (Hettich Zentrifugen, type 1610 D-78532 Tuttlingen, Rotor E819). The supernatant was discarded and the pellet saved at -80 °C for further protein extraction and *in vitro* binding assay-analysis.

100 mM IPTG stock: 23.8 mg/mL in dH_2O, 500 µL aliquots stored at – 20 °C

4.9 Plant methods

4.9.1 Seed harvesting and storage

Plants with mature siliques were cut, packed in a paper bag and allowed to completely dry for some days at RT. Dried seeds can be harvested by sieving the plant material through a metal sieve and collecting the seeds in 1.5 tubes to store them at RT.

4.9.2 Seed sterilization

Seeds (up to 100 µL) were sterilized in a 2 mL tube where they were resuspended in at least 1 mL of sterilization solution and incubated for 7 minutes with vigorous shaking. Afterwards the seeds were allowed to settle down until the solution can be removed and replaced by dH_2O. The seeds were further washed several times with dH_2O to remove the sterilizing solution thoroughly. Larger amounts of seeds were sterilized in 14 mL falcon tube with 7ml of sterilizing solution. The procedure is then the same as for smaller amounts of seeds. After sterilization the seeds can be stored for a short time in dH_2O at 4 °C.

Sterilization solution: 10 mL 12 % sodium hypochlorite (6 % v/v), 10 mL dH_2O and 100 µL 20 % Triton X-100 (0.1 % v/v), prepared freshly.

20 % Triton X-100 (v/v): 1 mL 100 % Triton X-100 diluted in dH_2O up to 5 mL, stored at RT up to 1 month

4.9.3 Cultivation on solid media

PN (plant nutrient) medium (Haughn and Somerville, 1986) was heated in a microwave oven and cooled to 55 °C in a water bath. Following steps were done under a laminar flow hood to preserve sterile conditions. 50 % sucrose was added to the media to a final concentration of 1 % (v/v) sucrose (PNS…PN with sucrose). PN media used for selection of primary transformants lack sucrose in order to reduce the contamination with *A. tumefaciens.* If necessary, media can be supplemented with selection drugs or hormones. Sterile seeds were resuspended in 0.1 % agarose and plated in parallel rows by using a 1 mL pipette tip. For T1 selection a higher amount of seeds were resuspended in 0.1 % agarose and distributed over the already hard agar

by circular movement. Afterwards the agarose was allowed to dry in the laminar stream for some minutes.

Dry plates were sealed with surgical tape Leukopor™ and incubated for at least 48 hours at 4 °C, before the plates can be transferred into a plant growth incubator/phytotron (Percifal Scientific Inc.) under following conditions: 12 h photo-period, 159 µmol/m^2/s light intensity, 50 % relative humidity and 22 °C. For the T1 selection the plates were incubated in a horizontal, for phenotypic analysis plates were incubated in a vertical position.

PN solid medium: 0.0931 g $Na_2EDTA*2H_2O$ (50 µM) dissolved in 500 mL dH_2O, 0.0695 g $FeSO_4*7\ H_2O$, 50 mL 250 mM KPO_4 pH 5.5 buffer system (2.5 mM), 50 mL 500 mM KNO_3 (5 mM), 50 mL 200 mM $Ca(NO_3)_2$ (2 mM), 50 mL 200 mM $MgSO_4$ (2 mM) and 5 mL 1000x micronutriens mix, dH_2O to 4500 mL, pH brought to 5.5 with 1 M KOH, dH_2O up to 5000 mL. 700 mL of this suspension filled into a 1000 mL glass bottle containing 7 g agar (1 %), autoclaved and stored at RT.

250 mM KPO_4 pH 5.5 buffer system: 31.98 g KH_2PO_4 (235 mM), 2.61 g K_2HPO_4 (15 mM), dH_2O to 1000 mL, autoclaved and stored at RT.

500 mM KNO_3: 50.55 g KNO_3, dH_2O to 1000 mL, autoclaved and stored at RT.

200 mM $Ca(NO_3)_2$: 47.23 g $Ca(NO_3)_2*4\ H_2O$, dH_2O to 1000 mL, autoclaved and stored at RT.

200 mM $MgSO_4$: 49.3 g $MgSO_4*7\ H_2O$, dH_2O to 1000 mL, autoclaved and stored at RT.

1000x micronutriens mix: 2.16 g H_3BO_3 (70 mM), 1.39 g $MnCl_2*4H_2O$ (14 mM), 0.02624 g $CuSO_4*5\ H_2O$ (0.5mM), 0.144 g $ZnSO_4*7$ H2O (1 mM), 0.242 g $Na_2MoO_4*2\ H_2O$ (0.2 mM), 0.2922 g NaCl (10 mM), 0.0024 g $CoCl_2*6\ H_2O$ (0.01 mM), dH_2O to 500 mL, autoclaved and stored at RT.

1M KOH: 5.61 g potassium hydroxide to 100 mL with dH_2O, stored at RT.

50 % sucrose: 100 g sucrose dissolved in dH_2O up to 200 mL, aliquoted to 50 mL, autoclaved and stored at RT.

0.1 % (w/v) Agarose: 0.4 g agarose to 400 mL with dH_2O, melted in a microwave oven and aliquoted in 50 mL, autoclaved and stored at RT.

Selection drugs: Antibiotics used for plant selection were filter sterilized, divided in 1 mL aliquots and stored at – 20 °C

Antibiotic	**Stock concentration in dH_2O**	**Final concentration for T1 plants**	**Final concentration for *T2* plants**
Gentamycin	50 mg/mL	75 µg/mL	60 µg/mL

4.9.4 Plant cultivation on soil

For further propagation or analysis of adult plant phenotypes, 2-3 weeks old plants were brought from plates to soil. Soil substrate was composed of 3 volumes of Einheitserde E 15 Typ P (Werkverband E.V.) and 1 volume of Granuperl Standard S 0-6 granules (Perlite). Pots (5x5 cm) were filled with soil substrate and put in a plastic tray holding 28 pots. After the soil was soaked with water, 5 plants were carefully transferred from agar plate to soil with tweezers. Each pot was labeled with a plastic stick. For the first days the plants were covered with a transparent plastic to avoid the loss of humidity and promote plant recovery. Plants were grown in climate chambers under long day conditions (16hours of light, 8 hours dark) at 22 °C at approximately 100 µM/m^2/s light intensity and 50 % relative humidity.

4.9.5 *A. tumefaciens* mediated plant transformation by the floral dip method

A single *A. tumefaciens* colony, already containing the desired gene construct by electroporation, was used to inoculate 5 mL LB containing all necessary selective antibiotics and grown over night at 29 °C. On the next day the 5 mL pre-culture were used to inoculate a large scale culture of 300-400 mL LB containing only the antibiotic selection for the plasmid, and grown at 29 °C overnight. The culture was centrifuged for 15 minutes at 4 °C in a Sorvall GAS rotor at 3000 rpm. The pellet was resuspended in 250 mL of infiltration medium and transferred into a 250 mL beaker, which fitted to the size of the plant pots. Plant pots were inverted into the *Agrobacterium*-containing medium and the plants were incubated for 15-20

minutes at RT (Clough and Bent, 1998). Afterwards the plants were placed horizontally into a plastic tray, covered with a plastic wrap to ensure efficient transformation and humidity. After several hours, the plants were transferred vertically into a plastic tray and incubated in the climate chamber for growth and seed formation.

Transformation medium: 2.15 g MS salts, 0.5 g MES (2-N-morpholino-ethanesulfonic acid), 50 g sucrose dissolved in 800 mL dH_2O, brought to a pH 5.7 with KOH, dH_2O to 900 mL. Before use 300 µL of Silwet L-77 (0.03 % Van Meeunwen Chemicals B.V., Netherlans) was added. Fresh prepared no autoclaving necessary.

4.9.1 Confocal Laser Scanning Microscopy (CLSM)

In order to select for T1 plants transformed with the *stol6* and the *stol6* mutated constructs, plant seeds were sterilized and transferred on PN plates with Gentamycin as selection marker. After germination wild type plants show impaired growth. Efficiently transformed plants continuously grow due to the presence of the plant vector (pPZP221) including the gene of interest under the control of the endogenous promoter and the gentamycin-resistance gene. Two homozygous T3 lines of each plant line were propagated and further analyzed.

To determine the localization of stol6 and mutant stol6 proteins in the root cells, live cell imaging with 6 to 10-day-old seedlings was performed. For image acquisition, a Leica SP5 (DM6000 CS) confocal laser-scanning microscope was used, equipped with a Leica HCX PL APO CS 63×1.20 glycerol-immersion objective. The Venus-tag was excited at 514 nm (fluorescence emission: 525–578 nm) and the fluorescence signals were processed with the Leica software LAS AF 3.

4.10 Biochemical methods

4.10.1 Extraction of recombinant proteins from BL21

Recombinant protein extraction from BL21 (DE3) was performed to obtain high level of soluble protein in a suitable quality for further analysis. The frozen protein pellet after induction was

resuspended in 1 mL of Sonication buffer with SDS and incubated for 30 minutes at 4 °C with rocking. Afterwards 1 mL of Sonication buffer without SDS was added to the cell suspension, before the cells were disrupted by the usage of ultrasonic frequencies during sonication procedure (Vibra cell^{TM}, Sonics and Material Danbury.CT. USA). Every sample was sonicated six times for 10 seconds. Between sonication pulses, the samples were allowed to chill on ice. Afterwards the samples were centrifuged at maximal speed for 10 minutes at 4 °C. The supernatant, containing the recombinant protein, was transferred to a 15 mL falcon tube and 3 mL of RIPA buffer, 500 µL 100 % Glycerol and ¼ of the complete mini EDTA free tablet (Roche) were added. For further analysis, 100 µL sample after extraction and one pellet after centrifugation were saved to determine the amount of recombinant protein in the soluble fraction, with respect to the amount in the pellet fraction. 500 µL aliquots of the supernatant in the RIPA buffer (soluble fraction) were frozen at – 80 °C for further binding assay procedure.

Sonicationbuffer with SDS: 800 µL 0.5 M Hepes/NaOH pH 7.4 (10 mM), 80 µL 0.5 M EDTA pH 8 (1 M), 1 mL 20 % SDS (0.5 % w/v), dH_2O to 40 mL, stored at. Before use 1 mM PMSF, 1 mM DTE and 1 mM Aprotinin/Leupeptin were added as efficient protease inhibitors.

Sonication buffer without SDS: 800 µL 0.5 M Hepes/NaOH pH 7.4 (10 mM), 80 µL 0.5 M EDTA pH 8 (1 M), dH_2O to 40 mL, stored at. Before use 1 mM PMSF, 1 mM DTE and 1 mM Aprotinin/Leupeptin were added as efficient protease inhibitors.

RIPA buffer: 5 mL 0.5 M Hepes/NaOH pH 7.4 (50 mM), 100 µL 0.5 M EDTA (1 mM), 2.8 mL 2.5 M NaCl (140 mM), 2.5 mL 20 % Triton X-100 (1 % w/v), 0.5 mL 10 % Na-deoxycholate (0.1 % w/v), dH_2O to 50 mL, stored at 4 °C. Before use 1 mM PMSF, 1 mM DTE and 1 mM Aprotinin/Leupeptin were added as efficient protease inhibitors.

0.5 M Hepes/NaOH pH 7.4: 4.77 g Hepes (4-(2-hdyroxyehtyl)-1-piperazineethanesulfonic acid) dissolved in 25 mL dH_2O, brought to pH 7.4 with concentrated NaOH, dH_2O to 40 mL, sterile filtered and stored at 4 °C.

0.5 M EDTA pH 8.0: 93.06 g $Na_2EDTA*2\ H_2O$ dissolved in 450 mL dH_2O and brought to a pH 8.0 with 10 M NaOH, with dH_2O to 500 mL, autoclaved and stored at RT.

20 % SDS: 10 g SDS (sodium dodecyl sulfate, w/v) dissolved in dH2O to 50 mL, autoclaved ant stored at RT.

1 M Aprotinin stock: 2 mg Aprotinin in 2 mL H_2O, aliquots of 50 µL were dried and stored at -20 °C.

1 M Leupeptin hemisulfate stock: 2 mg Leupeptin hemisulfate in 2 mL H_2O, aliquots of 50 µL were dried and stored at -20 °C.

0.5 M DTE: 7.7 mg DTE (2,3-Dihydroxybutane-1,4-dithiol) dissolved in 100 µL dH_2O, stored at -20 °C #

100 mM PMSF: 174 mg PMSF (Phenylmethylsulfonyl fluoride) dissolved in Isopropanol up to 10 mL, 200 µL aliquots, for short storage at -20 °C

20 % Triton X-100 (v/v): 1 mL 100 % Triton X-100 diluted in dH_2O up to 5 mL, stored at RT up to 1 month.

10 % Na-deoxycholate: 10 g of Na-deoxycholate dissolved in 100 mL dH_2O, autoclaved and stored at RT

2.5 M NaCl: 14.61 g NaCl dissolved in 100 mL dH_2O, autoclaved and stored at RT.

4.10.2 Binding Assay with glutathione-magnetic beads

The binding assay was performed to analyze the binding activity of a protein to a specific target (in our case ubiquitin) *in-vitro*. For this experiment ubiquitin was linked to Thermo Scientific Pierce Glutathione Magnetic Beads via a GST-tag (glutathione-S-transferase). In further steps, the protein of interest was added to the ubiquitin coupled glutathione-magnetic beads to test their ubiquitin binding activity by affinity purification.

Thermo Scientific Pierce Glutathione Magnetic Beads are composed of iron oxide particles, encapsulated by crosslinked agarose with a mean diameter of 1-10 µm with reduced glutathione (GSH) covalently attached to the surface.

Thermo Scientific Pierce Glutathione Magnetic Beads were stored in 25 % slurry of 20 % Ethanol with a binding capacity of 5-10 mg of GST fusion protein per 1 ml of settled beads (i.e., 4 ml of 25% slurry). According to the manufacturer's manual, 100 µL slurry, corresponding to 25 µL of

settled beads, was used for one sample. 100 µL slurry for one sample was transferred to a 1.5 mL tube and washed 3 times with 1 mL EB binding/wash-buffer, in between incubating for 10 minutes at 4 °C with gentle rocking. The tubes were placed into a magnetic stand (Promega™ MagneSphere™ Technology Magnetic Separation Stand), which quickly pulls down the beads to enable easy and efficient discarding of the supernatant. Afterwards the magnetic beads were resuspended in 500 µL EB binding/wash-buffer and transferred into a new 1.5 mL tube already containing 100 µL soluble extracted recombinant ubiquitin-GST fusion protein (see section 3.18.1) diluted in 400 µL EB binding/wash-buffer. The sample was incubated for 2 hours at 4 °C, gently rocking, allowing the Ubiquitin-GST fusion protein to bind to the Glutathione Magnetic Beads via its GST-tag. After the incubation time, the tubes were transferred into the magnetic stand to allow the beads to settle down and 50 µL of the supernatant was saved for further analysis by diluting in 50 µL Laemmli buffer (1:2) and finally stored at -20 °C. The ubiquitin coupled Glutathione Magnetic Beads in the remaining 1.5 mL tube were washed again 3 times with 1 mL EB binding/wash-buffer for 10 minutes at 4 °C, gently rocking. An appropriate amount of the protein of interest (20-100 µL, according to the expression efficiency) was diluted in 1mL of Resuspension buffer. Prior to the addition to the ubiquitin coupled Glutathione Magnetic Beads, 20 µL was saved for further analysis by diluting 1:2 in Laemmli buffer and freezing at -20 °C. The sample containing the ubiquitin coupled Glutathione Magnetic Beads together with the desired protein was incubated overnight at 4 °C, gently rocking. Next day 50 µL of the supernatant was saved for further analysis (1:2 with laemmli buffer and stored at -20 °C). After 6 washing steps (the same procedure as at the beginning) with resuspension buffer, the coupled Glutathione Magnetic Beads were resuspended in 50 µL Laemmli buffer and incubated for 10 minutes at 98 °C to (Concurrently, the high temperature caused the aggregation of Glutathione Magnetic Beads and loss of binding activity.) The supernatant was saved at -20 °C until analysis. Similar procedures were performed as control experiments using GST instead of ubiquitin-GST.

EB binding/wash-buffer: 2.5 mL 20x TBS, 1 mL 1 M Tris/HCl pH 7.4 (20 mM), 1.25 mL 20 % Triton X-100 (0.5 %), 500 µL 0.5 M EDTA pH 8 (5 mM), 5 mL 5 % CHAPS ((3-(3-cholamidopropyl) dimethylammonio)-1-

propanesulfonate) (0.5 %), dH_2O to 50 mL, stored at 4 °C. Before use 1 mM PMSF, 1 mM DTE and 1 mM Aprotinin/Leupeptin were added as efficient protease inhibitors.

Resuspension buffer: 1 mL 1M Tris/HCl 7.4 (20 mM), 4 mL 2.5 M NaCl (200 mM), 100 µL 0.5 M EDTA pH 8 (1 mM), dH_2O to 50 mL, stored at 4 °C. Before use 1 mM PMSF, 1 mM DTE and 1 mM Aprotinin/Leupeptin were added as efficient protease inhibitors.

2.5 M NaCl: 14.61 g NaCl dissolved in 100 mL dH_2O, autoclaved and stored at RT.

20x TBS: 121 g tris (2-Amino-2-(hydroxymethyl)-1,3-propanediol) (1 M), 175 g NaCL (3 M) dissolved in 900 mL dH_2O, brought to pH 7.5, dH_2O to 1000 mL, autoclaved and stored at RT.

1 M Tris/HCl pH 7.4: 60.6 g Tris (2-amino-2-hydroxymethylö-1,2-propanediol) dissolved in 480 ML dH_2O and brought to the pH 7.4 with concentrated HCl, dH_2O to 500 mL, autoclaved and stored at RT.

20 % Triton X-100 (v/v): 1 mL 100 % Triton X-100 diluted in dH_2O up to 5 mL, stored at RT up to 1 month

5 % CHAPS: 500 mg CHAPS ((3-(3-cholamidopropyl) dimethylammonio)-1-propanesulfonate) dissolved in 10 mL dH_2O, 1.5 mL aliquots stored at -20 °C.

0.5 M EDTA pH 8: 93.06 g $Na_2EDTA*2\ H_2O$ dissolved in 450 mL dH_2O and brought to a pH 8.0 with 10 M NaOH, with dH_2O to 500 mL, autoclaved and stored at RT.

1 M Aprotinin stock: 2 mg Aprotinin in 2 mL H_2O, aliquots of 50 µL were dried and stored at -20 °C.

1 M Leupeptin hemisulfate stock: 2 mg Leupeptin hemisulfate in 2 mL H_2O, aliquots of 50 µL were dried and stored at -20 °C.

0.5 M DTE: 7.7 mg DTE (2,3-Dihydroxybutane-1,4-dithiol) dissolved in 100 µL dH_2O, stored at -20 °C

100 mM PMSF: 174 mg PMSF (Phenylmethylsulfonyl fluoride) dissolved in Isopropanol up to 10 mL,200 µL aliquots, for short storage at -20 °C

SDS-Page using a Mini-Protean® II cell (BIO-RAD) was performed in order to separate proteins by electrophoresis due to their molecular weight. The electrophoresis was done in presence of SDS, which is responsible for protein denaturaturation and covering the charged amino acids of the protein resulting in a constant charge density. Additionally dithiothreitol (DTT) or β-mercaptoethanol as reducing agents was used to reduce the disulfide bonds and therefore completely unfold the protein. In order to make sure, that a large amount of protein start migrating from the same level, a discontinuous system, including a stacking gel and a separation gel, was used. The staking gel was responsible to make sure, that a large amount of protein start migrating from the same level, whereas the separating gel was liable for efficient protein separation according to their molecular weight.

Separation gel:

Component	Volume for 2 gels	Final concentration
30 % Acrylamid/Bisacrylamid (37.5:1)	5 mL	10 %
4x 1.5 M Tris/HCl pH 8.8	3.75 mL	375 mM
20 % SDS	75 µL	0.1 %
dH_2O	6.25 mL	-
10 % APS	75 µL	0.05 %
TEMED	15 µL	0.1 %

APS and TEMED were added just before pouring the gels. The components for the separation gel were mixed in a 50 mL falcon tube and poured into assembled gel plates using a pipette, but leaving enough space on top for the staking gel to be added later on. To avoid drying out of the separation gel isopropanol was added on the top of the gel. After at least 30 minutes of gel polymerization the isopropanol was removed and the gel rinsed with water and finally dried with filter paper. Afterwards the staking gel was added on top.

Staking gel:

Component	Volume for 2 gels	Final concentration
30 % Acrylamid/Bisacrylamid (37.5:1)	1 mL	4 %
4x 1.5 M Tris/HCl pH 8.8	1.875 mL	375 mM
20 % SDS	37.5 µL	0.1 %
dH_2O	4.625 mL	-
10 % APS	37.5 µL	0.05 %
TEMED	7.5 µL	0.1 %

The staking gel was prepared and poured in the same way as the separating gel. Finally combs were inserted avoiding air bubble formation. After the polymerization of the gels was finished, they were removed from their casting stand and assembled into the chamber for running the electrophoresis. The chamber was filled with 1x Running buffer and the protein samples already diluted in 2xLaemmli buffer 1:2 were heated up for at least 5 minutes at 98 °C , before they were loaded on the gels. The gels were run at 100-130 V until the bromphenol blue dye has reached the end of the separating gel.

1.5 M Tris/HCl pH 8.8: 36.33 g Tris (2-amino-2-hydroxymethyl-1,3-propanediol) dissolved in 160 mL dH_2O and brought to pH 8.8 with concentrated HCl, dH_2O to 200 mL, autoclaved and stored at RT

20 % SDS: 10 g SDS (sodium dodecyl sulfate, w/v) dissolved in dH_2O to 50 mL, autoclaved ant stored at RT.

0.5 M Tris/HCl pH 6.8: 30.3 g Tris (2-amino-2-hydroxymethyl-1,3-propanediol) dissolved in 480 mL dH_2O and brought to the pH 6.8 with concentrated HCl, dH_2O to 500 mL, autoclaved and stored at RT.

10% APS: 20 mg APS (Ammonium persulfate) dissolved in 200 µL dH_2O, short storage at -20 °C

Running buffer: 3 g Tris (2-amino-2-hydroxymethylö-1,2-propanediol) (25 mM), 14.4 g Glycine (192 mM), dissolved in 1000 mL dH_2O, 6 mL 20 % SDS (0.01 % w/v) were added afterwards.

2x Laemmli buffer: 2.0 mL glycerol (20 % v/v), 1.25 mL 1 M Tris pH 6.8 (125 mM), 2.0 mL 20 % SDS (4% w/v), 1 mg bromphenol blue (0.01 % w/v), 3.75 mL dH_2O to a final volume of 9 mL, stored at RT. Before use 10 µL β-mercaptoethanol was added to 90 µL 2x Laemmli buffer.

4.10.3 Coomassie blue staining

For analysis of the extracted protein quality, Coomassie blue staining was performed after SDS-PAGE. The detection limit of for Coomassie brilliant blue R-250 staining is approximately 30ng protein. After electrophoresis, the gel was transferred into a plastic bowl and 50 mL Coomassie staining solution was added to the gel and incubated for at least 1 hour at RT with gentle rocking. The Coomassie staining solution was removed and the gel rinsed several times with water, before it was transferred into a glas bowl with water and heated up in the microwave to destain. Water need to be refreshed several times. Finally, the gel was incubated overnight in water with a piece of paper towel in the water to soak up the excessive remaining Coomassie brilliant blue, until blue bands with a clear background were obtained.

Coomassie staining solution: 0.5 g Coomassie brilliant blue (0.25 % w/v), dissolved in a mixture of 80 mL dH_2Om 90 mL Methanol (45 % v/v) and 20 mL acetic acid (10 % v/v), dH_2O to 200 mL and stored at RT.

Coomassie destaining solution: 90 mL Methanol (45 % v/v) and 20 mL acetic acid (10 % v/v), dH_2O to 200 mL and stored at RT.

4.10.4 Western Blot and detection

After SDS PAGE the separated proteins from the polyacrylamide gel were transferred onto a solid membrane for further detection of a particular protein by interaction with specific Antibodies.

The wet transfer using a mini Trans-Blot cell (BIO-RAD) was performed with nitrocellulose membrane (Roth). Transfer buffer was prepared and stored at 4 °C; it can be re-used 3-4 times. Filter papers were cut slightly smaller than the fiber pad and the nitrocellulose membranes were cut slightly bigger than the polyacrylamide gel. After SDS-PAGE, the staking gel was removed and the remaining separation gel was equilibrated for at least 10 minutes in transfer

buffer. Nitrocellulose membrane, fiber pads and filter paper were soaked in transfer buffer, before the gel cassette was assembled with one layer of fiber pads and filter paper on each side of gel and membrane. Air bubbles were avoided by trying to assemble the gel cassette within a plastic bowl filled with transfer buffer. The gel cassette together with the gel holder, were transferred into electrode unit, taking care that the membrane was positioned next to the anode. The transfer chamber was filled with transfer buffer and placed into a big plastic bowl filled up with crashed ice for cooling. The transfer was carried out at constant 100 V for 1 hour (depend on the molecular weight of the protein). After the transfer the membrane was incubated in Ponceau S staining solution, to make sure that the transfer worked, for 5 minutes at RT rocking and afterwards rinsed with water several times to eliminate the background. The membrane was washed at least 4 times for 10 minutes with TBST and blocked for 1 hour in blocking solution at RT, rocking gently. The membrane was transferred to an adequately diluted primary antibody in blocking solution and incubated overnight at 4 °C, gently rocking. Next day the primary antibody was removed and the membrane washed 3 times for at least 10 minutes in TBST at RT until finally the membrane was incubated in a adequate dilution of secondary antibody in blocking solution for 2 hours at RT, gently rocking. After at least 4 washing steps of 10 minutes in TBST at RT, the membrane was rinsed with dH_2O and further transferred onto a plastic plate. The HRP chemiluminescence substrate (Pierce) was diluted 1:2 with dH_2O, distributed on the membrane and incubated for 2 minutes. Afterwards the membrane was transferred onto a plastic slide and excess of substrate was removed with a piece of paper towel. An X-ray film was exposed on the membrane in the dark room for 5-30 seconds and afterwards the film was developed.

Transfer buffer: 6.05 g Tris (25 mM), 28.75 g Glycine (192 mM), 200 mL 100 % Methanol (10 % v/v), dissolved in 2000 mL dH_2O, 3.75 mL 20 % SDS (0.05 % w/v) were added afterwards. Stored at 4 °C, can be used 3-4 times.

Ponceau staining solution: 0.25 Ponceau S (0.5 % w/v), 0.5 mL acetic acid (1 % v/v), dissolved in dH_2O up to 50 mL, stored at RT.

Blocking solution: 1.5 g BSA (bovine serum albumin, 3 % w/v), dissolved in TBST to a final volume of 50 mL, prepared fresh before use.

20x TBS: 121 g Tris (2-Amino-2-(hydroxymethyl)-1,3-propanediol) (1 M), 175 g NaCl (3 M) dissolved in 900 mL dH_2O, brought to pH 7.5, dH_2O to 1000 mL, autoclaved and stored at RT.

TBST: 50 mL 20x TBS, 10 mL 20 % Tween 20 (0.1 % v/v), dH_2O to 1000 mL, stored at RT.

5. Results

5.1 General information

In order to define and characterize the VHS and GAT domains as important UBDs in TOL proteins*, in vitro* and *in vivo* experiments were performed.

Ubiquitin itself functions as a covalent post-translational modification for diverse cargos to regulate different fundamental processes like protein degradation, endocytosis and vesicular trafficking (recently reviewed by (Hurley et al., 2006)). Generally ubiquitin can be seen as a sorting signal for cargo proteins within cellular transport mechanisms (Mizuno et al., 2003). UBDs, as present for example in the ESCRT complexes and other proteins involved in vesicular transport pathways, represent a widespread regulatory element for reversible non-covalent ubiquitin interaction (Prag et al., 2007; Dikic et al., 2009). α-helical UBDs, comprising the largest class of UBDs, are known to interact with a hydrophobic patch centered around the Isoleucin44 on ubiquitin (recently reviewed by (Hurley et al., 2006)). The UBDs of ESCRT-0 subdomains in yeast and mammals are well characterized (Prag et al., 2007; Wang et al., 2010). ESCRT-0 subunits share a N-terminal 140 aa long octahelical VHS domain with the conserved residues for ubiquitin binding in the α2- and α4- right handed helix (Wang et al., 2010). Furthermore ESCRT-0 subunits also contain UIMs and α3- helix-bundled GAT domain (Collins et al., 2003b; Zhu et al., 2003; Shiba et al., 2004; Prag et al., 2007).

5.1.1 VHS domain

Analyzing the VHS domain of STAM proteins with NMR chemical shift perturbation experiments helped to elucidate important amino acids for ubiquitin binding within the helix 2 and helix 4. This highlighted the crucial importance of a Tryptophan at position 26 (Trp26, W26) for the efficient binding of the UBD to ubiquitin (Hong et al., 2009) This amino acid is highly conserved within the VHS domains of the ESCRT-0, the GGAs and the TOM1-like proteins of mammals but also of their homologs in yeast and plants (see Figures 15-17). Furthermore important amino acids for the ubiquitin binding of the VHS domain were identified by co-crystallization of human

STAM1 with mono-ubiquitin. They were found to include the amino acids Tryptophan at position 26 (Trp26), Leucine at position 30 (Leu30, L30), which contribute to more than half the total interaction area, as well as Glycine at position 27 (Gly27, G27), Aspartate at positions 31 (Asp31, D31) and 34 (Asp34, D34), Alanine at 71 (Ala71, A71), Serine at 74 (Ser74, S74), and Asparagine at position 75 (Asn75, N75) (Ren and Hurley, 2010). Asn75 (STAM1) was also shown to be conserved and involved, but not essential, for the interaction of ubiquitin with the VHS domain (Ren and Hurley, 2010). Furthermore, NMR studies showed the Tryptophan in α2-helix and the Asparagine in α4-helix (Trp28 and Asn77) in STAM2 to represent highly conserved residues (Figure 15) providing a surface for efficient ubiquitin binding (Wang et al., 2010; Lange et al., 2011).

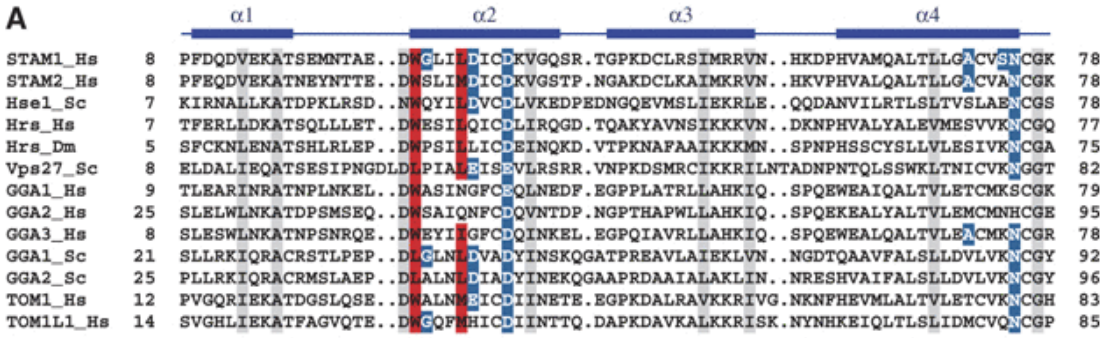

Figure 15: Sequence alignment of VHS domains of different proteins ; residues in red indicate most conserved amino acids, residues in blue are conserved in most proteins. (adapted from (Ren and Hurley, 2010))

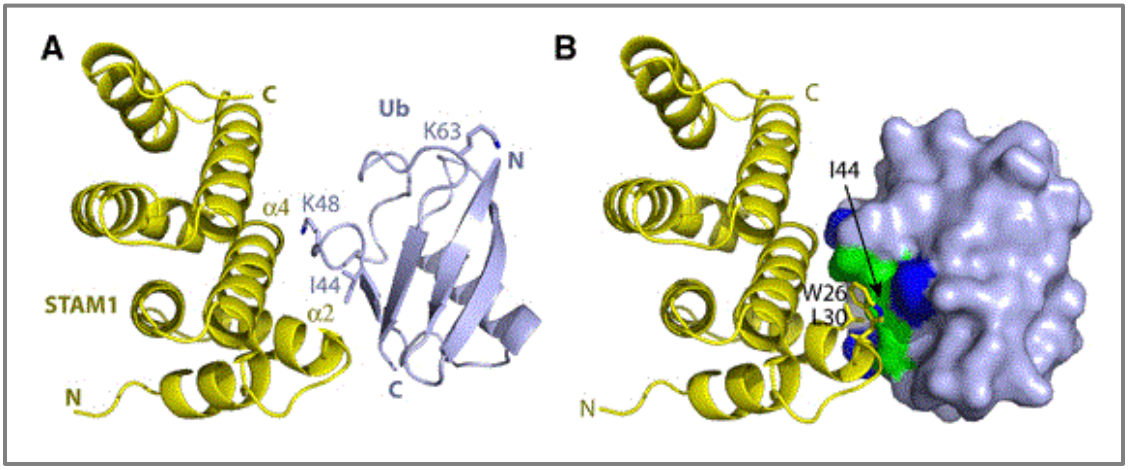

Figure 16: structure of STAM1 binding to ubiquitin , STAM1 shown in yellow, Ubiquitin shown in grey, (adapted from (Ren and Hurley, 2010)),

Summarized, all identified conserved residues are located in the α2- and α4-helix of the VHS domain (Wang et al., 2010). According to these results an alignment of all nine TOL proteins with Tom and STAM proteins was performed to elucidate whether these prominent residues, relevant for ubiquitin binding, are also conserved within the VHS domain of TOL proteins in *Arabidopsis thaliana* (Figure 17).

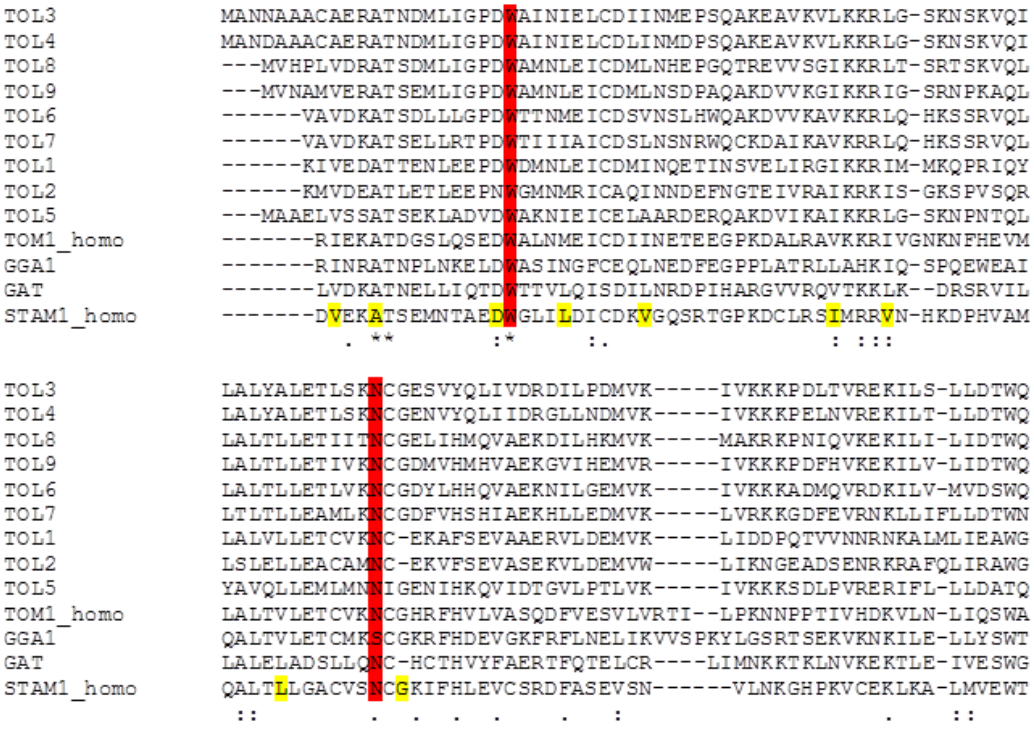

Figure 17: Alignment of TOL proteins and ESCRT-0 orthologues : VHS domain between 5-144 amino acids, most conserved amino acids within the alignment were marked in red.

The important Trp26 of STAM (Figure 17 in red), found in many studies to be essential for ubiquitin binding is highly conserved in all TOL proteins, unlike Leu30, which is not so conserved in the VHS domain containing TOL proteins. On the other hand, Asn75 (found in helix 4) is (Figure 17 in red) highly conserved in the TOLs. Therefore I focused on these two amino acids, the amino acid corresponding to Trp26 in α-helix 2 and the amino acid corresponding to Asn75 in α-helix 4 for my mutational analysis of the VHS domain of the TOL proteins within my master thesis.

The two most conserved amino acids Trp25 and Asn73 of TOL6 outlined in red (Figure 17) correspond to the already identified Trp28 and Asn77 relevant for ubiquitin interaction in STAM proteins VHS domain and were consequently chosen for site-directed mutagenesis: W25A, N73A in TOL6 to elucidate their involvement in ubiquitin binding.

5.1.2 GAT domain

GAT domains in ESCRT-0 subunits, GGAs and TOM1L1 proteins are three helical bundles (Collins et al., 2003a; Shiba et al., 2003; Zhu et al., 2003; Prag et al., 2007) susceptible for ubiquitin binding (Mattera et al., 2004; Scott et al., 2004; Shiba et al., 2004; Prag et al., 2007).

The GAT domain of GGA3 (Bilodeau et al., 2004) and Tom1 (Akutsu et al., 2005) include two ubiquitin interacting sites. The first is formed by the α1 and α3 helix and the second is located in the α3 helix (Bilodeau et al., 2004; Akutsu et al., 2005). Ubiquitin interaction site 1 of Tom1 seems to be predominantly determined by Glutamate at position 256 (Glu256, E256), although Methionine at position 237 (Met237, M237) show promising but slightly lower ubiquitin binding capacity and dissociation constant during surface plasmon resonance (SPR) experiments of Tom1 GAT mutants (Akutsu et al., 2005). In GGA3 Arginin at position 226 (Arg 226, A226), Leucine at position 227 (Leu227, L227), Serine at position 229 (Ser229, S229) and Glutamate at position 230 (Glu230, E230) located in the first ubiquitin binding site were shown to influence ubiquitin interaction by site directed mutagenesis and subsequently *in vitro*-pull down assay (Bilodeau et al., 2004). The second ubiquitin binding site in the α3-helix is mainly determined by Isoleucine at position 279 (Ile279, I279), Leucine at position 280 (Leu280, L280), Serine at position 283 (Ser283, S283) and Glutamate at position 284 (Glu284, E284) in GGA3 (Bilodeau et al., 2004) as well as Leucine at position 285 (Leu285, L285) and Aspartate at position 289 (Asp 289, D289) in Tom1 (Akutsu et al., 2005).

However, the residues for GGA and Tom proteins forming the two ubiquitin binding motives in α1/α2 and α2/α3 (Bilodeau et al., 2004; Prag et al., 2005) within the GAT domain are incompletely conserved in Vps27 and Hse1 as it can be seen in Figure 19 (Prag et al., 2007).

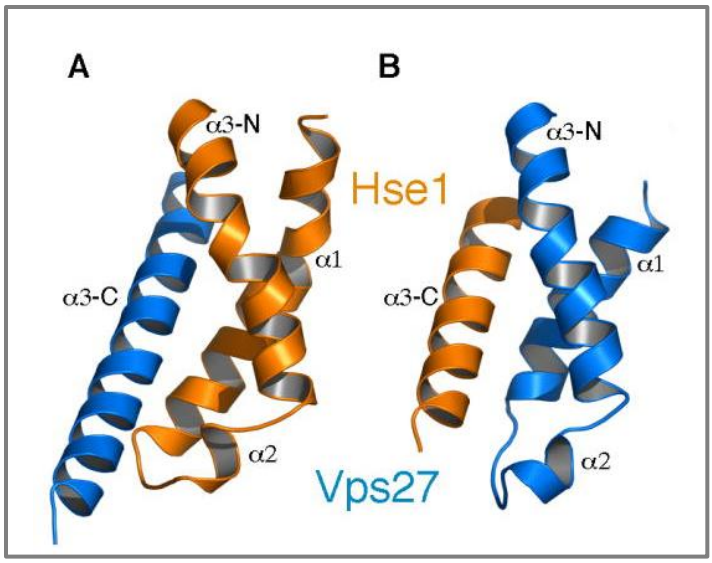

Figure 18: Vps27/Hse1 GAT domain : Each GAT domain consist of 3 α-helices interacting with each other resulting in a barbell-like structure. The middle narrow site of the α3-helix seems to be important for protein interaction, whereas the C and N-terminal part of the α3-helix together with the α1- and α2- helices forming bundles contribute to the complex stability. (adapted from (Prag et al., 2007)).

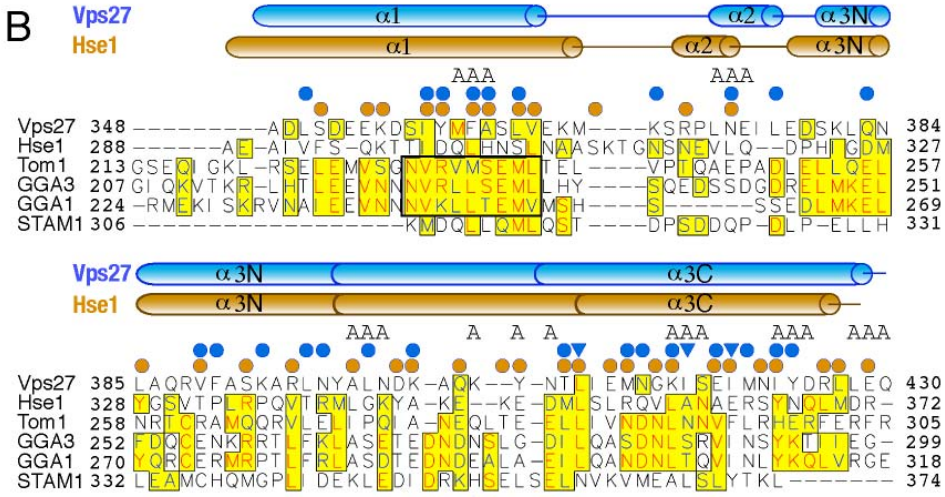

Figure 19: GAT domain sequence alignment of different vesicular trafficking proteins and corresponding secondary structure of Vps27 and Hse1 , The major site 1 ubiquitin-binding motif of GGA proteins and Tom1 is outlined in black. Conserved residues are marked in yellow, most conserved residues are written in red. (adapted from (Prag et al., 2007))

In order to determine the conserved residues involved in ubiquitin interaction in the GAT domain of the TOL proteins, a sequence alignment with different GAT containing GGA and TOM1 proteins was performed. As shown in Figure 20 six amino acids marked in yellow within the α-1 helix, which were found in GGA to participate in ubiquitin binding, are well conserved

through the TOL, GGA and TOM1L1, as their side chain properties remain consistent. This is in contrast to the second ubiquitin binding domain, found in α3-helix, which was only partially conserved in the plant TOL proteins. We thus focused on the first ubiquitin binding domain in our mutational analysis. To verify the impact of these amino acids on ubiquitin binding in TOL proteins, we performed site directed mutagenesis of DLL (246-248) to AAA and DML (250-252) to AAA in TOL6.

```
GGA1      DQKRMEKISKRVNAIEEVNNNVKLLTEMVMSHSQGGAAAGSSEDLMKELYQRCERMRPTL   210
TOM1L1    IAPTPEQIGKLRSELEMVSGNVRVMSEMLTELVPT-QAEPADLELLQELNRTCRAMQQRV   268
TOL6      EAMATEVEGLSLSSIESMRDVMDLLGDMLQAVDPS-DREAVKDEVIVDLVERCRSNQKKL   282
TOL3      SLQSDDASALSMEEIQSAQGSVDVLTDMLGALDPS-HPEGLKEELIVDLVEQCRTYQRRV   233
TOL9      PSAEPEFPTLSLSEIQNAKGIMDVLAEMLSALEPG-NKEDLKQEVMVDLVEQCRTYKQRV   233
```

Figure 20: Alignment of TOL proteins and ESCRT orthologs : amino acids 246-252 represent the most conserved part of the GAT domain

5.2 Mutagenesis strategies

5.2.1 General concept

TOL proteins, among them TOL6, have previously been shown to be essential for the down regulation of ubiquitinated PMPs and to thus to function as potential substitutes for the missing ESCRT-0 complex in plants (Korbei et al., 2013). TOL6, furthermore, is located at the PM and in EEs (Korbei et al., 2013) and its closest homolog in mammals is TOM1L1 (Richardson et al., 2011) , which has also been found at the PM and in EEs, where it assists in the endocytosis of the EGF receptor (Liu et al., 2009). In this master thesis, we therefore decided to focus on the mutational analysis of the UBDs of TOL6 as representative for the TOL protein family.

In previous, unpublished experiments, De Araujo, Korbei and co-workers have managed to show, that mutation of a single amino acid in the VHS domain of TOL6, the well conserved Tryptophan at position 25 to an alanine (W25A) (see section 5.1.1) , fails to fully rescue a higher order *tolQ* (see section 1.6.1) mutant phenotype. This is especially striking because it is expressed like functional *TOL6p::TOL6:mCherry*, which fully rescues the *tolQ* phenotype, and shows a similar subcellular localization (see Figure 21). Apart from that, the expression of

TOL6p::tol6^{W25A}*:mCherry* does not result in dominant negative effects, when expressed in plants (De-Araujo and Korbei, unpublished data).

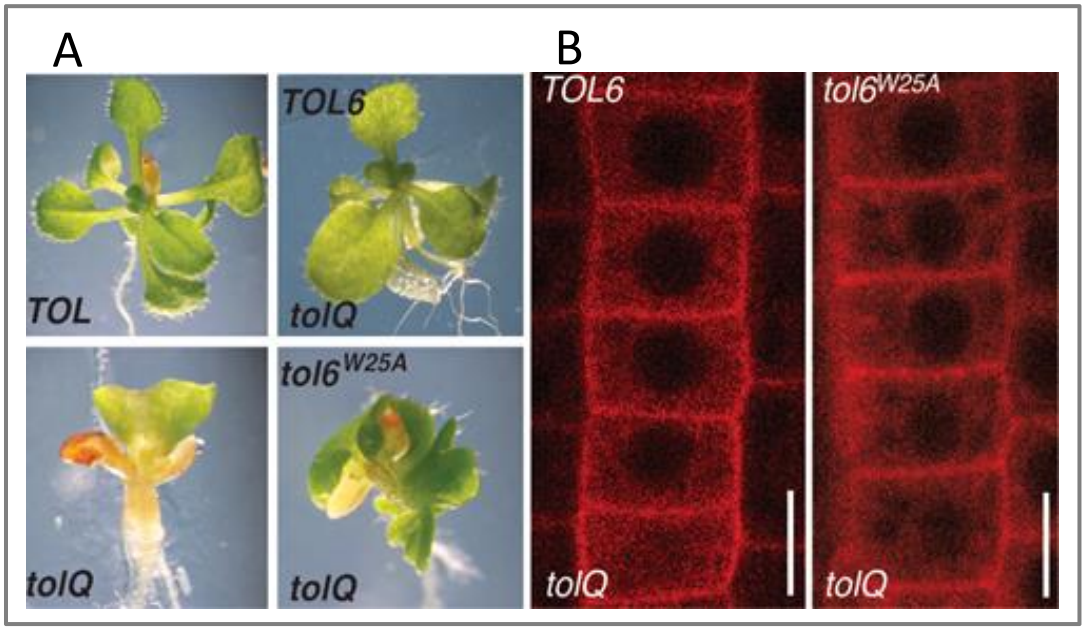

Figure 21*: TOL6p::TOL6:mcherry in tolQ Arabidopsis thaliana* , A) Rescue of *tolQ* plants and wild type *Arabidopsis* transformed with wild type TOL6 and mutated tol6 ^{W25A} **B)** Localization of wild type TOL6 and mutated tol6 ^{W25A} in *tolQ* root cells

The strategy in this master thesis was therefore to further mutate the VHS and analyzing the effects *in vitro* and *in planta*. Moreover, similar mutagenesis experiments will be initiated for the TOL GAT domain and for mutant combinations affected in both, VHS and GAT, domains. With these approaches I will determine the role of conserved TOL UBDs and their relevance for cargo recognition and sorting.

5.3 Mutagenesis and cloning of the mutated VHS and GAT domain to pTZ57R/T

To potentially obtain a TOL6 construct with a VHS domain that cannot bind to ubiquitin, I introduced a second mutation into the already mutated TOL6 construct (W25A) mutated in the α-helix 2. The second mutation comprised the highly conserve amino acid in the α-helix 4 of the TOL6 VHS domain, namely the Asparagine (Asn, N) at position 73, which was mutated to alanine (N73A). We called this construct: *tol6*$^{25A,\ N73A}$ = *tol6* ^{mVHS}.

To obtain the *tol6* ^{mVHS}, *tol6*^{W25A} cDNA (obtained from De-Araújo) in pTZ57R/T was amplified with oligos TOL6 N73Af and TOL6 N73Ar introducing an Alanine instead of an Asparagine at position 73, which resulted in *tol6*$^{W25A,\ N73A}$, which we called *tol6*^{mVHS}. Successful mutation was verified by sequencing.

To establish the TOL6 mutants potentially lacking ubiquitin binding of the GAT domain, *TOL6* cDNA (provided by de-Araujo) in pTZ57R/T was amplified with oligos TOL6 AAA1f and TOL6 AAA1f to replace DLL by AAA at position 246-248 (see Figure 21) resulting in *tol6*$^{DLL246\text{-}248AAA}$. Successful mutation was verified by sequencing. Further amplification of *tol6*$^{DLL246\text{-}248AAA}$ in pTZ57R/T vector with oligos TOL6 AAA2f and TOL6 AAA2r replaced DML by AAA at position 250-252, resulting in *tol6*$^{DLL246\text{-}248AAA,}$ which we called *tol6*^{mGAT}. Successful mutation was verified by sequencing.

The total mutant TOL6, including both VHS and GAT mutations, was obtained by using EcoRI as restriction enzyme to insert the first 424 bp from *tol6*^{mVHS} in pTZ57R/T into *tol6*^{mGAT}. Thus resulting in a TOL6 construct, which contains both fully mutated domains. This construct we called *tol6*^{mTOTAL}. Once again we checked this construct by sequencing of the entire construct.

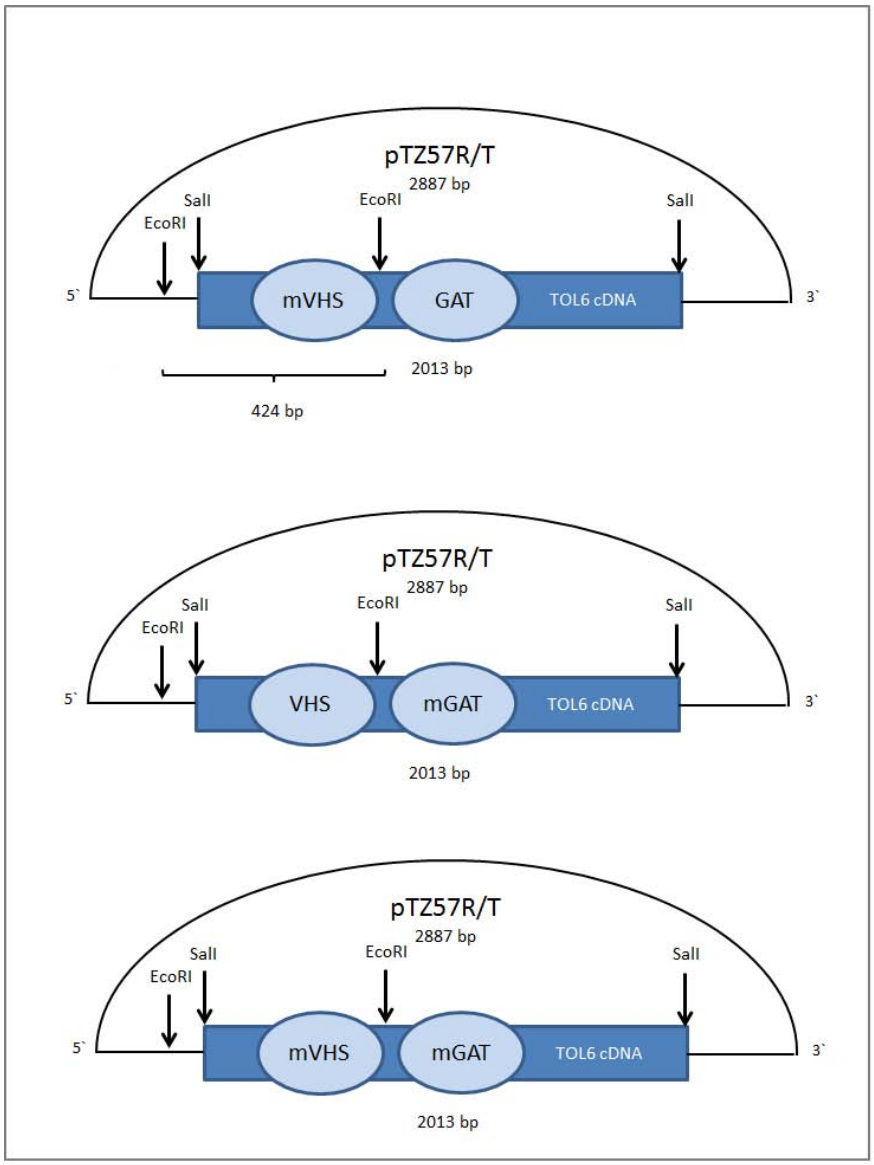

Figure 22: *in silico* visualization of the cloning procedure for the *tol6*^{mTOTAL} construct in the bacterial pTZ57R/T vector

When we obtained the sequencing results, we noticed that apparently during the cloning procedures a short nucleotide sequence between 1497 and 1605 bp was excised, encoding a short C-terminal Glutamine-rich amino acids stretch (HQQHQQQQGYSQPQHSQQQGYSQLQQPQPQQGYSQ) of TOL6.

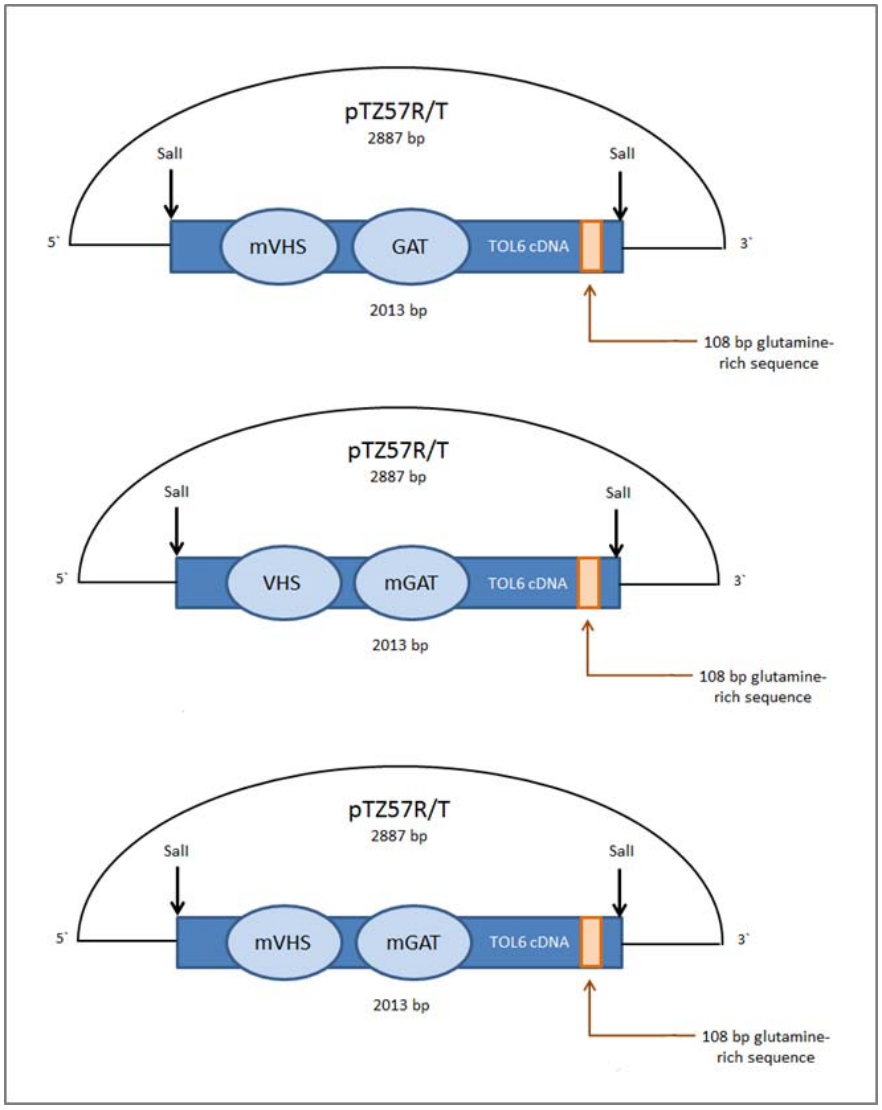

Figure 23: *in silico* visualization of the full length tol6 contructs in the bacterial pTZ57R/T vector

No alignment matches with this short sequence using BLAST were found, but a similar, albeit not as long sequence is also found in TOL9 and in a plant ENTH domain protein named epsin1 (Holstein and Oliviusson, 2005; Zouhar and Sauer, 2014). Due to the in frame deletion in the C-terminal part of these constructs, we named these shorter constructs short tol6 (*stol6*). In the further experiments we used these short constructs of TOL6 in their mutated and non mutated version, to additionally determine the impact of the short Glutamine-rich amino acid sequence at the C-terminal part of TOL6 protein on ubiquitin binding or protein location *in planta*.

Consequently 4 different TOL6 mutant lines were established:

tol6 $^{\Delta 499\text{-}535}$ = *stol6*

stol6$^{W25A,\ N73A}$ = *stol6*^{mVHS}

stol6$^{DLL246\text{-}248AAA,DML250\text{-}252AAA}$= *stol6*^{mGAT}

stol6$^{mVHS+mGAT}$= *stol6*^{mTOTAL}

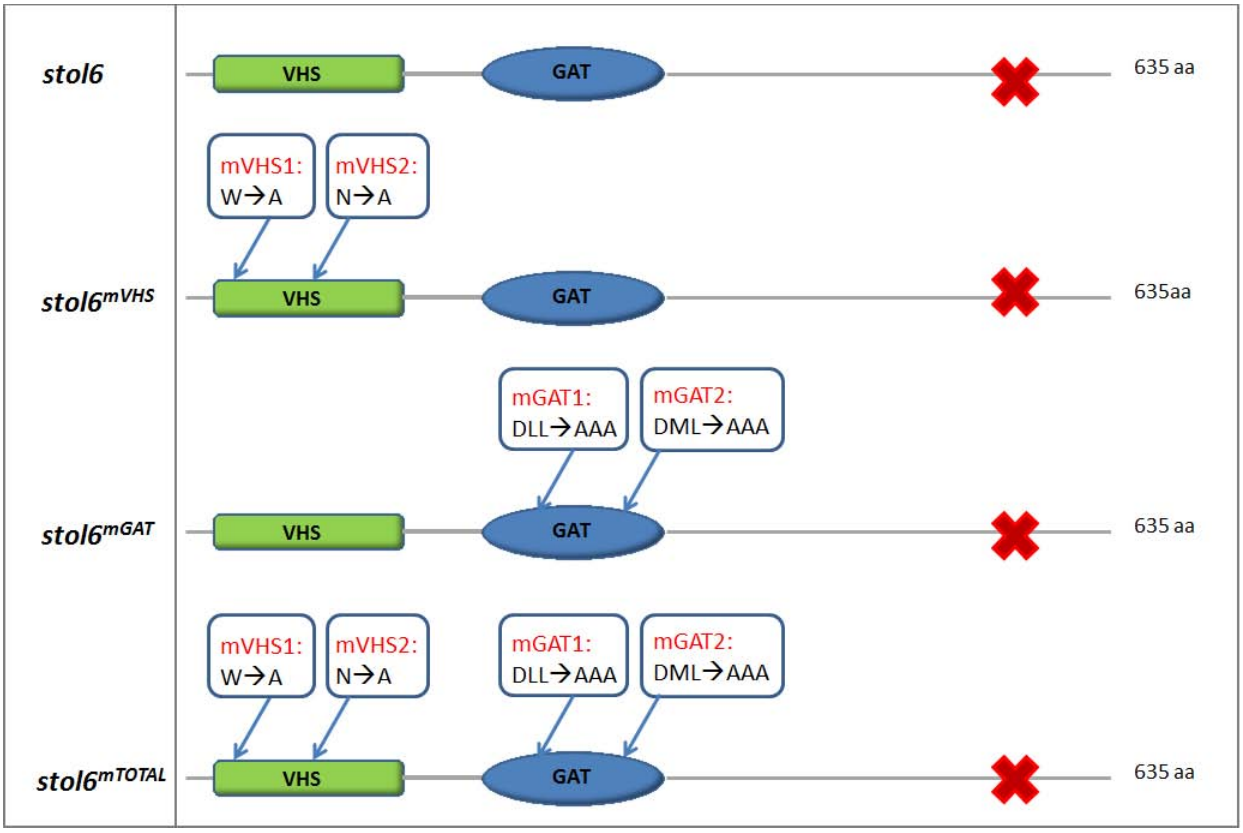

Figure 24: *In silico* visualization of the *stol6* constructs

5.4 Cloning of the mutated constructs into a bacterial expression vector

The mutated *stol6* clones in the pTZ57R/T vectors (see Figure 24) were amplified with oligos TOL6-SalIu and TOL6-SalId introducing in frame SalI sites at the very 5' and 3' end of the PCR product with proof reading polymerase. Furthermore T/A sticky ends were added to the PCR products by performing an additional PCR without primers and non-proof reading Taq-polymerase to ensure efficient ligation to the pTZ57R/T vector. After electroporation into

DH10B, positive colonies were selected by blue/white screening. Correct inserts were checked by control digestion with SalI and clones were further confirmed by sequencing.

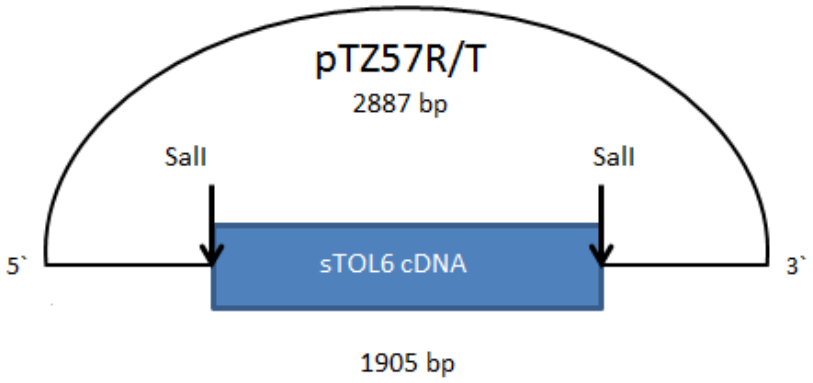

Figure 25*: in silico* visualization of sTOL6 in the bacterial cloning vector pTZ57R/T

The mutated *tol6* clones in pTZ57R/T were further sub-cloned via SalI into SalI digested, dephosphorylated pET24a vector. After ligation and electroporation into DH10B, positive colonies were checked by control digestion with SalI. Correct insert direction and reading frame was confirmed by control digestion with BamHI or EcoRI restriction endonuclease. The resulting clones were: *stol6*, *stol6*^{mVHS}, *stol6*^{mGAT} and *stol6*^{mTOTAL} in pET24a, thus in an inducible vector for protein expression and with a C-terminal His-tag.

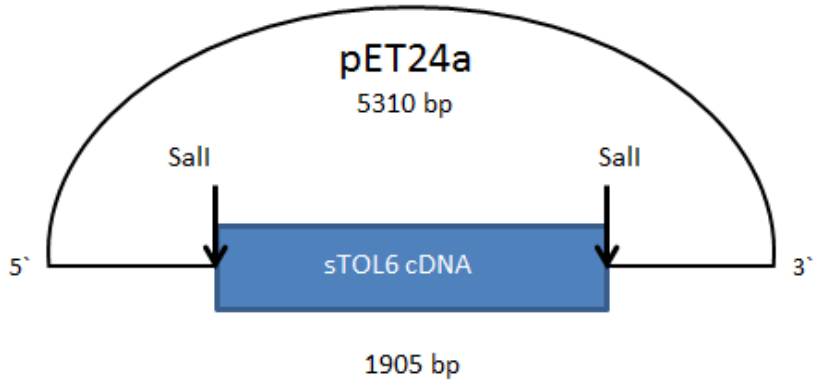

Figure 26: *in silico* visualization of *sTOL6* in the bacterial expression vector pET24a

5.4.1 Cloning strategy for full length TOL6-constructs

To account for the contribution of the deletion of the Q-stretch to the final phenotype, we also wanted to obtain the full-length constructs.

For this, the mutated *stol6* clones in pET24a, obtained from the previous cloning procedure were digested with BamHI and the first 765 bp, containing the mutated VHS and/or GAT domain, were eluated and ligated into the last 1248bp of a BamHI digested full length *TOL6* cDNA in pET24a. This was done for the *stol6*^{mVHS}, *stol6*^{mGAT} and *stol6*^{mTOTAL} to obtain the mutated full length constructs *tol6*^{mVHS},*tol6*^{mGAT} and *tol6*^{mTOTAL} respectively.

The resulting constructs were electroporated into DH10B, and checked by BamHI. Further EcoRI and HindIII control digestions were performed to verify the presence and the correct orientation of the 765 bp insert containing the mutated VHS and/or the mutated GAT domain.

The cloning procedure for the full-length mutant TOL6 constructs was performed by Lucinda De-Araujo.

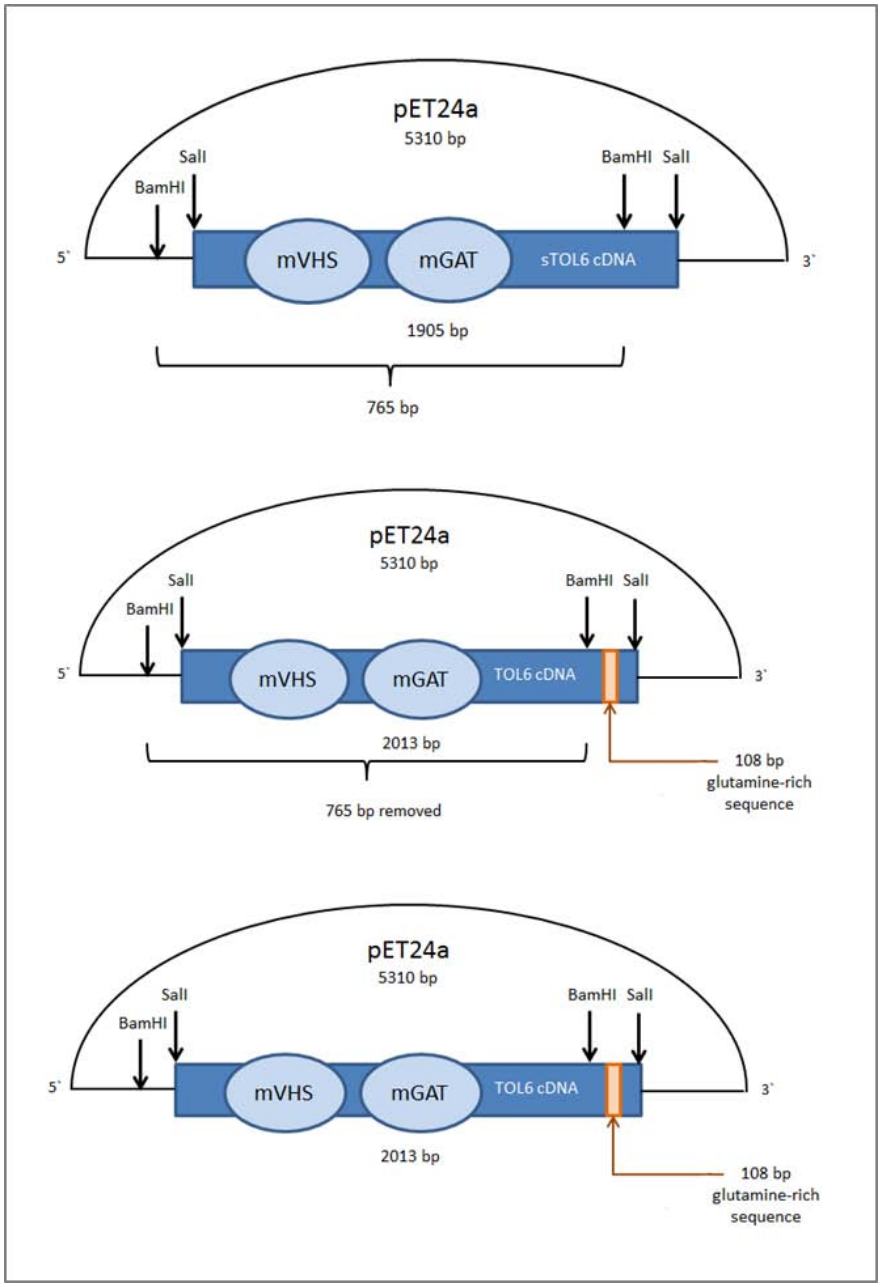

Figure 27: *In silico* visualization of the cloning procedure for the full length *tol6* constructs

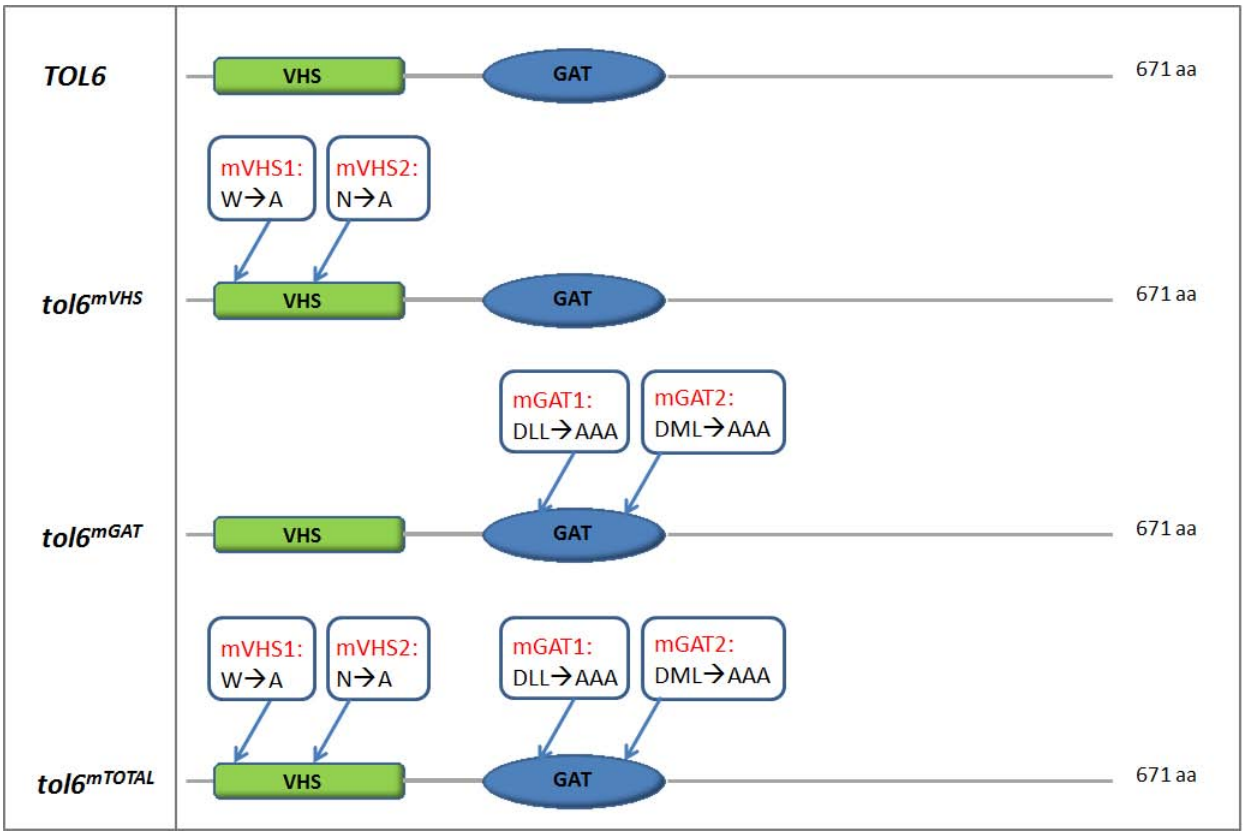

Figure 28: ***In silico*** **visualization of the full length** ***tol6*** **constructs**

5.4.2 Cloning of the mutated *TOL6* constructs for plant transformation

5.4.2.1 Cloning of Venus-tagged *stol6* constructs in pTZ57R/T

General cloning procedures were performed in pTZ57R/T. The finished constructs were further sub-cloned into the final vector of choice for *in planta* transformation, the pPZP221.

Stol6-Venus cDNA (Lucinda De Araújo Feitio) in pTZ57R/T was digested with BamHI. The eluated 1879bp fragment, containing the last 1143bp of *stol6* and the Venus tag, was ligated into the BamHI digested, eluated and dephosphorylated 3700 bp fragment of the different *stol6* constructs in pTZ57R/T. This resulted in the constructs *stol6*^{mVHS}*-Venus*, *stol6*^{mGAT}*-Venus* and *stol6*^{mTOTAL}*-Venus* in pTZ57R/T.

The same was done for the full-length constructs, ligating the 1987 bp BamHI fragment of *TOL6-Venus* (containing the last 1251bp of TOL6 and a Venus-tag) into the BamHI digested and dephosphorylated first 765bp of the mutated *stol6* constructs in pTZ57R/T resulting in:

tol6^{mVHS}*-Venus*, *tol6*^{mGAT}*-Venus* and *tol6*^{mTOTAL}*-Venus* in pTZ57R/T.

The obtained constructs were electroporated into DH10B. Control digests were performed with HindIII to verify the presence of the BamHI insert with the Venus-tag. Furthermore, the correct orientation of the insert was verified by restriction digest with PstI.

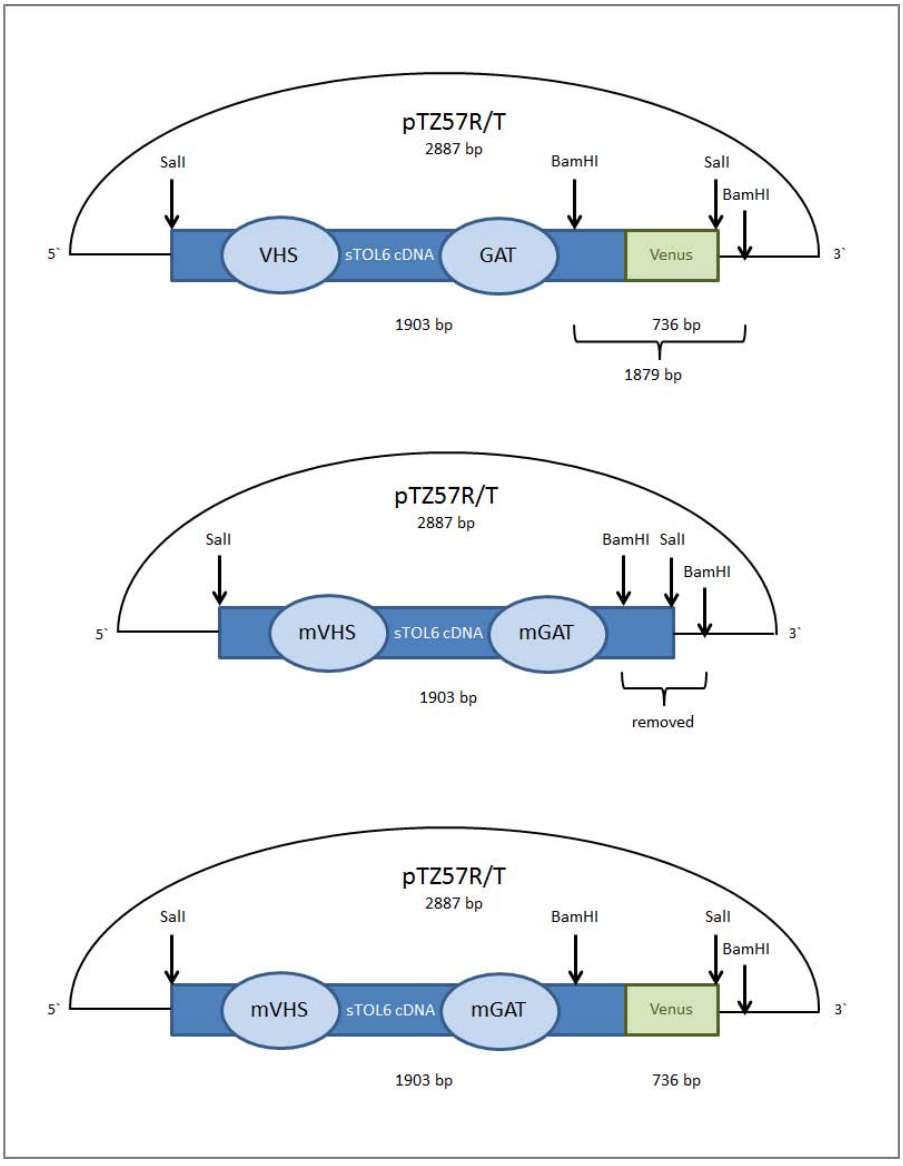

Figure 29: *in silico* visualization of the cloning procedure for the *stol6-Venus* constructs

5.4.2.2 Cloning of the stol6-Venus constructs into pPZP221 plant expression vector

The entire cassette (mutated s*tol6* or *tol6* cDNA with the C-terminal Venus tag) was then cut in frame out of the pTZ57R/T vector with SalI and cloned into the pPZP221. The pPZP221 already contained a 2000bp pTOL6 piece upstream and a pApA terminator sequence downstream, as was used for construction of the *pTOL6::TOL6:mcherry* constructs in Korbei et al., 2013. The construct was further electroporated into DH10B and selected using Spectinomycin as selection antibiotic for the pPZP221 plasmid. To control the presence of the mutated *tol6/stol6* construct within the pPZP221 vector the clones were digested using SalI. Directional digest to control the correct orientation of the insertion was performed with Pst and HindIII

5.4.3 *In vitro* binding assay to ubiquitin

5.4.3.1 General information

To assess the *in vitro* binding activity of mutated stol6 and mutated full length TOL6 protein constructs to ubiquitin, the constructs were cloned into pET24a plasmid (see section 1.4), which is a vector used for inducible high quality protein expression.

The plasmids were electroporated into electrocompetent BL21(DE3) cells, which are ideal *E.coli* for induced protein expression. Positive clones, selected by Kanamycin antibiotic, were inoculated in liquid cultures and further prepared for (large scale) induction of protein expression with IPTG. Expressed recombinant proteins were crudely purified from the cell culture broth by extraction and stored at -80°C for further use for the *in vitro* binding assay. Efficiency of protein expression by IPTG induction was confirmed by SDS PAGE stained with Coomassie, analyzing samples taken before and after the induction (see Figure 24). Furthermore, the solubility and purity of the proteins of interest were analyzed by examining the soluble and pellet fractions after extraction.

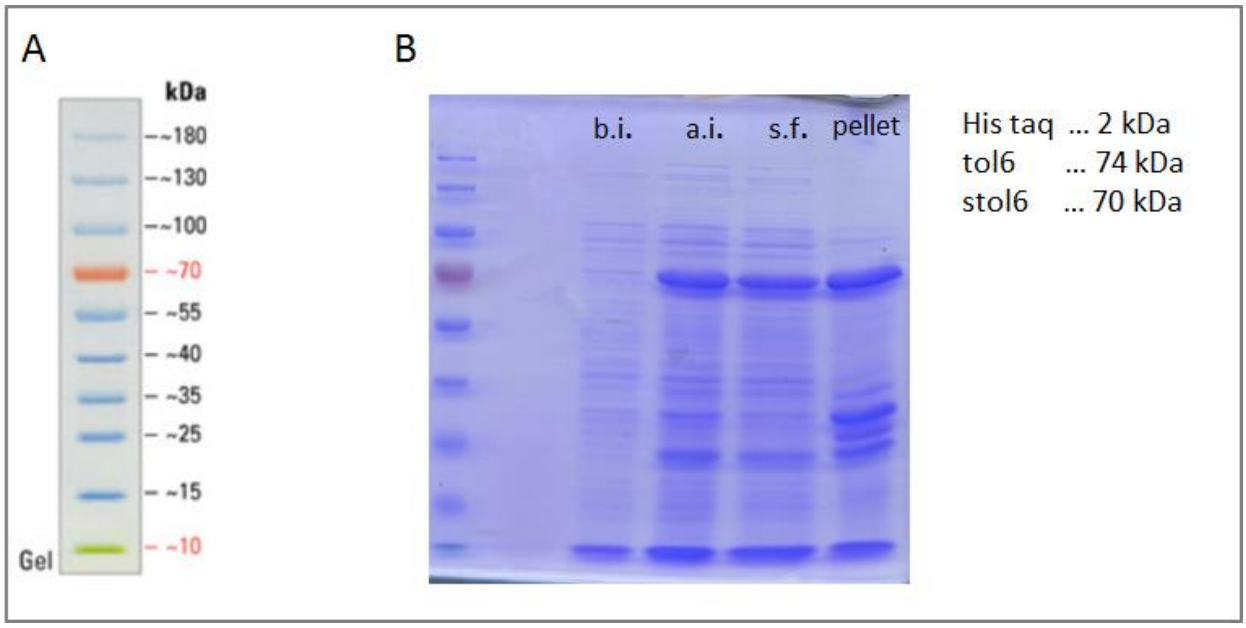

Figure 30: SDS-Page of induced protein expression and band profil ladder ; A) SDS-PAGE band profile of the Fermentas PageRuler Prestained Protein Ladder. **B)** SDS-PAGE stained with Coomassie, Induction of protein expression of mutated sTOL6; b.i.: before induction; a.i.: after induction, s.f.: soluble fraction; pellet.

Figure 30 show a typical picture of IPTG induced protein expression for the TOL6 constructs. The sample shown in the third lane of Figure 30 B was taken before induction (b.i.) with a very weak band at ~ 70 kDa do to the leakiness of the induction system. In lane 4, showing the sample taken after induction (a.i.), a strong band at 70 kDa was visible. This strong band is attributed to expressed mutated stol6 protein, which should have a calculated size of 70 kDa including the His-tag. Induction of protein expression by IPTG was efficient, as can be seen by the strong increase in the strength of the protein band from the third to the fourth lane. In the fifth lane, the soluble fraction (s.f.), obtained by protein extraction exhibited a strong band at 70 kDa pointing out the high efficiency of the extraction method for soluble protein. In the insoluble pellet fraction loaded on the last lane, there was still a band at 70 kDa visible, indicating, that some mutated stol6 is also found in the insoluble pellet fraction after extraction. But the extraction efficiency was high enough to obtain a suitable amount of soluble protein for further binding assay analysis.

5.4.3.2 *In vitro* binding assay

To determine the *in vitro* binding activity of the different mutated and non-mutated stol6 and full-length TOL6 proteins to ubiquitin I performed a pull down assay. For this assay, Pierce Glutathione Magnetic Beads were linked to bacterially expressed purified GST-tagged ubiquitin and further incubated with equal amounts of the different bacterially expressed purified His-tagged TOL6 protein constructs. The pelleted magnetic beads were analyzed by SDS-PAGE and further Western blotting to detect co-precipitated TOL6 constructs. As negative control, I used bacterially expressed and purified GST coupled to the beads. This allows me to assess the amount of His-tagged protein that binds non-specifically either to the beads or to GST.

An α-His antibody was used for detection of the TOL6 constructs and Coomassie staining was used to ensure that equal amounts of bound ubiquitin were employed in this assay. Furthermore, the extracts before binding were checked by SDS-PAGE and subsequent Coomassie staining or alternatively Western Transfer and immune-detection to confirm that equal amounts of purified TOL proteins were used. The extracts after binding were also analyzed with the before mentioned methods to assess the amount of non-bound protein. A typical experiment, with several of the above-mentioned controls, can be seen in Figure 31.

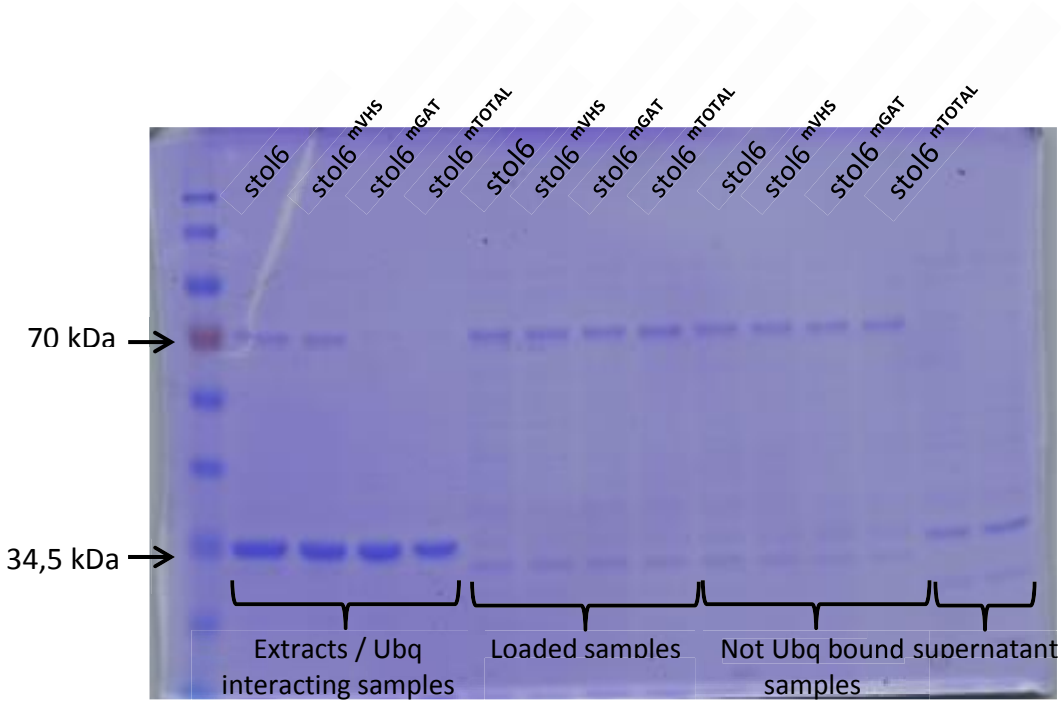

Figure 31: SDS-PAGE stained with Coomassie of the *in vitro* binding assay ; extracts: protein interacting with ubiquitin; loaded samples: amount of protein construct which was used for the binding assay; Not Ubq bounded samples: amount of protein construct which was not binding to ubiquitin at all in the second step; Supernatant; amount of ubiquitin which was not linked to the Glutathione magnetic beads in the first step

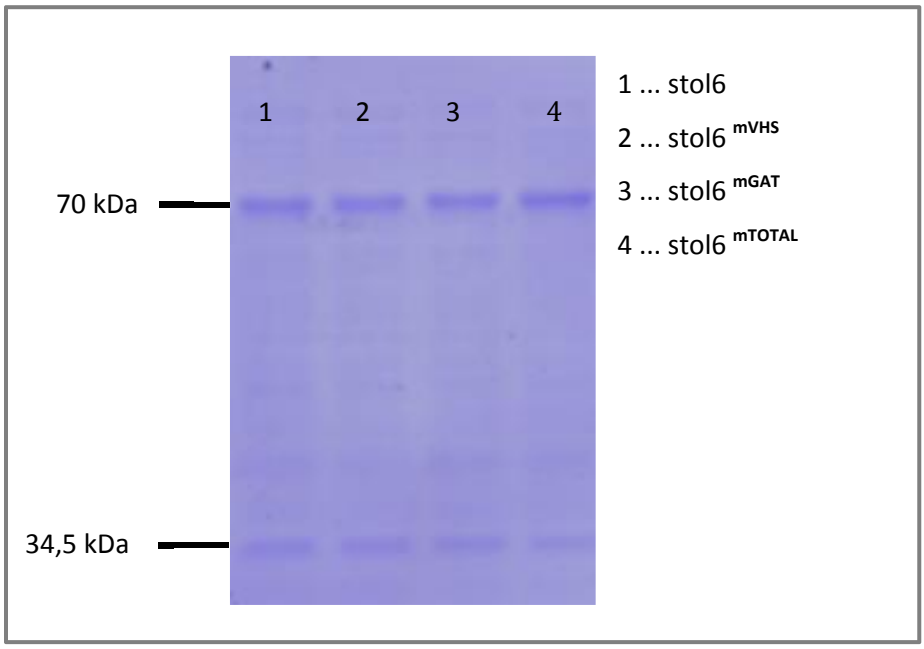

Figure 32: Amount of samples used for the *in vitro* binding assay loaded on SDS-PAGE stained with Coomassie ; stol6, stol6 ^{mVHS}, stol6 ^{mGAT}, stol6 ^{mTOTAL}

In Figure 32 (and Figure 31 lanes 6-9), the initial amounts of protein used for the experiment were loaded to ensure that equal amounts were used in the experiment. Comparing the band intensities of stol6 proteins at 70 kDa in a Coomassie stained gel, confirms that they are approximately equal, which allows for further comparison of protein band intensities of bound protein extracts in Figure 34. Due to the low sensitivity and specificity of Coomassie staining, the Western blot analysis was also used to be able to detect more subtle protein difference due to the more sensitive method (Figure 33).

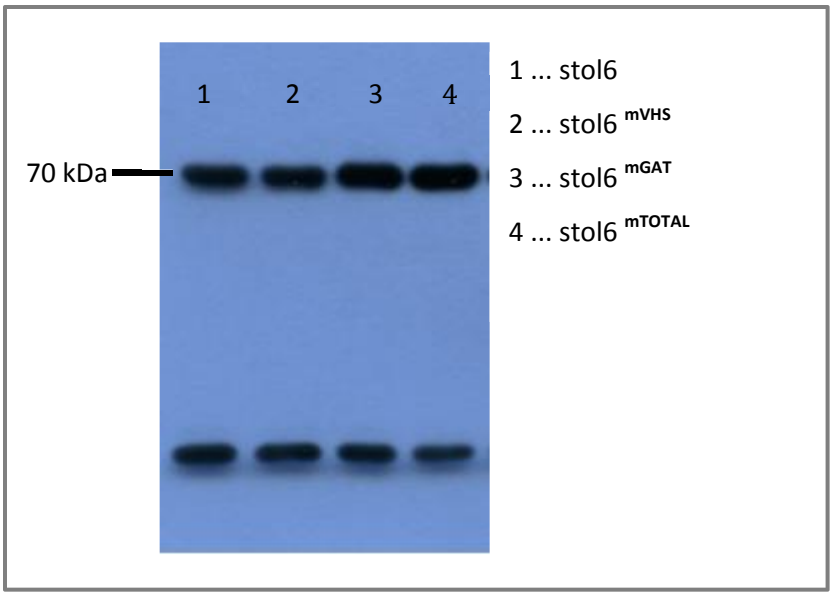

Figure 33: Amount of protein used for binding assay separated by SDS-PAGE with further western blotting detection ; stol6, stol6 ^{mVHS}, stol6 ^{mGAT}, stol6 ^{mTOTAL}

The western blot and immune-detection confirms the results from Figure 32 in that the initial amount of proteins used for the binding assay are comparable.

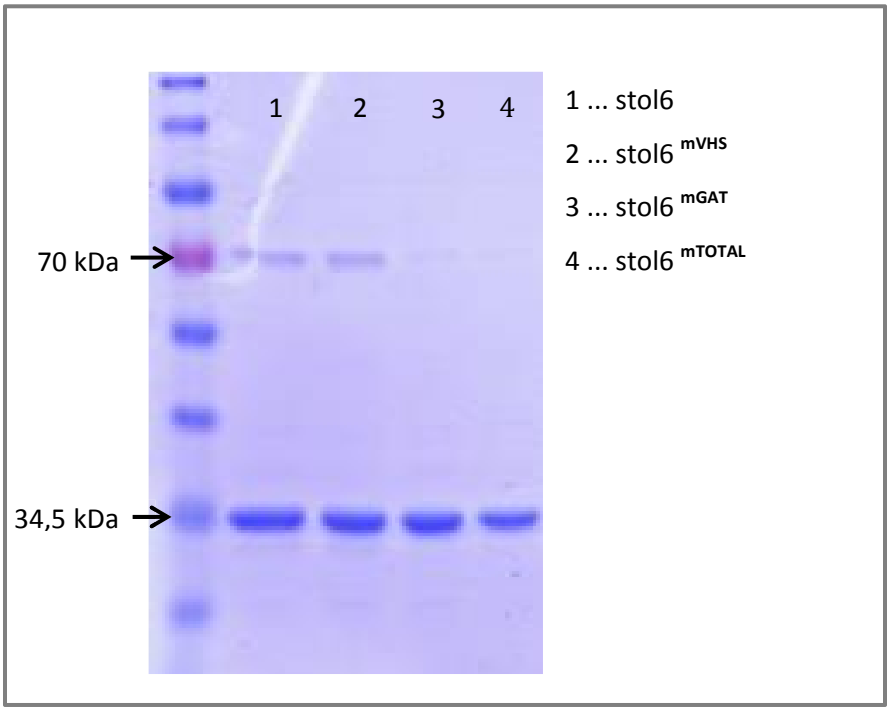

Figure 34: protein constructs interacting with ubiquitin from *in vitro* binding assay separated on SDS-PAGE stained with Coomassie ; stol6, stol6 ^{mVHS}, stol6 ^{mGAT}, stol6 ^{mTOTAL}

Figure 34 (and Figure 31 lanes 2-5) shows a typical *in vitro* binding assay with the different stol6 constructs. The protein bands at 70 kDa correspond to the stol6 protein constructs, which bound to the ubiquitin coupled beads during the *in vitro*-binding assay. The strength of the protein band in the stol6 sample (lane 1) is comparable to that of the stol6^{mVHS} sample (lane 2). Indicating that both short TOL6 constructs can bind ubiquitin with equal affinities. In contrast to wild type stol6, mutated stol6^{mGAT} bound with lower affinity to ubiquitin as demonstrated by the strongly reduced amount of the protein to co-precipitate with the ubiquitin beads. Mutated stol6^{mTOTAL}, representing the full-mutated construct showed the lowest binding affinity to ubiquitin. Thus ubiquitin binding is severely reduced in this construct.

The band at 34,5 kDa, which can be found in all four lanes represent GST:Ubiquitin, thus equal amount of GST-ubiquitin coupled beads were used in all four experimental set ups. Although Coomassie staining is not very sensitive and specific, the visual band intensities between the mutated shortTOL6 constructs and the wild type *stol6* indicated reduced ubiquitin binding. I further performed SDS-PAGE with subsequent Western Transfer and immune-detection to be able to compare the bound stol6 protein constructs more specifically and sensitively (Figure 35).

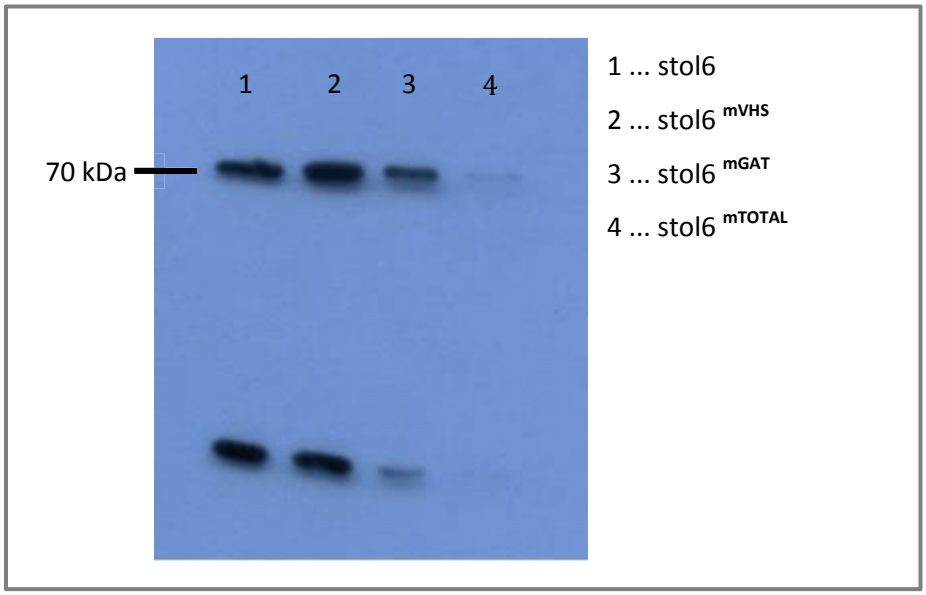

Figure 35: Protein constructs interacting with ubiquitin separated by SDS-PAGE and further western blotting detection ; stol6, stol6 ^{mVHS}, stol6 ^{mGAT}, stol6 ^{mTOTAL}

The band intensities in Figure 35 were in agreement to the results obtained by Coomassie staining in Figure 34. Both the stol6 and the stol6 ^{mVHS} bound with equal affinities to ubiquitin. There is a clear reduction in the amount of protein binding to ubiquitin for stol6 ^{mGAT} (lane 3), which thus revealed impaired ubiquitin binding activity. This is even more reduced in the fully mutated in stol6 ^{mTOTAL} (lane 4), where there is barely any binding to ubiquitin detectable. These fine differences, as between stol6 ^{mGAT} and stol6 ^{mTOTAL}, are better seen when employing western transfer and immune-detection rather that with the nonspecifically staining Coomassie.

To exclude unspecific protein binding to the Glutathione Magnetic beads or to GST, negative control reactions lacking ubiquitin were performed (Figure 36) alongside the *in vitro* binding assays with ubiquitin.

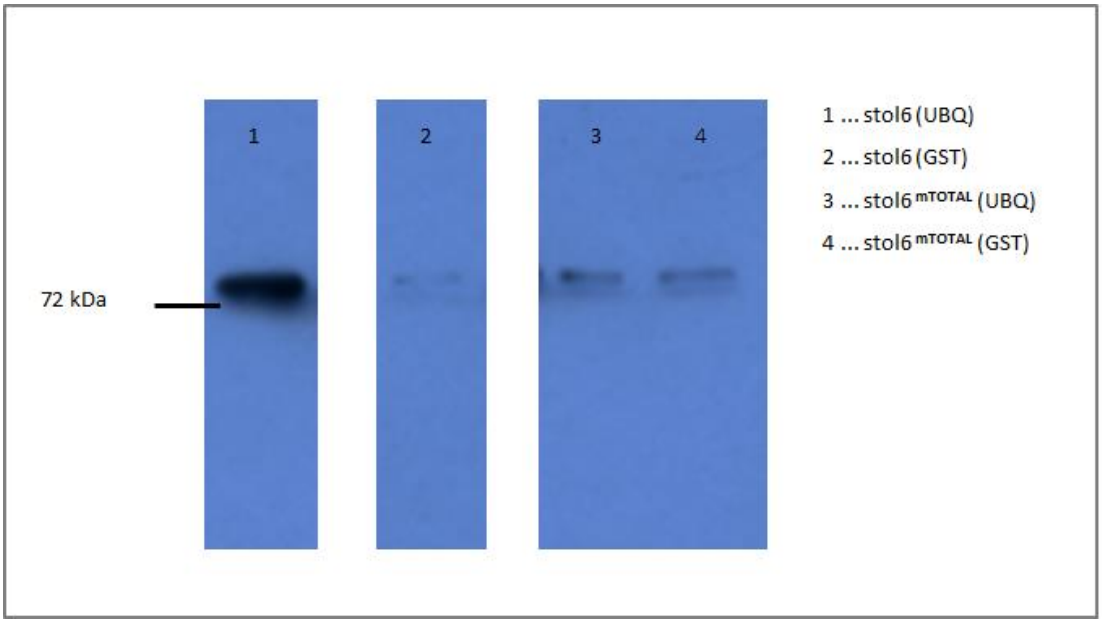

Figure 36: Protein interacting with Ubiquitin (1 and 3) or GST (2 and 4) from binding assay separated by SDS-PAGE and further western blotting detection ; stol6, stol6 ^{mVHS}, stol6 ^{mGAT}, stol6 ^{mTOTAL}

Figure 36 lane 1 shows a strong band at 70 kDa, once again confirming the strong binding of stol6 to ubiquitin. The negative control of stol6 loaded in lane 2 corresponds to the interaction of stol6 with the GST-coupled beads. Thus this weak band indicates slight unspecific interaction with the GST-coupled beads, which can be subsequently seen as background signal. The

interaction of stol6 ^{mTOTAL} with Ubiquitin depicted in Figure 36 lane 3 shows similar band intensities as the negative control of stol6 ^{mTOTAL} in lane 4. Consequently the binding of stol6 ^{mTOTAL} to ubiquitin is not much higher than the background, which represents unspecific binding to beads or GST.

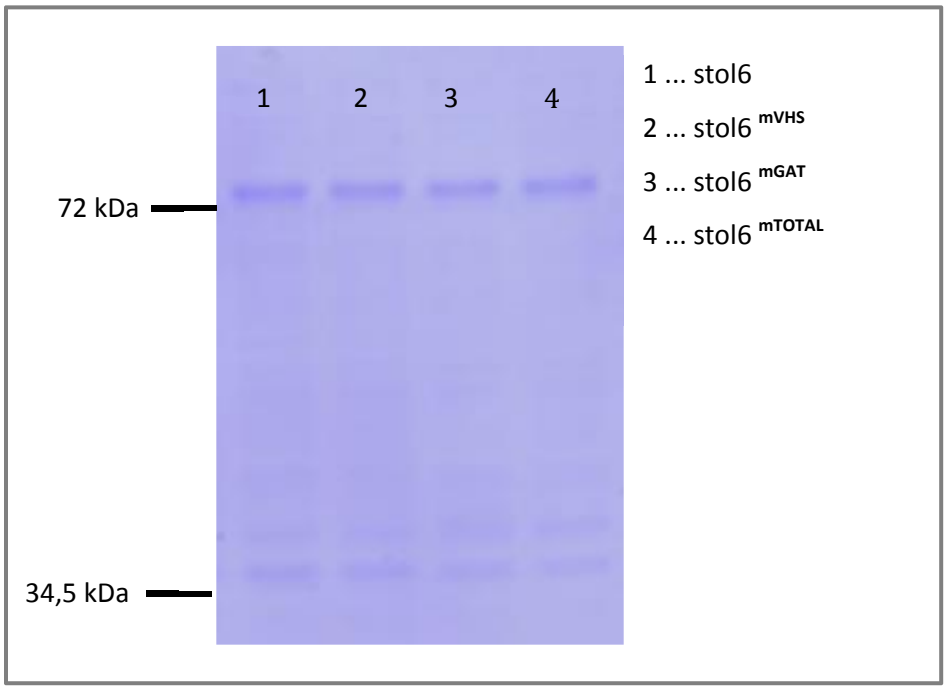

Figure 37: Amount of protein not bound to Ubiquitin separated on SDS-PAGE stained with Coomassie ; stol6, stol6 ^{mVHS}, stol6 ^{mGAT}, stol6 ^{mTOTAL}

Figure 37 shows the amount of protein, which did not bind to ubiquitin. They are also immunodetected as it can be seen in Figure 38.

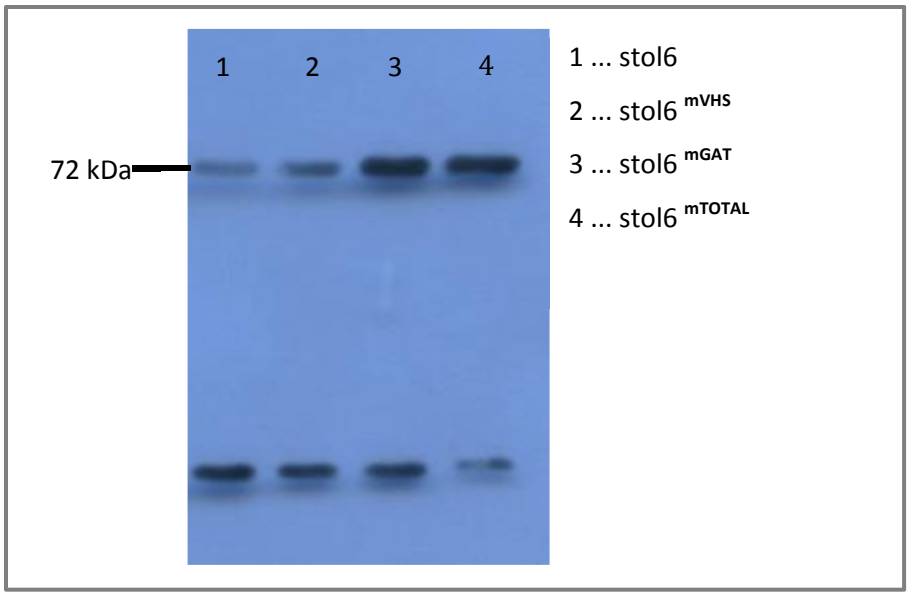

Figure 38: Amount of protein not bound to ubiquitin obtained by *in vitro* binding assay separated by SDS-PAGE with further western blotting detection ; stol6, stol6 ^{mVHS}, stol6 ^{mGAT}, stol6 ^{mTOTAL}

As compared to the band intensities of ubiquitin bound protein extracts in Figure 35 the protein bands obtained in Figure 38 showed mirror-inverted band intensities. As an example wild type stol6 protein bound with high affinity to ubiquitin resulting in a strong protein band in Figure 35 whereas only a weak band of not ubiquitin bound protein can be detected in Figure 38. These results mainly show that the amounts of proteins used in this study are adequate as it shows that the system is not completely saturated with His-tagged protein.

The experiments shown above represent a typical ubiquitin binding assays and were repeated several times with the similar outcome. In conclusion the *in vitro* analysis showed that, stol6 clearly and reproducibly binds to ubiquitin. Mutating just the VHS domain in two amino acids had no apparent effect on the ubiquitin binding capacity of TOL6 *in vitro*. On the other hand, mutating the GAT domain in 6 amino acids greatly reduced the ability of TOL6 to be able to bind to ubiquitin. Mutation of both the VHS and the GAT domain completely abolished the ubiquitin binding of TOL6 (stol6 ^{mTOTAL}), reducing it to background levels.

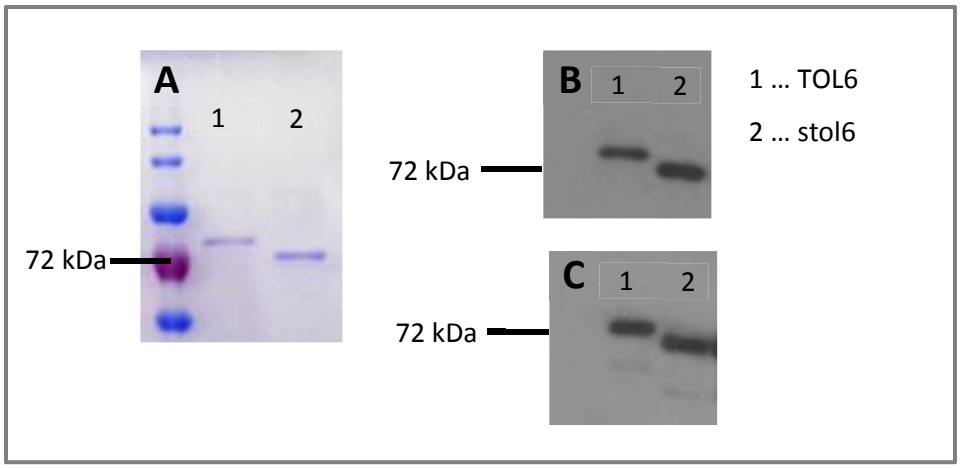

Figure 39: Binding assay with TOL6 and stol6 ; A) interaction of TOL6 and *stol6* with ubiquitin, separated by SDS Gel stained with Coomassie **B)** interaction of TOL6 and ***stol6*** with ubiquitin, SDS gel separation and Western blotting with primary α His **C)** Amount of TOL6 and stol6 used for the experiment, SDS gel separation and western blotting with primary α His.

In order to verify the comparability of stol6 and the full-length TOL6, binding assays shown in Figure 39, the *in vitro*-ubiquitin binding activity of TOL6 equals with that of stol6, indicating no obvious impact of the missing C-terminal Glutamine rich stretch in stol6 on the *in vitro*-ubiquitin interaction of TOL6.

Binding assay with the full length TOL6 and the mutated full length versions (TOL6, tol6 ^{mVHS}, tol6 ^{mGAT} and tol6 ^{mTOTAL}) were performed by Lucinda De-Araujo (Figure 40).

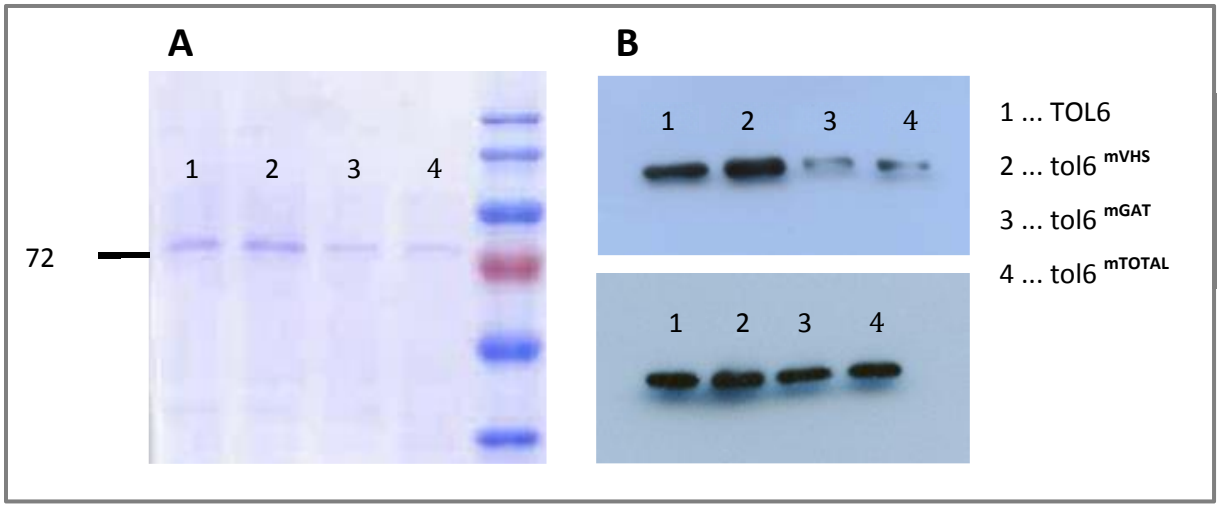

Figure 40: Binding assay with TOL6 and tol6 mutant constructs ; A) interaction of TOL6 and tol6 mutants with ubiquitin, separated by SDS Gel stained with Coomassie **B)** interaction of TOL6 and tol6 mutants with ubiquitin, SDS gel separation and Western blotting with primary α His, bottom: Amount of TOL6 and tol6 mutants used for the experiment, SDS gel separation and western blotting with primary α His., Lucinda De-Araujo.

TOL6 and tol6^{mVHS} revealed similar ubiquitin binding activity as stol6 and stol6^{mVHS}. Nevertheless tol6^{mGAT} show more reduced binding activity than stol6^{mGAT}. These differences need to be subjected to future studies. Overall these results support the results obtained for stol6 and mutated stol6 versions in that only upon mutation of both the VHS and the GAT domain binding to ubiquitin is completely abolished in TOL6.

5.4.4 In vivo analysis of TOL6 in *Arabidopsis thaliana*

5.4.4.1 General information

In order to determine the localization of mutated TOL6 constructs *in vivo*, different plant strains of *Arabidopsis thaliana* were transformed and further selected for expression of the desired TOL6 construct by Gentamycin. For efficient construct transformation into *Arabidopsis thaliana*, pPZP221 vector, already including promotor TOL6 for endogenous TOL6 expression in plants, was used. For detection of transformed proteins expressed *in planta,* the mutated tol6 constructs were cloned as fusion proteins containing a fluorescent GFP derived Venus-tag. Consequently, localization of transformed protein constructs can be determined by Confocal Laser Scanning Microscopy (CLSM).

5.4.4.2 Transformation of reporter constructs into *A. thaliana*

The obtained constructs (see 5.4.2) were transformed into *Agrobacterium tumefaciens* and transformed by the floral dip method into different *Arabidopsis thaliana* strains to analyze and visually detect the localization of the fusionprotein constructs within the plant roots. For transformation 3 different *Arabidopsis thaliana* strains were chosen: Columbia 0 ecotype (wt), *tol6-1* (a T-DNA insertion plant line lacking expression of full length endogenous TOL6) and *tol2-1/tol2-1 tol3-1/TOL3 tol5-1/tol5-1 tol6-1/tol6-1 tol9A-1/tol9A-1 (tolQ het)*. Columbia represents the control, whereas the other two *Arabidopsis thaliana* strains serve as analysis platform for not mutated and mutated TOL6 and stol6 constructs. As *tol6-1* is deficient in full length TOL6 expression, transformation of mutated *tol6* and *stol6* constructs to *tol6-1* can reveal differences in their localization within the endosomal system as well as aberrant PMP degradation. Homozygous mutant plant lines as *tol6-1* show no obvious phenotype (Korbei et al., 2013). This

phenomenon might be explained by the large amount of different TOL proteins in the TOL family, being possibly able to overtake the role of each other due to their ubiquitously expression pattern in nearly all plant organs (Korbei et al., 2013).

To analyze possible defects in the correct function of the different tol6 mutants with respect to the non-mutated TOL6, I used the third strain, the *tolQ het* and transformed it with the mutated *tol6/stol6* constructs. *tolQ het* is a multiple T-DNA insertion line lacking endogenous TOL2,5,6 and 9 and heterozygous for the T-DNA insertion line lacking full length TOL3. It has no obvious phenotype, while *tolQ* (which is also homozygous for the TOL3 T-DNA insertion line and thus also lacks TOL3, see Figures 21) is developmentally severely affected. Thus I transformed the different TOL6 constructs into the *tolQ het* to then obtain transformants in the *tolQ* background in the next generation. TOL6:mcherry has been shown to fully rescue the *tolQ* phenotype while the tol6^{W25A}:mCherry showed only a partial rescue ((Korbei et al., 2013) and section 5.2.1). The transformation of the different stol6 and TOL6 constructs into the *tolQ* background will therefore give us valuable information about the *in vivo* function of the TOL6 UBDs and potentially also about the short Glutamine rich stretch in the C-terminus of TOL6.

Unfortunately the further genotyping of the next generation and the analysis of the potential rescue phenotypes requires a long time period and therefore the analysis of the rescue experiments could not be carried out with in this master thesis, although I performed all the transformations. Initial analysis of some of the transformants, in the Col0 and *tol6-1* strains, were carried out though (Figure 41).

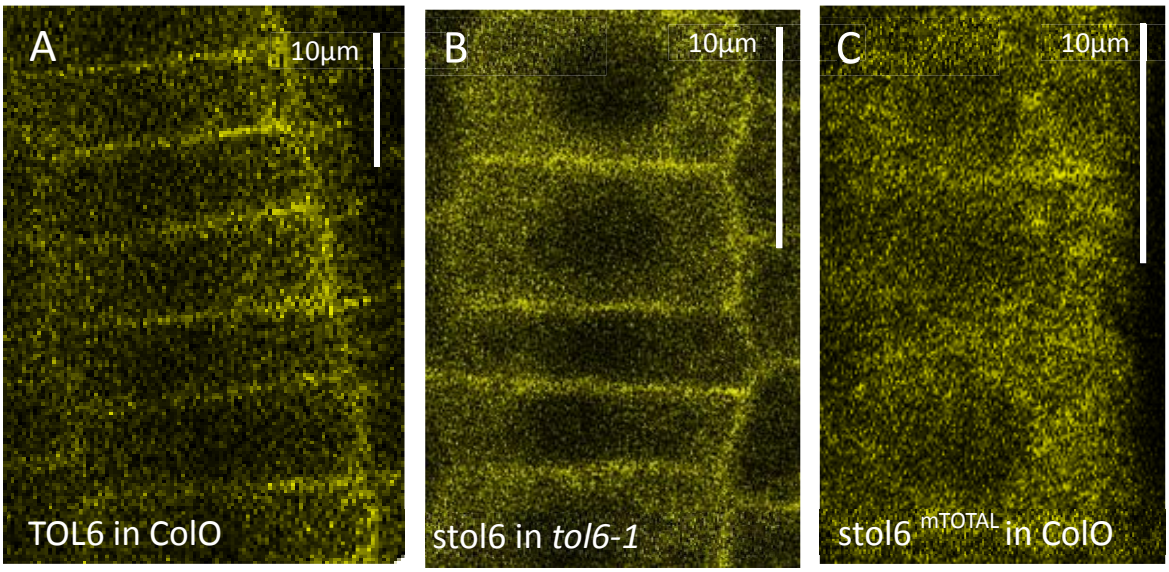

Figure 41: *In vivo*-localization of TOL6, stol6 and stol6 ^{mTOTAL} : A) TOL6p::TOL6:Venus in ColO root meristem cells of 10 day old seedlings **B)** TOL6p::stol6:Venus in tol6-1 root meristem cells of 10 day old seedlings **C)** TOL6p**::** stol6 ^{mTOTA}:Venus in ColO root meristem cells of 10 day old seedlings

Full length TOL6:Venus (Figure 41A) is primarily localized at the PM similar to TOL6:mCherry (Korbei et al., 2013) as expected. As can be seen in Figure 41B stol6 in *tol6-1* is mainly localized at the PM and partially at TGN/EE similar to TOL6, suggesting no obvious influence of the missing 100bp C-terminal stretch of stol6 on the cellular localization of the protein. However stol6 localization seems to be not that tightly restricted to the PM compared to TOL6. As this is only preliminary data, further experiments will have to clarify this issue. Furthermore, analysis of the stol6:Venus in *tolQ* background will be essential to determine a potential role of the 100bp C-terminal Q-rich stretch in the function of TOL6, asides from its localization.

Interestingly, the fully mutated version (stol6 ^{mTOTAL}) does not localize to the PM anymore, it is completely cytoplasmic (Figure 41C). This is surprising, as the altered localization has to be attributed to the impaired ubiquitin binding activity of stol6 ^{mTOTAL}, caused by the introduced mutations in the VHS and GAT domain. Thus ubiquitin binding and localization must be interconnected. Further tests, including the complementation analysis will need to be carried out to further investigate these differences in localization.

6. Discussion

6.1 *In vitro*-ubiquitin interaction

In-vitro binding assay revealed equal ubiquitin binding activity of TOL6 and stol6 constructs indicating no effect of the C-terminal Glutamine rich stretch, which is missing in stol6, on *in vitro*-ubiquitin binding. The stol6^{mVHS} mutant shows slightly reduced ubiquitin binding activity compared to the non-mutated stol6 construct, whereas the stol6^{mGAT} mutant revealed a more decreased binding activity (Figure 42). For stol6^{mTOTAL} binding to ubiquitin was reduced to background levels in the *in vitro* binding assay, indicating a complete loss of ubiquitin binding (see Figure 42).

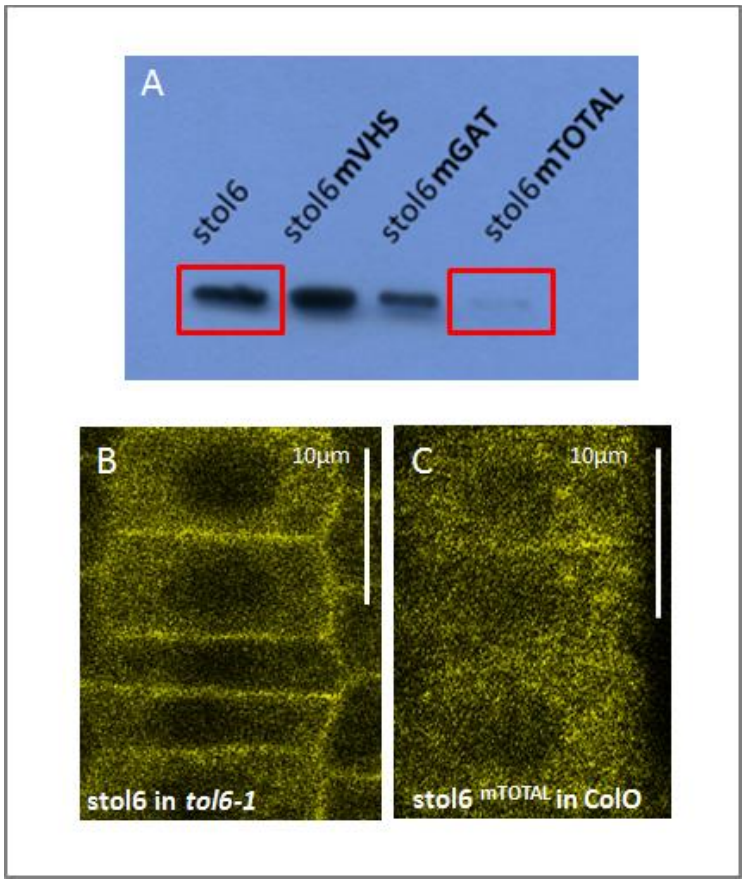

Figure 42: *In vitro* and *in vivo* results for stol6 constructs ; A.) *In vitro* binding assay showing stol6 constructs interacting with ubiquitin, separated by SDS-PAGE and detected by Western blotting **B) and C**) *In vivo* localization of TOL6p::stol6:Venus and TOL6p::stol6^{mTOTAL}:Venus constructs in *tol6-1* and ColO strains, detected by confocal laser scanning microscopy (CLSM)

The octahelical VHS domain includes highly conserved amino acids within the second α-helix pointing towards the surface of the protein to interact with the Ile 44 patch of ubiquitin (recently reviewed by (Wang et al., 2010)).

As shown by different groups, Tryptophan at position 26 (Trp26, W26) in STAM1 (Hong et al., 2009) and Tryptophan at position 28 (Trp28, W28) in Vps27 and Hse1 (Ren and Hurley, 2010) corresponding to Tryptophan at position 25 (Trp25, W25) in TOL6 is located in the α2-helix of the VHS domain and was demonstrated to have a high impact on ubiquitin binding (Hong et al., 2009). In contrast Asparagine at position 75 (Asn75, N75) in Vps27 and Hse1 corresponding to Asparagine at position 73 (Asp73, N73) in TOL6 was thought to be relevant, but not necessary for ubiquitin interaction (Ren and Hurley, 2010). Lange et al underline the importance of these two amino acids, as both experience the highest chemical shift perturbation in their NMR studies (Lange et al., 2011). Due to these facts, we chose these amino acids for site directed mutagenesis in the VHS domain. Yet in our assay, these mutants show no strong alteration in ubiquitin binding. This could be due to the fact, that additional amino acids might be involved in ubiquitin interaction. On the other hand, the binding of the VHS domain in plants might be less important than that of the GAT domains. To clarify this issue, we would need to construct deletion mutants of TOL6 and the mutated TOL6 constructs comprising only the VHS domain or only the GAT domain. These deletion mutants could then be tested in our *in vitro* binding assay for altered binding to ubiquitin.

Furthermore, other amino acids, which could potentially be involve in ubiquitin binding in the VHS domain could also be mutated.

The three-helical GAT domain of Tom1 and GGA3 include 2 ubiquitin interaction sites (Bilodeau et al., 2004; Akutsu et al., 2005). Sequence alignment with TOL proteins revealed 6 amino acids in one of the interaction sites within the GAT domain of the TOL proteins as being efficiently conserved according to their side chain properties: Aspartate at position 246 (Asp 246, D246), Leucine at position 247 (Leu247, L247), Leucine at position 248 (Leu248, L248), Aspartate at position 250 (Asp250, D250), Methionine at position 251 (Met251, M251) and Leucine at

position 252 (Leu252, L252). Site directed mutagenesis of these amino acids in the GAT domain result in impaired *in vitro*-ubiquitin affinity of stol6^{mGAT}.

Due to the decreased binding affinity of stol6^{mGAT} mutant in contrast to the stol6^{mVHS} mutant, the degree of contribution of the GAT domain to the ubiquitin binding activity seems to be higher than that of the VHS domain. This unequal importance can be referred to different mechanisms of TOL6 interaction with ubiquitin or on a more general level this could also reflect differences between plants and mammalian UBDs. Mutation of both domains was essential though to completely eliminate ubiquitin binding, although this is not as strongly visible in the full-length mutant (tol6^{mTOTAL}).

In summary, we have managed to create a TOL6 mutant that cannot bind ubiquitin anymore and we can use this mutant to assess the importance of the functionality of both UBDs *in vivo*.

6.2 *In planta* analysis

In planta analysis of the different TOL6 mutants gave essential insight into the function of the UBDs. I transformed the mutant constructs into three different plant strains to test for alterations in the localization of the mutant proteins with respect to the endogenous protein the ability to complement the severe *tolQ* phenotype, which should give indications about the function of the protein.

Non-mutated full-length Venus-tagged TOL6 was used as a reference and it localized predominantly at the PM, as would be expected of the endogenous TOL6 (Korbei et al., 2013). stol6:Venus in *tol6-1* (Figure 41 B and Figure 42 B) looked similar to TOL6:Venus, indicating no obvious alteration in the localization due to the 100 bp Glutamine-rich stretch lacking in the stol6 constructs. On the other hand, stol6^{mTOTAL} in Col0 (Figure 41 C and Figure 42C) accumulated predominantly in the cytosol, demonstrating its impaired recruitment to or binding at the PM.

TOL6 in ColO, as shown in Figure 41 A, serves as a control and is predominantly localized at the PM. s*tol6* in *tol6-1* (Figure 41 B and Figure 42 B) is localized similar to TOL6, indicating no obvious but slightly alteration due to the 100 bp Glutamine-rich stretch lacking in the *stol6*

constructs. Consequently more punctate signals of *stol6* were detected in the cytosol. stol6 ^{mTOTAL} in ColO (Figure 41 C and Figure 42 C) accumulates in the cytosol, which indicates disabled/impaired recruitment to the PM.

These preliminary results were not further advanced in this master thesis do to time constraints. Similarly, analysis of the other TOL6 mutants as well as complementation assays, which will allow us to differentiate more subtly between the different mutant lines, were out of the time frame of this master thesis.

Thus, summarizing the data so far, we can conclude that loss of ubiquitin binding results in loss of PM localization.

6.3 Models for function of UBDs

Based on the *in vitro*- and *in vivo*-result **2 potential modes of interaction** can be hypothesized.

Interactions of UBD with ubiquitin are generally weak, promoting the idea of a network-like interaction of different UBDs to create a rapidly assembled transiently stable and reversible complex for interaction with, for example, ubiquitinated cargo (Hicke et al., 2005)). Therefore many switches are present to disrupt the network-interaction (Hicke et al., 2005) One point mutation within a UBD can disrupt the weak transiently interaction between UBD and ubiquitin and consequently destabilize the network-like interaction of different UBDs (Hicke et al., 2005). Processes like for example vesicle budding for clathrin mediated endocytosis of ubiquitinated cargo from the PM requires a network of different UBDs (Hicke et al., 2005). Subsequent reversible ubiquitination of proteins including a UBD can induce a protein switch to start the assembling of a network-like interaction (Hicke et al., 2005). This **intermolecular interaction mode** is based on the finding, that some UBD-containing proteins, for example GGAs (Shiba et al., 2004), and ESCRT-0 proteins (Hrs and STAM) are themselves ubiquitinated, which might represent an important regulation step (Erpapazoglou et al., 2014). However, the influence of this post-translational modification on protein sorting needs to be subjected to more detailed analysis in the future.

On the other hand ubiquitination of a TOL6 might cause **intramolecular** binding of the UBD and thus induce a conformational change. This conformational change could subsequently trigger the activation of ubiquitin binding activity or the recruitment to the PM by other means of TOL6. Based on my *in vitro* results, exhibiting higher reduction of ubiquitin binding activity for stol6^{mGAT} in contrast to stol6^{mVHS} (see Figure 42 A), the GAT domain seems to be the most promising UBD for this intramolecular binding for protein activation. The identification of a possible ubiquitination site of GGA1 and 2 within the GAT domain in a manner dependent on the GAT-ubiquitin interaction (Shiba et al., 2004) and the idea of a protein activation switch induced by ubiquitination (Hicke et al., 2005) in particular support the hypothesis of a GAT domain ubiquitination dependent TOL6 activation. Nevertheless the involvement of the VHS domain cannot be excluded as both UBD might interact with each other in a network-like way.

An special feature of TOL6 (and TOL9) proteins is the C-terminal Glutamine rich stretch, which was found similarly in epsin 1 (At5g11710) an ENTH/ANTH plant proteins (Zouhar and Sauer, 2014).Figure 41he polyglutamine rich stretches are present in more than 60 human proteins and seem to play an extended role in stabilizing protein-protein interactions (Schaefer et al., 2012). These findings would support my hypothesis, that the Glutamine-rich stretch found in TOL6 (and TOL9) provide an interaction/attaching surface for other proteins within a network-like interaction.

PM associated localization of TOL6 suggests early involvement in the recognition of ubiquitinated PM proteins destined for degradation (Korbei et al., 2013). The major mechanism for endocytosis of PMPs is through clathrin coated vesicle formation at the PM (Zouhar and Sauer, 2014). Different types of accessory proteins mediate the clathrin coated vesicle formation (CCV) by serving as linkers between cargo, clathrin and adaptor proteins (Zouhar and Sauer, 2014). ENTH/ANTH/VHS domain-containing proteins represent one type of accessory proteins found in mammals and plants (Zouhar and Sauer, 2014). They share an N-terminal ENTH, ANTH or VHS domain interacting with endomembranes (recently reviewed by (Zouhar and Sauer, 2014). TOL proteins include a VHS domain next to the GAT domain and are thought to represent ESCRT-0 orthologs in plants (Korbei et al., 2013). The PM associated localization of TOL6 indicates its potential involvement in early steps of cargo recognition at the PM.

The ESCRT-0 complex, as part of the ESCRT-machinery, can be seen as a main regulator for the recognition of ubiquitinated PMP and subsequent sorting-procedure. TOL proteins as potential orthologs of ESCRT-0 complex in *Arabidopsis thaliana* consequently could function as a novel regulatory protein family in *planta* for PMP degradation. Their ability to interact with ubiquitinated cargo via a transient interaction between their UBDs and ubiquitin underlines the importance of UBDs in regulating PMP distribution at the PM. Thus, loss of PM localization of TOL6, due to mutations in the UBD, represents and interesting and novel regulation step in the assembly of the ESCRT machinery and the fine-tuning of PMP degradation. Consequently the findings of this master thesis will serve as corner stone for future studies intended to unravel the fate of ubiquitinated PMP and thus how sessile organisms like plants efficiently translate environmental cues into cellular signals.

7. References

Akutsu, M., Kawasaki, M., Katoh, Y., Shiba, T., Yamaguchi, Y., Kato, R., Kato, K., Nakayama, K., and Wakatsuki, S. (2005). Structural basis for recognition of ubiquitinated cargo by Tom1-GAT domain. FEBS Lett **579,** 5385-5391.

Alberts, B. (2008). Molecular Biology of the Cell: Reference edition. (Garland Science).

Babst, M. (2011). MVB Vesicle Formation: ESCRT-Dependent, ESCRT-Independent and Everything in Between. Current opinion in cell biology **23,** 452-457.

Bilodeau, P.S., Winistorfer, S.C., Kearney, W.R., Robertson, A.D., and Piper, R.C. (2003). Vps27-Hse1 and ESCRT-I complexes cooperate to increase efficiency of sorting ubiquitinated proteins at the endosome. J Cell Biol **163,** 237-243.

Bilodeau, P.S., Winistorfer, S.C., Allaman, M.M., Surendhran, K., Kearney, W.R., Robertson, A.D., and Piper, R.C. (2004). The GAT domains of clathrin-associated GGA proteins have two ubiquitin binding motifs. J Biol Chem **279,** 54808-54816.

Bonifacino, J.S. (2004). The GGA proteins: adaptors on the move. Nat Rev Mol Cell Biol **5,** 23-32.

Clough, S.J., and Bent, A.F. (1998). Floral dip: a simplified method for Agrobacterium-mediated transformation of Arabidopsis thaliana. The Plant journal : for cell and molecular biology **16,** 735-743.

Collins, B.M., Watson, P.J., and Owen, D.J. (2003a). The structure of the GGA1-GAT domain reveals the molecular basis for ARF binding and membrane association of GGAs. Dev Cell **4,** 321-332.

Collins, B.M., Watson, P.J., and Owen, D.J. (2003b). The Structure of the GGA1-GAT Domain Reveals the Molecular Basis for ARF Binding and Membrane Association of GGAs. Developmental cell **4,** 321-332.

Dell'Angelica, E.C., Puertollano, R., Mullins, C., Aguilar, R.C., Vargas, J.D., Hartnell, L.M., and Bonifacino, J.S. (2000). GGAs: a family of ADP ribosylation factor-binding proteins related to adaptors and associated with the Golgi complex. J Cell Biol **149,** 81-94.

Dettmer, J., Hong-Hermesdorf, A., Stierhof, Y.D., and Schumacher, K. (2006). Vacuolar H+-ATPase activity is required for endocytic and secretory trafficking in Arabidopsis. Plant Cell **18,** 715-730.

Dikic, I., Wakatsuki, S., and Walters, K.J. (2009). Ubiquitin-binding domains [mdash] from structures to functions. Nat Rev Mol Cell Biol **10,** 659-671.

Driscoll, P.C. Solving the FYVE domain--PtdIns(3)P puzzle. (Nat Struct Biol. 2001 Apr;8(4):287-90.).

Engel, A., and Gaub, H.E. (2008). Structure and mechanics of membrane proteins. Annu Rev Biochem **77,** 127-148.

Erpapazoglou, Z., Walker, O., and Haguenauer-Tsapis, R. (2014). Versatile Roles of K63-Linked Ubiquitin Chains in Trafficking. Cells **3,** 1027-1088.

Foresti, O., and Denecke, J. (2008). Intermediate organelles of the plant secretory pathway: identity and function. Traffic **9,** 1599-1612.

Geldner, N. (2004). The plant endosomal system--its structure and role in signal transduction and plant development. Planta **219,** 547-560.

Grant, B.D., and Donaldson, J.G. (2009). Pathways and mechanisms of endocytic recycling. Nat Rev Mol Cell Biol **10,** 597-608.

Haughn, G.W., and Somerville, C. (1986). Sulfonylurea-resistant mutants of Arabidopsis thaliana. Molecular and General Genetics MGG **204,** 430-434.

Herman, E.K., Walker, G., van der Giezen, M., and Dacks, J.B. (2011). Multivesicular bodies in the enigmatic amoeboflagellate Breviata anathema and the evolution of ESCRT 0. Journal of Cell Science **124,** 613-621.

Hicke, L., Schubert, H.L., and Hill, C.P. (2005). Ubiquitin-binding domains. Nat Rev Mol Cell Biol **6,** 610-621.

Hirsch, E., Costa, C., and Ciraolo, E. (2007). Phosphoinositide 3-kinases as a common platform for multi-hormone signaling. J Endocrinol **194,** 243-256.

Holstein, S.E., and Oliviusson, P. (2005). Sequence analysis of Arabidopsis thaliana E/ANTH-domain-containing proteins: membrane tethers of the clathrin-dependent vesicle budding machinery. Protoplasma **226,** 13-21.

Hong, Y.H., Ahn, H.C., Lim, J., Kim, H.M., Ji, H.Y., Lee, S., Kim, J.H., Park, E.Y., Song, H.K., and Lee, B.J. (2009). Identification of a novel ubiquitin binding site of STAM1 VHS domain by NMR spectroscopy. FEBS Lett **583,** 287-292.

Huotari, J., and Helenius, A. (2011). Endosome maturation. The EMBO journal **30,** 3481-3500.

Hurley, J.H. (2010). The ESCRT Complexes. Critical reviews in biochemistry and molecular biology **45,** 463-487.

Hurley, James H., Lee, S., and Prag, G. (2006). Ubiquitin-binding domains. Biochemical Journal **399,** 361-372.

Korbei, B., Moulinier-Anzola, J., De-Araujo, L., Lucyshyn, D., Retzer, K., Khan, Muhammad A., and Luschnig, C. (2013). Arabidopsis TOL Proteins Act as Gatekeepers for Vacuolar Sorting of PIN2 Plasma Membrane Protein. Current Biology **23,** 2500-2505.

Lange, A., Hoeller, D., Wienk, H., Marcillat, O., Lancelin, J.M., and Walker, O. (2011). NMR reveals a different mode of binding of the Stam2 VHS domain to ubiquitin and diubiquitin. Biochemistry **50,** 48-62.

Lemmon, S.K., and Traub, L.M. (2000). Sorting in the endosomal system in yeast and animal cells. Curr Opin Cell Biol **12,** 457-466.

Leung, K.F., Dacks, J.B., and Field, M.C. (2008). Evolution of the multivesicular body ESCRT machinery; retention across the eukaryotic lineage. Traffic **9,** 1698-1716.

Liu, N.S., Loo, L.S., Loh, E., Seet, L.F., and Hong, W. (2009). Participation of Tom1L1 in EGF-stimulated endocytosis of EGF receptor. The EMBO journal **28,** 3485-3499.

Luzio, J.P., Pryor, P.R., and Bright, N.A. (2007). Lysosomes: fusion and function. Nat Rev Mol Cell Biol **8,** 622-632.

Mao, Y., Nickitenko, A., Duan, X., Lloyd, T.E., Wu, M.N., Bellen, H., and Quiocho, F.A. (2000). Crystal structure of the VHS and FYVE tandem domains of Hrs, a protein involved in membrane trafficking and signal transduction. Cell **100,** 447-456.

Mattera, R., Puertollano, R., Smith, W.J., and Bonifacino, J.S. (2004). The trihelical bundle subdomain of the GGA proteins interacts with multiple partners through overlapping but distinct sites. J Biol Chem **279,** 31409-31418.

McMahon, H.T., and Boucrot, E. (2011). Molecular mechanism and physiological functions of clathrin-mediated endocytosis. Nat Rev Mol Cell Biol **12,** 517-533.

Mizuno, E., Kawahata, K., Kato, M., Kitamura, N., and Komada, M. (2003). STAM proteins bind ubiquitinated proteins on the early endosome via the VHS domain and ubiquitin-interacting motif. Mol Biol Cell **14,** 3675-3689.

Moulinier-Anzola, J., De-Araujo, L., and Korbei, B. (2014). Expression of Arabidopsis TOL genes. Plant Signaling & Behavior **9,** e28667.

Prag, G., Lee, S., Mattera, R., Arighi, C.N., Beach, B.M., Bonifacino, J.S., and Hurley, J.H. (2005). Structural mechanism for ubiquitinated-cargo recognition by the Golgi-localized, gamma-ear-containing, ADP-ribosylation-factor-binding proteins. Proc Natl Acad Sci U S A **102,** 2334-2339.

Prag, G., Watson, H., Kim, Y.C., Beach, B.M., Ghirlando, R., Hummer, G., Bonifacino, J.S., and Hurley, J.H. (2007). The Vps27/Hse1 complex is a GAT

domain-based scaffold for ubiquitin-dependent sorting. Developmental cell **12,** 973-986.

Puertollano, R., and Bonifacino, J.S. (2004). Interactions of GGA3 with the ubiquitin sorting machinery. Nat Cell Biol **6,** 244-251.

Ren, X., and Hurley, J.H. (2010). VHS domains of ESCRT-0 cooperate in high-avidity binding to polyubiquitinated cargo. The EMBO journal **29,** 1045-1054.

Reyes, F.C., Buono, R., and Otegui, M.S. (2011a). Plant endosomal trafficking pathways. Curr Opin Plant Biol **14,** 666-673.

Reyes, F.C., Buono, R., and Otegui, M.S. (2011b). Plant endosomal trafficking pathways. Curr Opin Plant Biol **14,** 666-673.

Richardson, L.G., and Mullen, R.T. (2011). Meta-analysis of the expression profiles of the Arabidopsis ESCRT machinery. Plant Signal Behav **6,** 1897-1903.

Richardson, L.G.L., Howard, A.S.M., Khuu, N., Gidda, S.K., McCartney, A., Morphy, B.J., and Mullen, R.T. (2011). Protein–Protein Interaction Network and Subcellular Localization of the Arabidopsis Thaliana ESCRT Machinery. Frontiers in plant science **2,** 20.

Saftig, P., and Klumperman, J. (2009). Lysosome biogenesis and lysosomal membrane proteins: trafficking meets function. Nat Rev Mol Cell Biol **10,** 623-635.

Saksena, S., Sun, J., Chu, T., and Emr, S.D. (2007). ESCRTing proteins in the endocytic pathway. Trends in Biochemical Sciences **32,** 561-573.

Sauer, M., and Friml, J. (2014). Plant biology: gatekeepers of the road to protein perdition. Curr Biol **24,** 019.

Schaefer, M.H., Wanker, E.E., and Andrade-Navarro, M.A. (2012). Evolution and function of CAG/polyglutamine repeats in protein-protein interaction networks. Nucleic acids research **40,** 4273-4287.

Scheuring, D., Viotti, C., Kruger, F., Kunzl, F., Sturm, S., Bubeck, J., Hillmer, S., Frigerio, L., Robinson, D.G., Pimpl, P., and Schumacher, K. (2011). Multivesicular bodies mature from the trans-Golgi network/early endosome in Arabidopsis. Plant Cell **23,** 3463-3481.

Scott, C.C., Vacca, F., and Gruenberg, J. (2014). Endosome maturation, transport and functions. Semin Cell Dev Biol **31,** 2-10.

Scott, P.M., Bilodeau, P.S., Zhdankina, O., Winistorfer, S.C., Hauglund, M.J., Allaman, M.M., Kearney, W.R., Robertson, A.D., Boman, A.L., and Piper,

R.C. (2004). GGA proteins bind ubiquitin to facilitate sorting at the trans-Golgi network. Nat Cell Biol **6,** 252-259.

Shahriari, M., Richter, K., Keshavaiah, C., Sabovljevic, A., Huelskamp, M., and Schellmann, S. (2011). The Arabidopsis ESCRT protein-protein interaction network. Plant Mol Biol **76,** 85-96.

Shen, B., Li, C., Min, Z., Meeley, R.B., Tarczynski, M.C., and Olsen, O.A. (2003). sal1 determines the number of aleurone cell layers in maize endosperm and encodes a class E vacuolar sorting protein. Proc Natl Acad Sci U S A **100,** 6552-6557.

Shiba, T., Kawasaki, M., Takatsu, H., Nogi, T., Matsugaki, N., Igarashi, N., Suzuki, M., Kato, R., Nakayama, K., and Wakatsuki, S. (2003). Molecular mechanism of membrane recruitment of GGA by ARF in lysosomal protein transport. Nat Struct Biol **10,** 386-393.

Shiba, Y., Katoh, Y., Shiba, T., Yoshino, K., Takatsu, H., Kobayashi, H., Shin, H.W., Wakatsuki, S., and Nakayama, K. (2004). GAT (GGA and Tom1) domain responsible for ubiquitin binding and ubiquitination. J Biol Chem **279,** 7105-7111.

Sommerville, L.E., and Hartshorne, D.J. (1986). Intracellular calcium and smooth muscle contraction. Cell Calcium **7,** 353-364.

Sorkin, A., and von Zastrow, M. (2009). Endocytosis and signalling: intertwining molecular networks. Nat Rev Mol Cell Biol **10,** 609-622.

Spitzer, C., Schellmann, S., Sabovljevic, A., Shahriari, M., Keshavaiah, C., Bechtold, N., Herzog, M., Muller, S., Hanisch, F.G., and Hulskamp, M. (2006). The Arabidopsis elch mutant reveals functions of an ESCRT component in cytokinesis. Development **133,** 4679-4689.

Stenmark, H. (2009). Rab GTPases as coordinators of vesicle traffic. Nat Rev Mol Cell Biol **10,** 513-525.

Uemura, T., and Nakano, A. (2013). Plant TGNs: dynamics and physiological functions. Histochemistry and Cell Biology **140,** 341-345.

Viotti, C., Bubeck, J., Stierhof, Y.D., Krebs, M., Langhans, M., van den Berg, W., van Dongen, W., Richter, S., Geldner, N., Takano, J., Jurgens, G., de Vries, S.C., Robinson, D.G., and Schumacher, K. (2010). Endocytic and secretory traffic in Arabidopsis merge in the trans-Golgi network/early endosome, an independent and highly dynamic organelle. Plant Cell **22,** 1344-1357.

Wang, T., Liu, N.S., Seet, L.F., and Hong, W. (2010). The emerging role of VHS domain-containing Tom1, Tom1L1 and Tom1L2 in membrane trafficking. Traffic **11,** 1119-1128.

Welsch, S., Habermann, A., Jager, S., Muller, B., Krijnse-Locker, J., and Krausslich, H.G. (2006). Ultrastructural analysis of ESCRT proteins suggests a role for endosome-associated tubular-vesicular membranes in ESCRT function. Traffic **7,** 1551-1566.

Williams, R.L., and Urbe, S. (2007). The emerging shape of the ESCRT machinery. Nat Rev Mol Cell Biol **8,** 355-368.

Winter, V., and Hauser, M.T. (2006a). Exploring the ESCRTing machinery in eukaryotes. Trends Plant Sci **11,** 115-123.

Winter, V., and Hauser, M.-T. (2006b). Exploring the ESCRTing machinery in eukaryotes. Trends in plant science **11,** 115-123.

Xiang, L., Etxeberria, E., and Van den Ende, W. (2013). Vacuolar protein sorting mechanisms in plants. Febs J **280,** 979-993.

Zhang, C., Hicks, G.R., and Raikhel, N.V. (2014). Plant vacuole morphology and vacuolar trafficking. Front Plant Sci **5**.

Zhu, G., Zhai, P., He, X., Terzyan, S., Zhang, R., Joachimiak, A., Tang, J., and Zhang, X.C. (2003). Crystal structure of the human GGA1 GAT domain. Biochemistry **42,** 6392-6399.

Zouhar, J., and Sauer, M. (2014). Helping hands for budding prospects: ENTH/ANTH/VHS accessory proteins in endocytosis, vacuolar transport, and secretion. Plant Cell **26,** 4232-4244.

8. Abbreviations

CCV
clathrin coated vesicle formation 92
CLSM
Confocal Laser Scanning Microscopy 26
CUE
coupling of ubiquitin conjugation to endoplasmatic reticulum degradation 17
DUIM
double sided UIM 17
EE
Early endosomes 10
ESCRT-machinery
Endosomal Sorting Complex required for Transport 11
FYVE
Fab 1 (yeast orthologue of PIKfyve), YOTB, Vac 1 (vesicle transport protein), and EEA1 15
GAT
GGA and Tom 15
GGA
Golgi-localized, gamma-ear containing, ADP-ribosylation factor binding 18
HRS
hepatocyte growth factor (HGF) regulated Tyr-kinase substrate 15
ILVs
intraluminal vesicles 12
LE
late endosomes 10
LE/MVB
late endosome/multivesicular bodies 11
MIU
motive interacting with ubiquitin 17
PI-3-kinase
Phosphoinositide-3-kinase 12
PI-3P
Phosphoinositide 3-Phosphate 12
PIPs
Phosphoinositides 12
PM
plasma membrane 9
PMP
plasma membrane proteins 9
RE
recycling endosomes 10

9. Table of figures